Physical Mechanisms of Ca-ATPase Regulation in the Heart

Vidhya Sivakumaran

Dissertation submitted to the faculty of the Virginia Polytechnic Institute and State University in partial fulfillment of the requirements for the degree of

Doctor of Philosophy
In
Biochemistry

James E. Mahaney
Peter J. Kennelly
Erin L. Dolan
Richard P. Wyeth

August 9th, 2010
Blacksburg, VA

Keywords: SERCA2a, Ca-ATPase, Phospholamban, EPR, Fluorescence

Physical Mechanisms of Ca-ATPase Regulation in the Heart

Vidhya Sivakumaran

ABSTRACT

The Ca-ATPase is an integral membrane enzyme which translocates two calcium ions from the cytoplasm of the cell to the sarcoplasmic reticulum lumen utilizing ATP breakdown as its energy source, in order to promote muscle relaxation. The focus of this research is the cardiac isoform of the Ca-ATPase which undergoes allosteric regulation by the phosphoprotein phospholamban (PLN). The Ca-ATPase is thought to be a target for nitrative stress and is affected by several chronic diseases of the heart.

In the heart, age-based nitration of the Ca-ATPase inhibits Ca^{2+} transport activity but the physical mechanism by which nitration inhibits Ca-ATPase activity is not understood. Conversely, nitroxyl (HNO), a new candidate for drug therapy for congestive heart failure (CHF), improves overall cardiovascular function by increasing Ca-ATPase activity in the heart. However, the physical mechanism for this activation is unknown. Therefore, we have used enzyme kinetics, fluorescence spectroscopy, and EPR spectroscopy studies to determine the effects of $ONOO^-$ and HNO on the Ca-ATPase and the physical regulation of the Ca-ATPase by PLN.

Treatment of Ca-ATPase with a nitrating agent, $ONOO^-$, inhibited Ca-ATPase activity, and the [$ONOO^-$]-dependent inhibition of the Ca-ATPase was more effective in the presence of PLN. $ONOO^-$ did not affect the [Ca^{2+}]-

dependence of Ca-ATPase activity either in the presence or absence of PLN. $ONOO^-$ had no effect on Ca-ATPase rotational mobility or oligomeric interactions, as affected by PLN, but $ONOO^-$ decreased the amplitude of the Ca^{2+}-dependent E2 to E1•Ca_2 conformational change, both in the absence and presence of PLN.

Treatment with HNO had no affect on the [Ca^{2+}]-dependence of Ca-ATPase activity in the absence of PLN; however in the presence of PLN, the [Ca^{2+}]-dependent activity was shifted to lower Ca^{2+} levels and corresponded to the uncoupling of PLN from the Ca-ATPase. HNO decreased Ca-ATPase rotational mobility and increased the Ca-ATPase Ca^{2+}-dependent conformational transition, consistent with uncoupling PLN from the Ca-ATPase.

Taken together, these results suggest that $ONOO^-$ inactivates a fraction of enzyme units to lower overall enzyme activity, whereas HNO uncouples PLN from the Ca-ATPase with increases in Ca-ATPase conformational flexibility and Ca-ATPase activity.

DEDICATION

To my mother

ACKNOWLEDGEMENTS

First, I would like to thank my advisor, Dr. James E. Mahaney without whom this dissertation could not have been completed. He has always had confidence in my abilities, to learn, to write, and most significantly to become a well-rounded scientist. Thank you for teaching me how to think like a scientist, and for always being patient when I just didn't understand or was frustrated with my work. The time, effort, and encouragement have not gone unnoticed.

I would also like to thank my graduate committee, Dr. Peter Kennelly, Dr. Erin Dolan, and Dr. Richard Wyeth. I am extremely grateful for all the advice and the time taken to help me when it was needed. I appreciate the time taken for meetings, presentations, and the patience with all of my questions. Thank you.

I would next like to thank the American Heart Association and all persons responsible for awarding me with a pre-doctoral fellowship (2008-2010) in order to support my studies here at Virginia Tech.

I would like to thank the Mahaney lab, both past and present: Chevon Thorpe, Lesly De Arras, Johnathan Bermudez, Cara Marie Jackson, and Christian Bergman for the long talks, problem solving, and overall fun times in the lab (especially in the cold room while dissecting those hog hearts)!

I would like to thank the faculty and staff members within the department of Biochemistry for their support throughout the past four years.

I would like to thank my friends, for the constant encouragement and support: Leslie Tawiah, Andre' Ellis, Jennifer Lam, and the Reverend Dr. Terrence Walker. Thank you for the support, faith, and reassurance.

Finally, I thank my mother, Pat, my father, Siva, and my sister, Dheepa for their constant love, support, and encouragement. Thank you for always being there and for supporting me through every accomplishment, but most importantly for always believing in me and never giving up on me, through every drawback and/or struggle. Without all of you, I could not have done this. To my sister, thank you for the unwavering support and for always being a helping hand; I am truly lucky to have an older sister that has always put me before herself. Thank you!

TABLE OF CONTENTS

LIST OF FIGURES

Chapter 1: Introduction

Chapter 2: Physical Mechanism of Ca-ATPase Inhibition by Peroxynitrite

Chapter 3: Physical Mechanism of Ca-ATPase Activation by HNO

Chapter 4: Preliminary Investigation of 1-nitrosocyclohexyl acetate as a potential HNO donor, and its role in the physical mechanism of Ca-ATPase stimulation

Appendix A: The Induction of Heat Shock Protein 70 at Specific Hypothermic Intervals in an Isolated and Perfused Rat Heart Model – Implications for Cardiac Transplantation

LIST OF ABBREVIATIONS

2A7-A1	monoclonal antibody against SERCA2a
2D12	monoclonal antibody against phospholamban
Å	angstrom
ATP	adenosine 5'-triphosphate
Ca^{2+}	ionized calcium
CaM	calmodulin
CaM Kinase	calmodulin kinase
CSR	cardiac sarcoplasmic reticulum
DHPR	dihydropyrodine receptor
DMF	dimethyl fomamide
dsDNA	double-stranded DNA
EGTA	ethylene glycol bis(-aminoethyl ether)-*N, N, N', N'*-tetraacetic acid
EP	phosphoenzyme
EPR	electron paramagnetic resonance spectroscopy
FITC	fluorescein isothiocyanate
HCl	hydrochloric acid
HF	High Five insect cells
HNO	nitroxyl
$K_{0.5}$ value	ionized [Ca^{2+}] giving half-maximal activation of the Ca-ATPase
kDa	kilodalton
Mg^{2+}	Magnesium
mM	millimolar
MOPS	3-(*N*-morpholino)propanesulfonic acid
NCX	sodium-calcium exchanger
$ONOO^-$	peroxynitrite
PBS	phosphate buffered saline
PCA	perchloric acid
PCR	polymerase chain reaction

P_i	inorganic phosphate
PKA	protein kinase A
PLN	phospholamban
PMCA	plasma membrane Ca-ATPase
PVDF	polyvinylidene difluoride
RyR	Ryanodine receptor
SDS-PAGE	sodium dodecyl sulfate polyacrylamide gel electrophoresis
SERCA	sarco(endo)plasmic reticulum Ca-ATPase
-SH	thiols
SR	sarcoplasmic reticulum
TnC	troponin C
TnI	troponin I
TnT	troponin T
μM	micromolar
V_{max}	maximum activity
WT	wild type

Chapter 1

Introduction

Cardiac Sarcoplasmic Reticulum

The sarcoplasmic reticulum (SR) is an intracellular membranous system that serves as a reservoir for storing calcium (Ca^{2+}) ions. It serves as the primary source of Ca^{2+} ions involved in excitation-contraction coupling, and thereby in muscle contraction and relaxation. The SR regulates the intracellular Ca^{2+} level. It contains three important components that are required for the regulation of Ca^{2+} levels: 1) The Ca-ATPase (SERCA), which is involved in Ca^{2+} uptake from the cytosol back into the SR lumen; 2) phospholamban (PLN), which regulates Ca^{2+} uptake; 3) and the ryanodine receptor (RyR), which is involved in Ca^{2+} release from the SR lumen into the cytosol (Walker and Spinale, 1999, Bigelow et al., 1986, Mahaney et al., 2003). These components aid in inducing quick changes in intracellular Ca^{2+} concentrations: Ca^{2+} release into the cytoplasm through the RyR promotes muscle contraction, while the accumulated Ca^{2+} is drawn from the cytoplasm by SERCA to promote muscle relaxation (Mintz and Guillain, 1997).

Calcium plays a key role in the regulation of all muscles, including the heart. Muscle fibers are surrounded by the SR. Depolarization leads to a change in membrane potential and then to the opening of the voltage-gated Na^{+} channel and the voltage-gated Ca^{2+} channel. The opening of the voltage-gated Na^{+} channel and the resulting influx of Na^{+} leads to the initial cardiac action potential. The action potential is then maintained by an influx of extracellular Ca^{2+} ions, which enter the cytoplasm through the dihydropyridine receptor (L-

type Ca^{2+} channel, DHPR). The influx of Ca^{2+} through the DHPR stimulates the SR Ca^{2+} release channels (Ryanodine receptors, RyR), which induces a large-scale release of Ca^{2+} ions into the cytosol from the SR, increasing the cytosolic Ca^{2+} levels from resting level of less than 0.1 μM to 5 μM or more (Walker and Spinale, 1999, Meldrum et al., 1996). The RyR is located at the interface between the SR and the T-tubule where the DHPR is located (Zhang et al., 1997)(**Figure 1-1**). The location of the RyR facilitates calcium-induced calcium release (CICR), which is the mechanism by which the RyR releases calcium in cardiac muscle. The DHPR allows Ca^{2+} ions into the cytosol (calcium induction), to which the RyR is sensitive. This activates the RyR for a large-scale release of Ca^{2+} ions into the cytosol (calcium release), which initiates muscle contraction (Endo, 1977).

As Ca^{2+} is released from the SR and its cytosolic concentration increases, the contractile proteins, myosin, actin, tropomyosin, and the troponin complex (contractile apparatus), are activated, triggering muscle contraction. Myosin is the thick filament, and is composed of a filamentous tail and a globular head region. This globular head region contains the actin binding site, as well as the catalytic site for ATP hydrolysis. Actin is the contractile protein found within the thin filament that interacts with the globular head of myosin. When ATP is present, a crossbridge is formed, which leads to a shortening of the sarcomere and thus contraction. Tropomyosin is another protein found in the thin filament and serves to add rigidity to the thin filament by sitting on either side of actin. Its function is to block contraction by not allowing myosin and actin to bind. The troponin complex is composed of three proteins: troponin T (TnT), troponin

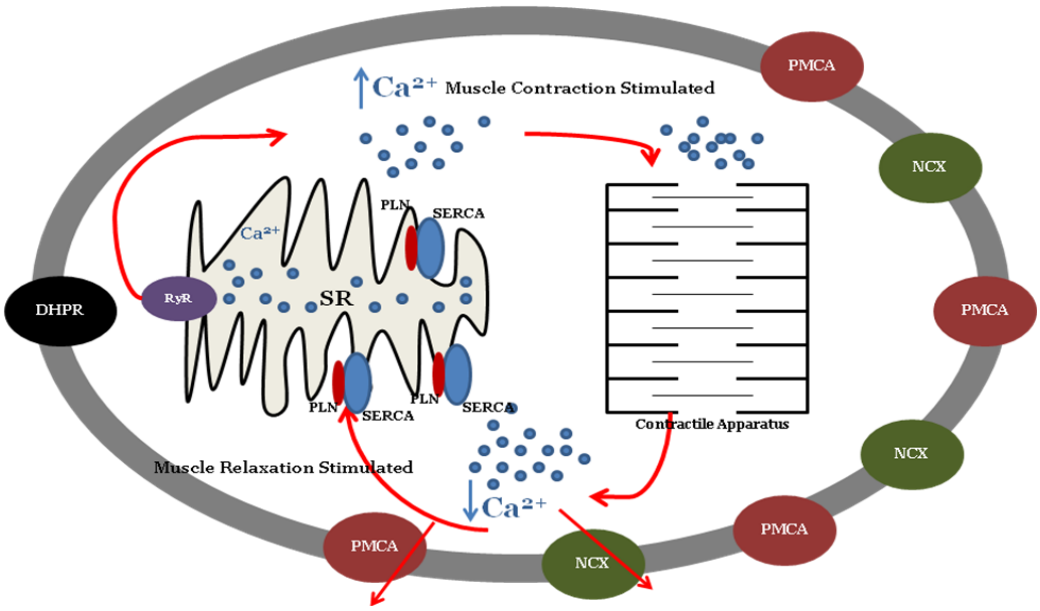

Figure 1-1. Ca^{2+} handling in cardiac myocytes. An action potential leads to an influx of extracellular Ca^{2+} ions through the L-type Ca^{2+} channel (DHPR). The Ca^{2+} ions bind to the Ca^{2+} release channel (RyR) of the sarcoplasmic reticulum (SR), and induce a conformational change within the RyR that allows release of Ca^{2+} from the SR Ca^{2+} store. This process is referred to as Ca^{2+}-induced Ca^{2+}-release (CICR), and it increases the intracellular Ca^{2+} level from < 0.1 μM to 5 μM. Cytoplasmic Ca^{2+} binds then to the troponin complex within the contractile apparatus, stimulating muscle contraction by myosin and actin filaments. When the contraction signal terminates, the RyR closes and the cytoplasmic Ca^{2+} is removed from the cytoplasm. Three mechanisms work to remove Ca^{2+}, the Na^{+}-Ca^{2+} exchanger (NCX), the plasma membrane Ca-ATPase (PMCA), and the sarco(endo)plasmic reticulum Ca-ATPase (SERCA). The majority of Ca^{2+} is removed by SERCA. As the cytoplasmic Ca^{2+} level drops to the resting level of < 0.1 μM, Ca^{2+} dissociates from the troponin complex, halting muscle contraction and allowing the filaments to relax.

C (TnC), and troponin I (TnI). The troponin complex controls the extent of crossbridge formation and contributes to the structural stability of the sarcomere. TnC binds Ca^{2+} ions to produce a conformational change in TnI. TnI binds to actin and holds the troponin-tropomyosin complex in place. When phosphorylated, TnI weakens the affinity of troponin C for calcium. TnT binds to tropomyosin, interlocking them to form a complex between troponin and tropomyosin. The rise in $[Ca^{2+}]$ leads to the binding of Ca^{2+} to TnC. Upon binding, TnC will bind to TnI, so that the troponin-tropomyosin complex binds more tightly to the actin filament and the myosin head can interact with actin more readily. The interaction between myosin and actin activates neighboring actin and TnC sites allowing for increased contraction to occur (Bers, 2008).

To initiate relaxation and terminate contraction, Ca^{2+} levels must be brought back to resting levels, which requires the removal of Ca^{2+} from the cytoplasm. The Ca^{2+} release channels close, stopping Ca^{2+} influx; and Ca^{2+} ions are then pumped out of the cytoplasm following their dissociation from the contractile apparatus. Some of the Ca^{2+} leaves byway of the plasma membrane sodium-calcium exchanger (NCX) and the plasma membrane Ca-ATPase (PMCA); however the majority of the Ca^{2+} ions are transported back into the SR by the sarco(endo)plasmic reticulum Ca-ATPase (SERCA). Due to the high levels of Ca-ATPase present in muscle cells, a single turnover or two of the pump is usually sufficient to decrease cytoplasmic $[Ca^{2+}]$ back to its resting level of less than 0.1 μM, thereby promoting rapid muscle relaxation (Bigelow and Squier, 2006). As the levels of free Ca^{2+} decrease, more Ca^{2+} dissociates from the contractile apparatus allowing the muscle to relax.

There are additional calcium binding proteins, such as calmodulin and calsequestrin, which are also important in muscle relaxation and for moderating the rate of Ca^{2+} uptake. Calmodulin will bind intracellular Ca^{2+}, which in turn activates the PMCA to expel intracellular Ca^{2+}. Calmodulin also binds to the RyR to ensure the channel stays closed (Feher and Fabiato, 1990). Calsequestrin is the main calcium storage protein inside the SR. It binds luminal calcium, lowering the free calcium concentration to prevent precipitation of SR calcium. Calmodulin and calsequestrin facilitate additional calcium uptake by the SR Ca-ATPases (Katz, 1993).

SR function tightly controls the beat-to-beat cardiac cycle. The rate and extent of myocardial relaxation is determined by the rate and extent of Ca^{2+} uptake from the cytoplasm into the SR. The rate and extent of myocardial contraction is determined by the rate and extent of Ca^{2+} release into the cytoplasm (Meldrum et al., 1996). Regulatory agents that affect Ca-ATPase performance, such as phospholamban (PLN, described later), have significant effects on the rate of relaxation of cardiac muscle. Likewise, chemical factors that affect Ca-ATPase performance, such as $ONOO^-$ or HNO (described later); can also exert considerable effects on the rate of cardiac muscle relaxation. The focus of this project is to better understand the mechanisms, by which Ca-ATPase nitration inhibits Ca-ATPase activity, and by which HNO stimulates the Ca-ATPase in terms of the effects of Ca-ATPase function and its regulation by PLN (described further later).

Ca^{2+} Transport: the Sarco(endo)plasmic Reticulum Ca-ATPase

The sarco(endo)plasmic reticulum Ca-ATPase (SERCA, or the Ca^{2+} Pump) is a 110 kDa integral membrane enzyme that promotes muscle relaxation by utilizing ATP as its energy source to sequester Ca^{2+} ions from the muscle cytosol into the SR lumen. The Ca-ATPase belongs to the family of P-type ATPases, a group of cation transporters that form an aspartyl-phosphoryl-enzyme intermediate from ATP during the reaction cycle. The free energy of ATP breakdown is captured by this high energy phosphoprotein to drive a series of conformational changes that translocate ions across the membrane against the normal ion concentration gradient (Kuhlbrandt, 2004, Scarborough, 1999, Pedersen and Carafoli, 1987). The Ca-ATPase translocates two Ca^{2+} ions from the cytoplasm of the cell to the SR lumen per ATP used (Inesi, 1987, Inesi et al., 1980).

There are three isoforms of the Ca-ATPase: fast twitch skeletal muscle (SERCA1), cardiac, slow twitch, and smooth muscles (SERCA2), and a ubiquitous non-muscle form of the enzyme (SERCA3), which serves to transport Ca^{2+} into the endoplasmic reticulum (East, 2000, Martonosi and Pikula, 2003). SERCA1 and SERCA2a share 84% sequence identity (Toyoshima et al., 2000, Toyoshima and Nomura, 2002). SERCA2 is a splice variant where SERCA2a is the cardiac isoform and SERCA2b is the smooth muscle isoform. The focus of this research is the Ca-ATPase of cardiac muscle SR (SERCA2a).

The mechanism of calcium transport by the cardiac Ca-ATPase has been studied in detail (Tada et al., 1980, Sumida et al., 1980, Dode et al., 2003, Mahaney et al., 2005). The most widely accepted model for Ca^{2+} transport is

shown in **Figure 1-2.** The Ca-ATPase can adopt two major conformational states, called "E1" and "E2." E1 is the high affinity state of the enzyme for cytoplasmic Ca^{2+} and ATP, while E2 is the low affinity state for Ca^{2+} because the sites face into the SR. It also has low affinity for ATP and phosphate (P_i). Two Ca^{2+} ions and ATP bind to the E1 state, leading to ATP-dependent phosphorylation, forming E1P, which stimulates a conformational change to the E2 state, E2P. E2P releases the two Ca^{2+} ions back into the SR lumen. Phosphate is then released, shifting the enzyme back to the E2 state, and the enzyme cycle starts again.

The enzyme cycle is reversible and can also lead to ATP synthesis. This can occur if the vesicles are loaded with calcium, and have Mg^{2+}, ADP, and P_i in the absence of a calcium gradient (Chiesi et al., 1984). The Ca-ATPase in the E2 state is phosphorylated by inorganic P_i in the presence of Mg^{2+}. When vesicles are not loaded with calcium, the E2P state is stable. However, if loaded, E2P will bind the calcium, which causes a conformational change to E1P(Ca_2) (de Meis, 1988, Masuda and De Meis, 1973). This allows for ADP binding and the transfer of covalently bound P_i to ADP, forming ATP. ATP dissociates from the enzyme, as do the calcium ions.

SERCA is comprised of a single polypeptide chain that comprises 994 amino acids in length that contains 10 transmembrane α-helices (M1-M10). The pump consists of two major regions, (1) the cytoplasmic region which contains 440 amino acid residues and is more than half the total mass of the protein.

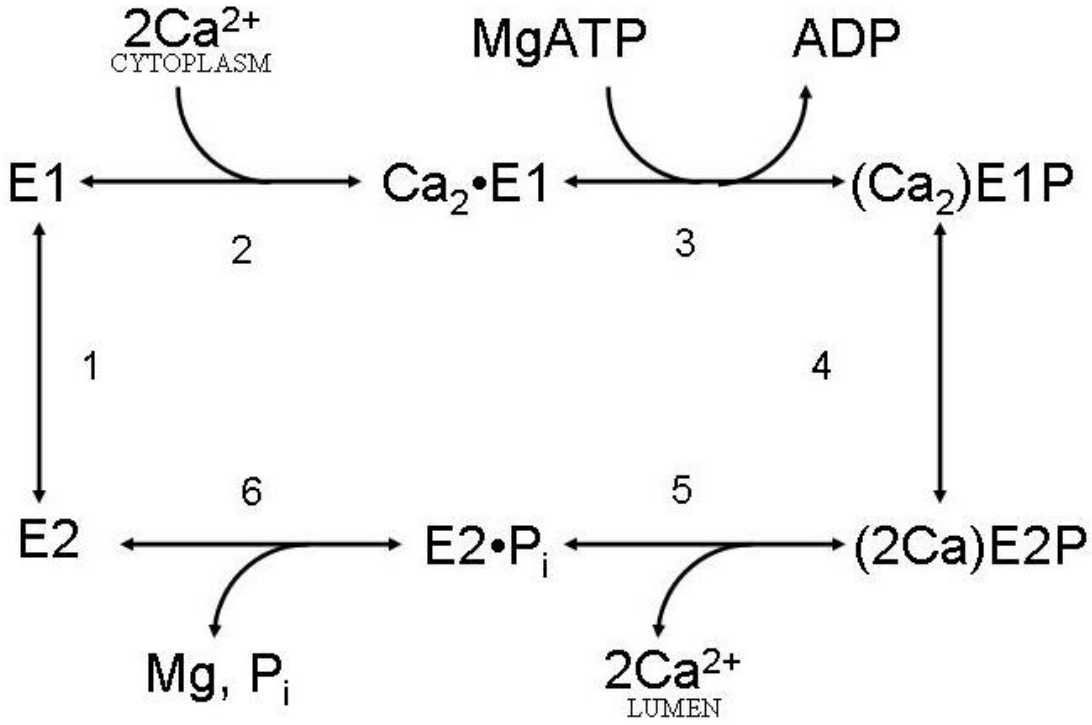

Figure 1-2. Reaction cycle of the Ca-ATPase. In the absence of substrate and ligands, the Ca-ATPase exists in equilibrium between the E2 and E1 conformations, which exhibit low and high affinity for Ca^{2+}, respectively. Two cytoplasmic Ca^{2+} ions bind with high affinity to the E1 conformation of the Ca-ATPase, which activates the enzyme for ATP-dependent phosphorylation at Asp-351, forming a phosphoenzyme intermediate with occluded Ca^{2+} ions. Phosphorylation of the enzyme induces a conformational change that drives the transition from (Ca_2)E1P to (2Ca)E2P that moves the Ca^{2+} ions across the membrane. The E2 intermediate has low affinity for Ca^{2+}, so the two Ca^{2+} ions are then released into the SR lumen. The phosphoenzyme is then hydrolyzed to release inorganic phosphate, forming the E2 state.

The cytoplasmic region contains three distinct domains: the phosphorylation domain (P domain), the actuator domain (A domain), and the nucleotide domain (N domain); (2) the transmembrane region consists of one domain known as the transmembrane domain (M domain), where Ca^{2+} binding occurs. The globular domains that make up the cytoplasmic part of the enzyme are physically distinct, but are composed of amino acids spread throughout the primary sequence. This complex arrangement allows for long range conformational changes and coupling of ATP utilization and ion transport. For example, the P domain is connected to M4 and M5 helices, where M5 actually serves as the backbone of the enzyme extending through the membrane and well into the P and N domains (Toyoshima and Inesi, 2004). The P domain contains the phosphorylation site, Asp-351. The N domain contains the residues involved in nucleotide binding. The N domain, with its insertion point inside the P domain, serves as a bridge between ATP binding and phosphorylation (Toyoshima, 2009). The A domain serves as an actuator for the N domain that aids in conformational flexibility and long range movements between helices during phosphorylation and Ca^{2+} binding. It also regulates Ca^{2+} binding and release, as it is directly connected to M1-M3. The M domain contains the 10 α-helices. The coordinated movements between the cytoplasmic and transmembrane domains facilitate Ca^{2+} transport through the membrane, allowing Ca^{2+} release into the SR.

To date, there are over 20 crystal structures capturing nine different states that cover the entire reaction cycle (Toyoshima and Nomura, 2002, Sørensen et al., 2004, Toyoshima, 2008, Toyoshima and Inesi, 2004, Olesen et al., 2007, Zhang et al., 1998, Obara et al., 2005, Toyoshima et al., 2000, Toyoshima and

Mizutani, 2004, Møller et al., 2005). These structures confirm that the Ca-ATPase undergoes a series of conformational changes as it progresses through its enzyme cycle. For example, **figure 1-3** shows a non-hydrolyzable ATP analogue 2'3'-0-(2,4,6-trinitrophenyl)-adenosine monophosphate (TNP-AMP) bound to the N domain, which is known to occur in the vicinity of Lys-515, Lys-492, and Phe-487 (Toyoshima et al., 2000). Upon binding, domain movements take place so that the N domain, which is 25 Å away from Asp-351, is close enough for the γ-phosphate transfer from ATP onto the Ca-ATPase to take place. The Ca^{2+} transport sites are located in the transmembrane domain and are formed by helices M4, M5, and M6. In the E1 conformation, the Ca^{2+} binding sites are oriented toward the cytoplasm and display high affinity Ca^{2+} binding. In the E2 conformation, the Ca^{2+} binding sites are oriented toward the SR lumen, and the structure changes to one with a low Ca^{2+} affinity to promote Ca^{2+} release into the lumen. Agents that affect these conformational changes may modify Ca-ATPase function.

In the E1 state, the Ca^{2+} binding sites face toward the cytoplasmic side of the lipid bilayer. The two high affinity binding sites were identified by Toyoshima and colleagues (Toyoshima et al., 2000), which were dubbed them site I and site II (MacLennan et al., 1997). Site I is located between M5 and M6 where the side-chain oxygen atoms of residues Asn-768, Glu-771, Thr-799, Asp-800, and Glu-908 contribute to this site and Ca^{2+} binding. Site II is formed by the M4 helix and partial contribution by M6. The main chain carbonyl oxygen atoms of residues Val-304, Ala-305, and Ile-307 contribute to Ca^{2+} binding of site II. These sites

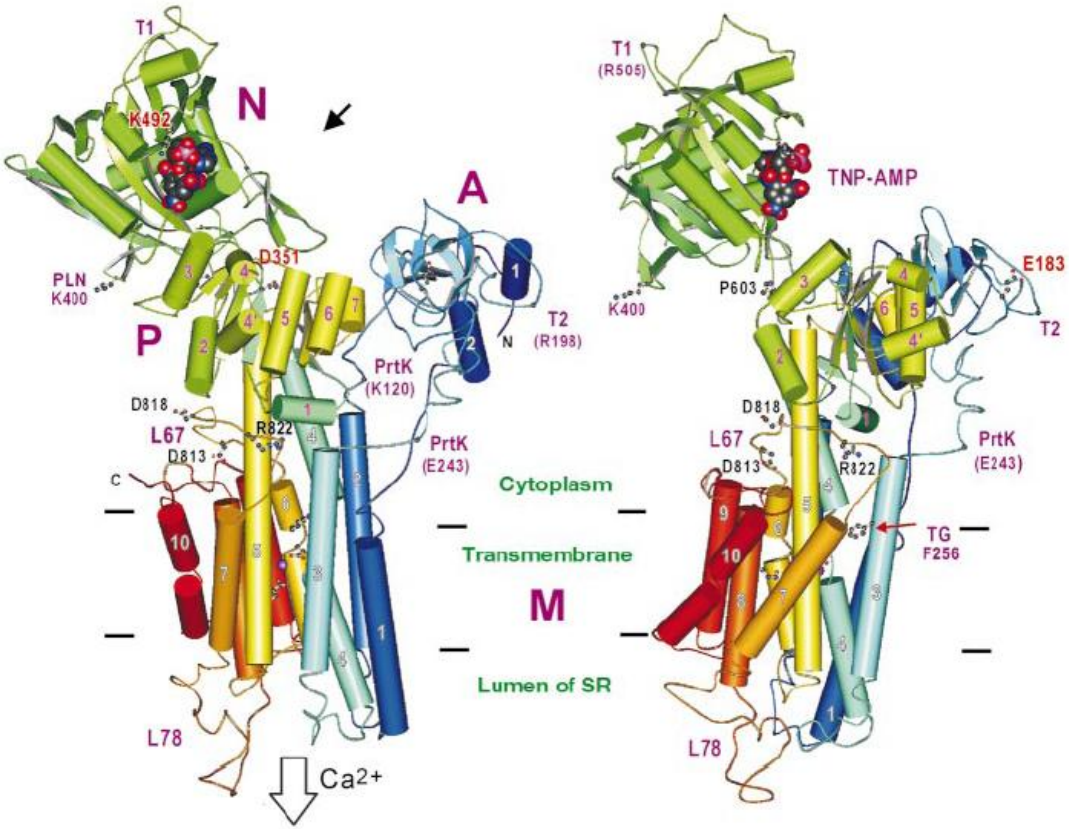

Figure 1-3. 2.6 Å resolution structure of the sarco(endo)plasmic reticulum Ca-ATPase (SERCA1). This figure shows the two major conformational states of SERCA1: the Ca^{2+}-bound E1 form (left) and the Ca^{2+} free E2 form (right). The four major domains are labeled: T, transmembrane; A, actuator, P, phosphorylation; and N, Nucleotide domains. The 10 transmembrane helices are labeled 1-10. Asp-351, where phosphorylation occurs, is labeled D351 in red. Reprinted by permission from Macmillan Magazines Ltd: Nature, (Chikashi Toyoshima and Hiromi Nomura, "Structural Changes in the Calcium Pump Accompanying the Dissociation of Calcium," 418 (605-611)), copyright (2000).

are stabilized by hydrogen-bonding between the residues (Toyoshima et al., 2000, Toyoshima et al., 2003, Inesi et al., 1980).

Ca^{2+} binding occurs in a sequential fashion, where one Ca^{2+} ion must first bind and cause a slight conformational change that exposes the second Ca^{2+} binding site such that the next Ca^{2+} ion can bind (Inesi, 1987). Structurally, the binding of the second Ca^{2+} ion straightens helix M5 (the backbone helix, mentioned above), which moves the P domain into a new position opening up the previously closed structure of the cytoplasmic region **(Figure 1-4)**. This opening allows ATP binding and phosphorylation to occur at Asp-351. Phosphorylation of the enzyme and Ca^{2+} binding to the enzyme shifts the enzyme into its E2 conformation, causing long-range conformational changes to take place in the A domain. Rearrangement of the M1-M6 helices breaks open the Ca^{2+} binding sites, opening the sites to the luminal side of the protein and releasing the Ca^{2+} into the SR lumen (Toyoshima et al., 2007). P_i is then released and the cycle repeats itself.

Ca-ATPase Regulation:

The Ca-ATPase is reversibly regulated by the small 52 amino acid integral membrane phosphoprotein phospholamban (PLN), which is an α- helical structure **(Figure 1-5)**. It regulates the Ca-ATPase in cardiac, slow twitch and smooth muscles. It serves as a modulator of cardiac contractility (MacLennan and Kranias, 2003, Koss and Kranias, 1996). The physical mechanism by which PLN regulates the Ca-ATPase has been studied extensively (Voss et al., 1994, Mahaney et al., 2000a, Kimura et al., 1997, Kimura et al., 1996). In its

dephosphorylated state, PLN acts as an allosteric inhibitor of the Ca-ATPase to decrease enzyme Ca^{2+} sensitivity ($k_{0.5}$) without affecting the maximum activity (V_{max}). When PLN is phosphorylated, inhibition is relieved (Autry and Jones, 1997).

PLN is predicted to contain three domains (Simmerman and Jones, 1998). Domain Ia is highly charged and helical in nature, containing amino acids 1-20 and the sites of regulatory phosphorylation by the cAMP-dependent protein kinase (PKA), at Ser-16, and Ca^{2+}/camodulin-dependent protein kinase II (CaM kinase II), at Thr-17 (Brittsan and Kranias, 2000, MacLennan and Kranias, 2003, Koss and Kranias, 1996). Domain Ib is polar and contains a β-hairpin structure. It contains residues 21-30. It contains a high percentage of Asn and Gln residues. Domain II is hydrophobic, neutral, and helical in structure. It forms transmembrane portion of the protein, and contains residues 31-52 (Simmerman and Jones, 1998).

Monomers of PLN (MW 6 kDa) spontaneously associate to form a homo-pentamer (MW 30 kDa). While these two forms are in equilibrium in the SR membrane, it is the monomeric form of PLN that binds to and regulates the Ca-ATPase (Cornea et al., 1997), as shown in **Figure 1-6**. It has been demonstrated that pentameric PLN is held together by a series of leucine-isoleucine motifs (Cornea et al., 2000, Simmerman et al., 1996). Cross-linking and mutagenesis studies have been used to identify the specific contact interactions between the transmembrane and cytosolic sequences between PLN and the Ca-ATPase. These

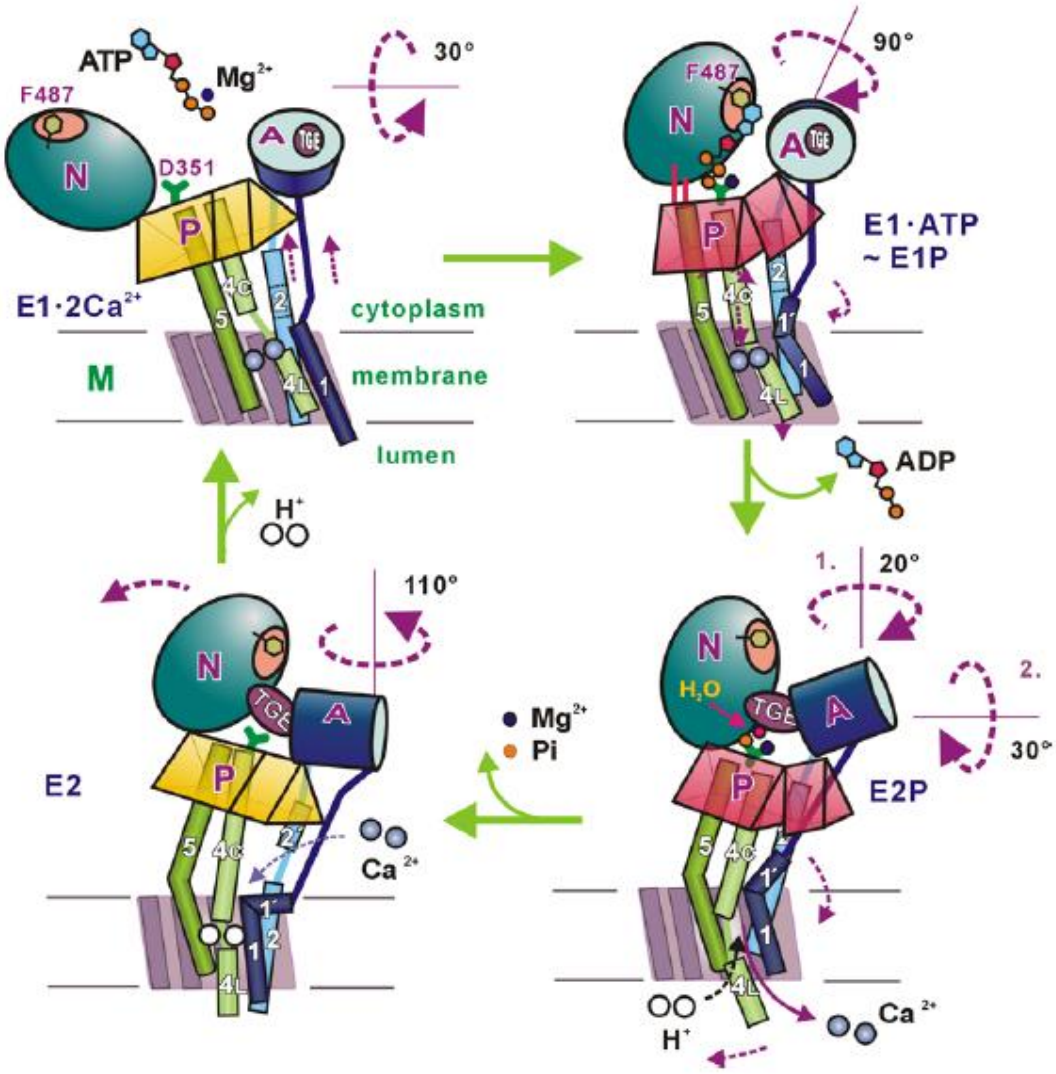

Figure 1-4. Illustration of the structural changes the Ca-ATPase undergoes during its reaction cycle. Structural changes illustrating the different transition states the Ca-ATPase undergoes during its reaction cycle. Reprinted from Archives of Biochemistry and Biophysics (Chikashi Toyoshima, "Structural Aspects of Ion Pumping by Ca^{2+}-ATPase of Sarcoplasmic Reticulum", 476:1 (3-11), copyright (2008)), with permission from Elsevier.

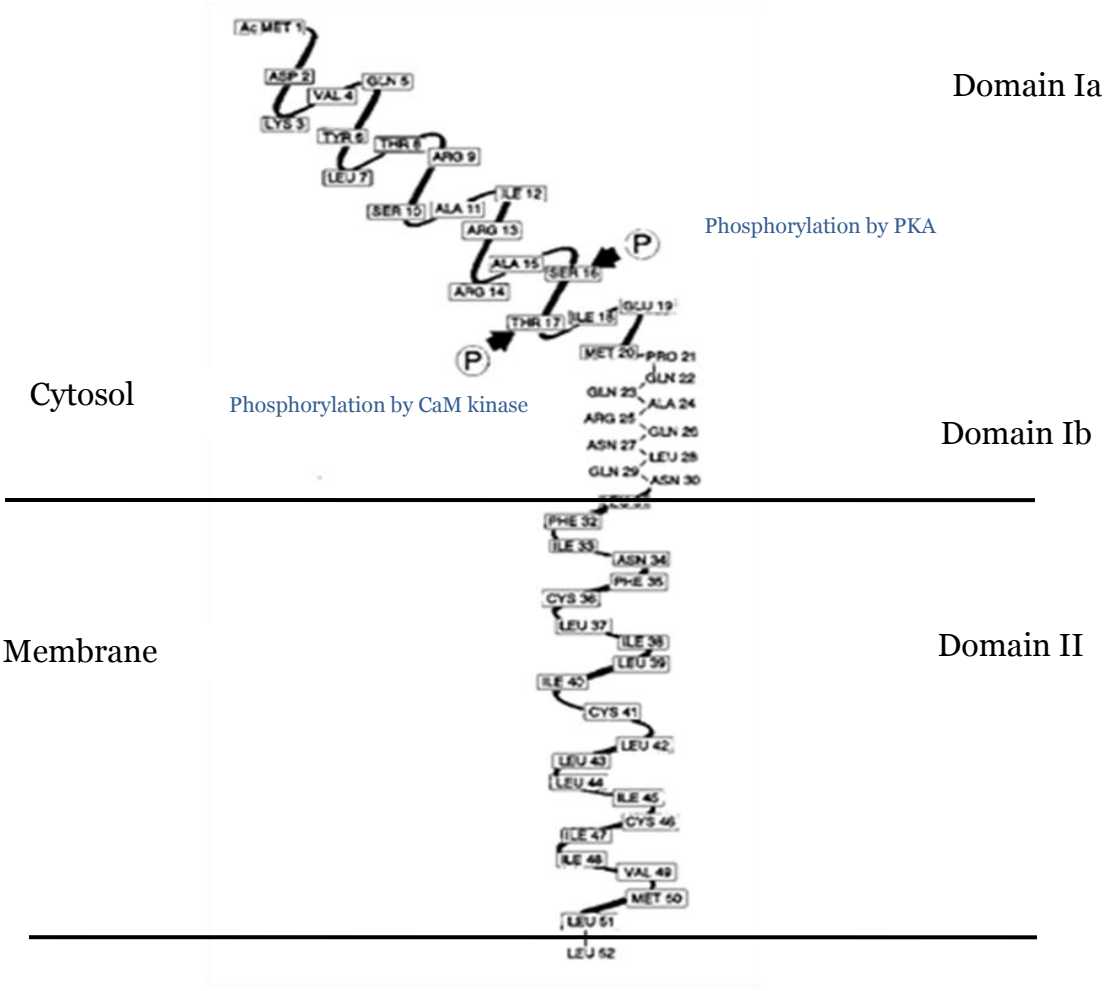

Figure 1-5. Structural model of phospholamban (PLN). PLN consists of two helical portions connected by a less structured hinge region. Amino acids 1-20 (domain Ia) are cytoplasmic and contain the phosphorylation sites for protein kinase A (PKA) at Ser-16 and Ca^{2+}/calmodulin kinase (CaM Kinase) at Thr-17. Amino acids 21-30 (domain Ib) contain several Asn and Gln residues. Amino acids 31-52 (domain II) form a transmembrane helix.

studies reveal that residues in both the cytoplasmic and transmembrane portions of PLN interact directly with the Ca-ATPase. It is suggested that PLN assumes an extended arrangement when coupled to the Ca-ATPase (**Figure 1-6 and 1-7)** (Li et al., 2003, Lamberth et al., 2000, Toyoshima et al., 2003, James et al., 1989, Kimura et al., 1997, Pollesello and Annila, 2002).

PLN stabilizes the Ca-ATPase in the E2 conformational state **(Figure 1-7),** and inhibits the Ca^{2+}-dependent conformational transitions (steps 1 and 2, **Figure 1-3**) that promote the cooperative Ca^{2+} binding and activate ATP-dependent phosphorylation (Mahaney et al., 2005, Waggoner et al., 2007). Consequently, PLN decreases the Ca^{2+} sensitivity of the Ca-ATPase (increases $k_{0.5}$ for Ca^{2+}), which causes the enzyme to operate at approximately half its normal maximal activity during the peak of cytosolic Ca^{2+}concentrations (**Figure 1-8**). The sigmoidal nature of the [Ca^{2+}]-dependent activity is characterized in terms of maximal activity (V_{max}) and the Ca^{2+} concentration that induces half maximal ATPase activity ($K_{0.5}$). As mentioned earlier, in its dephosphorylated state PLN inhibits Ca-ATPase activity, by decreasing the Ca-ATPase apparent affinity for Ca^{2+}, which manifests as a right-shift of the curve and a shift of $K_{0.5}$ to higher levels of Ca^{2+}.

Inhibition is relieved by phosphorylation of PLN at Ser-16, which restores the Ca-ATPase to operate at full activity. Phosphorylation of Ser-16 follows activation of protein kinase A (PKA) by the ß-adrenergic receptor pathway. Phosphorylation of threonine-17, which also relieves inhibition, is catalyzed by a Ca^{2+}-dependent calmodulin (CaM)-dependent protein kinase. Mutagenic studies show that phosphorylation of PLN at Ser-16 disrupts the “L-shaped” structure of

monomeric PLN (Metcalfe et al., 2005). Experimentally, we can use the monoclonal antibody, 2D12, against PLN to relieve inhibition of the Ca-ATPase that mimics the effect of phosphorylation (Autry and Jones, 1998, Autry and Jones, 1997). Over-regulation of the Ca-ATPase by PLN has been shown to be a causative factor for heart disease (Frank et al., 2003, MacLennan and Kranias, 2003, Haghighi et al., 2001, Schmidt et al., 2001), which in combination with age-based or disease-based loss of Ca-ATPase function due to Ca-ATPase oxidation may represent a challenge for muscle relaxation to take place.

Oxidation

Living Organisms and the proteins within them are constantly exposed to reactive oxygen/nitrogen species (ROS/RNS). These oxidants are produced as a normal byproduct of aerobic metabolism (Sies, 1997) and are known to participate in several harmful reactions (Allen, 1998, Allen and Tresini, 2000). They are produced by multiple enzymes that use molecular oxygen (O_2) as a substrate to directly generate free radicals, such as superoxide ($O_2^{\bullet -}$). By definition, free radicals are any atom or molecule that has at least one unpaired electron in its outer-most shell. This is a highly reactive unpaired electron. They are produced intracellularly, but can also be derived from outside sources, being taken up directly by cells (Martindale and Holbrook, 2002). Free radical reactions have been studied extensively and have been found to influence biochemical reactions that can cause direct changes to cells during aging and differentiation (Allen, 1998, Allen and Balin, 1989, Allen and Tresini, 2000). There are several mechanisms involving the oxidation of proteins that have been

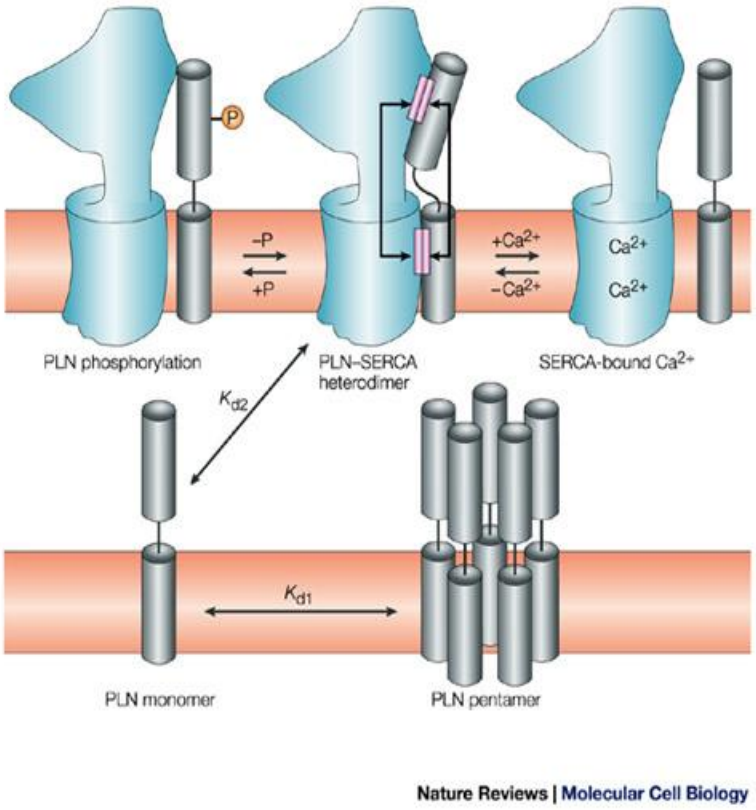

Figure 1-6. Monomeric and pentameric forms of PLN. PLN, in its monomeric state, binds to and regulates the Ca-ATPase through specific contact interactions. Association of PLN with Ca-ATPase is thought to be strongest for the Ca^{2+}-free E2 intermediate. Phosphorylation of PLN alters the structure of its cytoplasmic domain, reducing its affinity for Ca-ATPase, resulting in increased Ca-ATPase activity. Likewise, high Ca^{2+} levels stimulate the E1 form of the enzyme which is less susceptible to PLN regulation. Free PLN monomers self assemble into homopentamers, which are thought to be an inactive storage form of PLN. Reprinted by permission from Macmillan Publishers Ltd: Nature (David H. MacLennan and Evangelina Kranias, "Phospholamban: A Crucial Regulator of Cardiac Contractility", 4:7 (566-577)) copyright (2003).

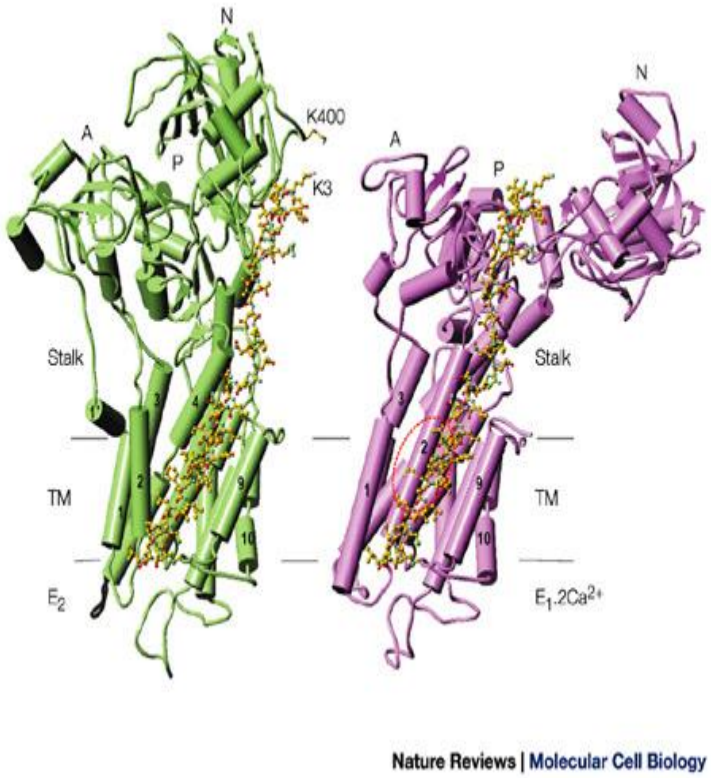

Figure 1-7. PLN assumes an extended arrangement when coupled to the Ca-ATPase. PLN binds to a major groove in Ca-ATPase that is most prominent when the enzyme is in the E2 state, and nearly non-existant for the enzyme in the E1 intermediate form. Nearly every residue in PLN interacts with the Ca-ATPase, contributing to regulation of the Ca-ATPase. Reprinted by permission from Macmillan Publishers Ltd: Nature (David H. MacLennan and Evangelina Kranias, "Phospholamban: A Crucial Regulator of Cardiac Contractility", 4:7 (566-577)) copyright (2003).

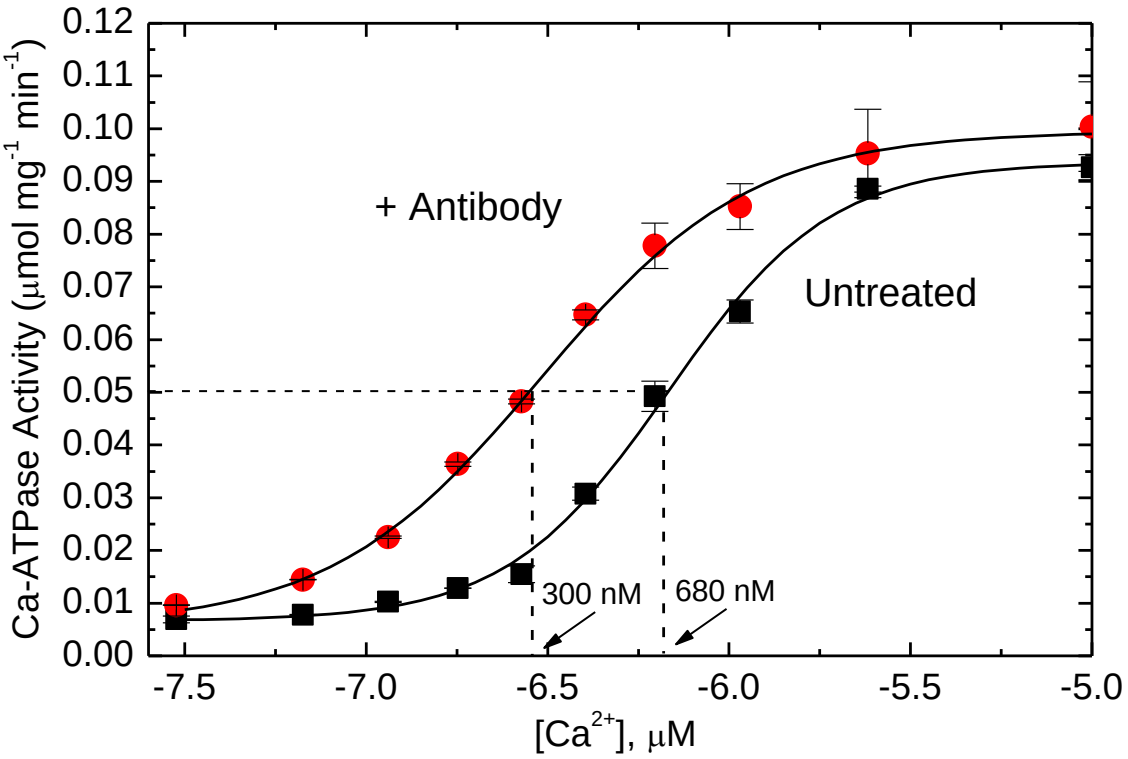

Figure 1-8. PLN decreases the effective Ca^{2+} affinity of Ca-ATPase. PLN binding to Ca-ATPase decreases the Ca^{2+}-sensitivity of the Ca-ATPase, resulting in a rightward shift in the $[Ca^{2+}]$-dependent ATPase activity profile. Because of this, in the presence of PLN, Ca-ATPase operates at about half its normal activity at most Ca^{2+} levels. Phosphorylation of PLN relieves its inhibitory influence, increasing Ca-ATPase Ca^{2+} sensitivity resulting in a leftward shift in the $[Ca^{2+}]$-dependent ATPase activity profile. Expermimentally, the effects of PLN phosphorylation can be mimicked using an anti-PLN monoclonal antibody, 2D12, that binds to and uncouples PLN from Ca-ATPase (Autry and Jones, 1997; Mahaney et al., 2000).

elucidated through several studies in which protein, peptides, and amino acids were exposed to ionizing radiation (Garrison, 1987, Garrison et al., 1962, Garrison and Weeds, 1962). These results suggested that radical-mediated oxidation of proteins leads to fragmentation of the polypeptide chain, oxidation of amino acid side chains, and generation of protein-protein cross linkages (Stadtman, 2006). In biological systems, oxygen-containing free radicals are generally the most common, in particular $O_2^{\bullet-}$, nitric oxide (NO), and the hydroxyl radical ($OH^{\bullet-}$). NO is a relatively unreactive free radical. However, in the presence of $O_2^{\bullet-}$, it forms peroxynitrite ($ONOO^-$), a species that reacts directly with amino acid side chains in proteins. The Ca-ATPase, for instance, is susceptible to oxidative damage from $ONOO^-$.

The SR, and therefore Ca-ATPase, is located contiguous to the mitochondria, which is described as "the cell's powerhouse" because of its ATP producing activities through the electron transport chain. Mitochondria are found in large quantities in cells that are the most metabolically active, such as neuron or muscle cells. The electron transport chain (ETC) couples the reactions of an electron donor to an electron acceptor, so that H^+ ions can be translocated across a membrane during aerobic respiration, producing ATP. The ETC is found in the inner mitochondrial membrane and is seen to be "leaky;" where these side reactions are considered to be toxic. ROS production occurs at two points in the ETC, at complex I (NADH dehydrogenase) and at complex III (ubiquinone-cytochrome c reductase). Electrons transferred to coenzyme Q, which subsequently leads to two sequential reductions and the production of the unstable intermediate $^{\bullet}Q^-$, can lead to $O_2^{\bullet-}$ production. In addition, the outer

mitochondrial membrane enzyme monoamine oxidase (MAO) catalyzes the deamination of the biogenic amines and also produces H_2O_2, which can lead to $O_2^{\bullet-}$ formation and the hydroxyl radical ($OH^{\bullet-}$) formation. The mitochondria converts about 1-2% of the oxygen molecules consumed into $O_2^{\bullet-}$ (Finkel and Holbrook, 2000, Boveris and Chance, 1973).

ROS/RNS can initiate degradative processes; although they are not always harmful. Mild amounts of oxidative damage, such as typically occurs during exercise, can serve as a stimulus for beneficial physiological reactions, such as mitochondrial biogenesis (Cadenas and Davies, 2000). In large amounts, however, ROS/RNS are toxic to the cellular environment leading to cell damage and loss of function. ROS/RNS also increase as we age; this underlies the central dogma of "The Free Radical Theory of Aging". In 1956 (Harman, 1956), it was suggested that free radicals that were produced during aerobic respiration cause cumulative oxidative damage, which later results in aging and death. The theory was extended in the 1970s to include mitochondrial production of ROS (Cadenas and Davies, 2000, Harman, 1956, Beckman and Ames, 1998, Harman, 1980). Cellular activities are subject to oxidative damage and stress and can be seen as a biomarker of aging (Sohal et al., 2002). In support of this theory, numerous signs of oxidative damage have been observed in the aged heart. This is not to say that all oxidation of proteins is necessarily toxic; harnessing the use of an oxidant can actually be useful as part of a pharmaceutical therapy, which will be described in a later section.

Free radical damage can be counteracted by an intricate antioxidant defense system. Within this system, $O_2^{\bullet-}$ can be converted to H_2O_2, and H_2O_2 can

be converted to water by a series of antioxidant enzymes, superoxide dismutase (SOD), catalase, and glutathione peroxidase. Antioxidants can also be taken in through diet. An antioxidant is a substance that, when in present in lower concentrations as compared to an oxidizable substrate works to delay the oxidation of a particular substrate by reacting with and scavenging radical species (Halliwell, 2007); this in turn slows the process of aging by preventing free radicals from oxidizing molecules. There is a parallel increase in the activity of SOD (Lammi-Keefe et al., 1984) and glutathione peroxidase (Yang et al., 2006) which may be a response to an increase in the cell's oxidative stress (Muscari et al., 1996). Oxidative stress can also occur due to the influence of environmental stimuli including ultra-violet light or chemotherapeutic agents, which can then perturb the normal redox balance. A fine balance between the production of free radicals and the antioxidant system exists and determines the degree of oxidative stress.

Nitrotyrosine Formation on the Ca-ATPase

During aging, Ca-ATPase oxidation occurs via the NO–mediated free radical, peroxynitrite ($ONOO^-$). The Ca-ATPase of cardiac muscle is subject to tyrosine nitration, forming 3-nitrotyrosine. Peroxynitrite, the product of the chemical reaction between NO and $O_2^{\bullet-}$, is the most-likely nitrating agent (Viner et al., 1999a). For the skeletal muscle Ca-ATPase (SERCA1), modification of several cysteine residues (Cys-344, Cys-349, Cys-476, Cys-498, Cys-525, and Cys-614) by $ONOO^-$ leads to enzyme inactivation (Viner et al., 1999b). At even higher concentrations of $ONOO^-$, Cys-636, Cys-670, and Cys-675 were also modified

(Viner et al., 1999b). In contrast, for the cardiac muscle (SERCA2a), $ONOO^-$ primarily targets tyrosine residues (Knyushko et al., 2005).

Knyushko and colleagues (2005) found that in young adult rats (6 month-old), approximately one molar equivalent of nitrotyrosine is distributed over five tyrosine residues, with minimal effects on Ca-ATPase activity. In senescent rats (24 month-old), this ratio increased to 3.5 molar equivalents per mole of Ca-ATPase. Nitrotyrosine formation occurs at three specific sites (Tyr-294, Tyr-295, and Tyr-753) as can be seen in **Figure 1-9**. Studies in cardiac SR vesicles isolated from young rat heart titrated with peroxynitrite in vitro corroborated the in vivo results: $ONOO^-$ treatment induced nitration preferentially at Tyr-294 and Tyr-295, with concurrent inhibition of enzyme activity by about 40% (Knyushko et al., 2005). Tyr-294 and Tyr-295 are conserved residues in SERCA1 and SERCA2a, which share 18 out of 24 tyrosine residues (Viner et al., 1999b). Tyr-294 and Tyr-295 are located near the Ca^{2+} binding and release sites which; so these tyrosine residues may be important for the change from the E1 to E2 conformation. Also Tyr-753 is located between the Ca^{2+} binding sites and the phosphorylation site, Asp-351, suggesting it may also have some functional relevance to these conformational transitions **(Figure 1-9)** (Smallwood et al., 2003, Zhang et al., 2003, Souza et al., 1999).

The physical mechanism by which nitration decreases Ca-ATPase activity is still not understood. Therefore, we have combined biochemical kinetics and

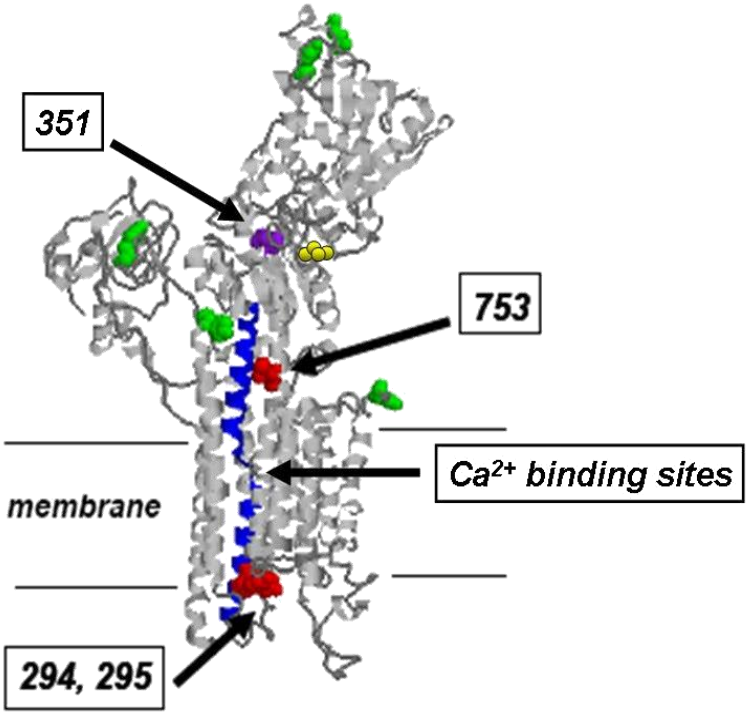

Figure 1-9. Ca-ATPase tyrosine residues nitrated specifically during aging. Age-based nitration at tyrosine residues 294, 295 and 753 (red) may induce structural changes in the vicinity of the Ca^{2+} binding sites and the phosphorylation domain (D-351) thus inhibiting Ca-ATPase activity. Reprinted with permission from Biochemistry (Knuyshko et al. "3-Nitrotyrosine Modification of SERCA2a in the Aging Heart: A Distinct Signature of the Cellular Redox Environment", 44:39 (13071-13081), copyright (2005), American Chemical Society.

biophysical spectroscopy experiments to determine how Ca-ATPase nitration leads to a loss of Ca^{2+} transport activity.

Oxidation of Phospholamban

Congestive heart failure (CHF) is the leading cause of human morbidity and mortality (Schmitt et al., 2003), and may soon surpass infectious disease as the major cause of death worldwide (Benjamin and Schneider, 2005). CHF is a life-threatening disorder characterized by a heart that progressively loses the ability to pump blood to the body. During early onset of the disease, cardiac remodeling allows the heart to compensate for pathological changes. Later, the heart loses the ability to compensate, leading to failure. Due to decreased blood flow, many organs do not receive sufficient oxygen and nutrients, which damages them as well. Heart failure affects both phases of the heart beat: systole (i.e., the contraction phase: excitation, Ca^{2+} release, myofilament activation) performance is depressed and diastole (i.e., the relaxation phase: Ca^{2+} removal from the sarcoplasm) is dysfunctional, resulting in abnormal Ca^{2+} cycling and disrupted Ca^{2+} homeostasis. Despite being a very complicated condition, CHF has been studied in detail in humans and in animal models, and many of the genes, proteins, signaling pathways, and factors involved in CHF have been identified and studied (Benjamin and Schneider, 2005). Likewise, considerable effort is being directed to finding, developing and testing new strategies, drugs and therapies for CHF patients to help them live longer and healthier lives. A prime example is the class of drugs known as nitroxyl donors. Nitroxyl (HNO), the one electron reduction product of nitric oxide (NO) and has properties and activities

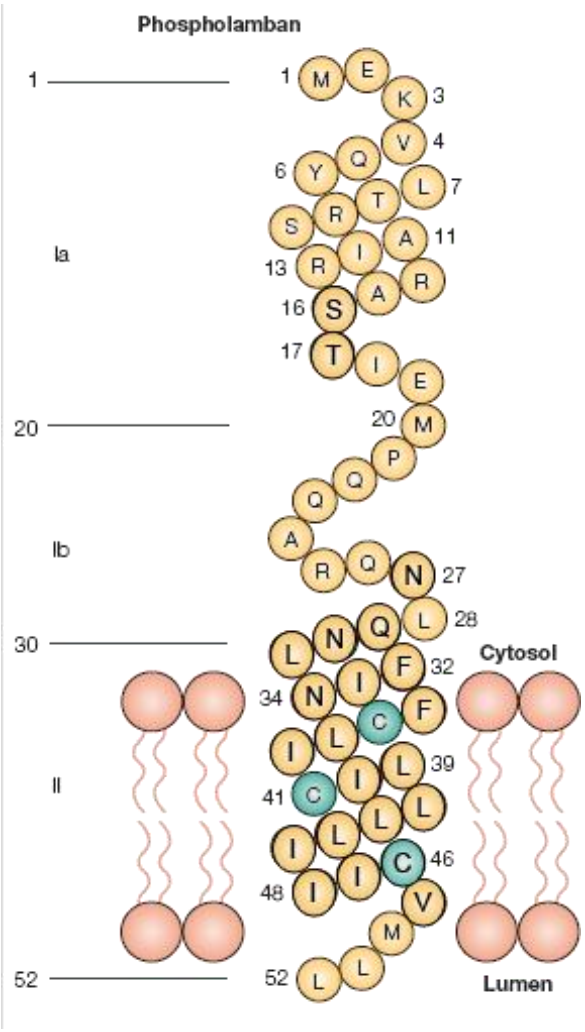

Figure 1-10. Molecular model of PLN highlighting the 3 proximal cysteine residues at 36, 41, and 46. HNO is a potent thiol oxidant that may modify one or more of the three PLN cysteine residues (Froehclich et al., 2008). HNO-dependent perturbation of PLN transmembrane structure could uncouple PLN from the Ca-ATPase, thereby relieving inhibition of the Ca-ATPase. Adapted by permission from Macmillan Publishers Ltd: Nature (David H. MacLennan and Evangelina Kranias, "Phospholamban: A Crucial Regulator of Cardiac Contractility", 4:7 (566-577)) copyright (2003).

that are clearly distinct from NO (Paolocci et al., 2007). In recent years, nitroxyl donors have been shown to stimulate both systolic (Dai et al., 2007) and diastolic (Tocchetti et al., 2007) function in failing hearts, making it truly unique among the many other CHF treatments available (Solaro, 2007). However, the mechanisms by which HNO stimulates cardiac function remain largely unknown. It is important, therefore, study of the effect of HNO on the key proteins of cardiac contraction and relaxation, in order to promote progress in evaluating HNO donors as therapeutic agents for the prevention and/or treatment of CHF. The goal of this project is to determine the effects of HNO on the function of the SR Ca-ATPase, which is the major agent controlling Ca^{2+} uptake to drive cardiac relaxation during diastole, and PLN, the endogenous regulatory agent controlling Ca-ATPase activity. Ca^{2+} transport activity by the Ca-ATPase declines during CHF, partly due to over-regulation of the enzyme by PLN (Schmidt et al., 2001). We propose that HNO stimulates Ca-ATPase, at least in part, by relieving the inhibitory influence of PLN on the enzyme **(Figure 1-10)**.

Overview of Dissertation Research

The link between protein oxidation and pathophysiological conditions within the heart is well established. A key step in understanding how these conditions affect the heart is to understand on a molecular level how age-based oxidation affects individual proteins. The Ca-ATPase is one such protein, along with its regulation by PLN. With CHF on the rise and increasing worldwide, it is important to test new drug candidates which may have improved pharmaceutical properties for cardiac function. In both cases, the Ca-ATPase and its regulation

by PLN represent important “players” in cardiac function that are affected by each process. Therefore, the goal of this dissertation research was to elucidate the physical mechanism of Ca-ATPase inhibition by $ONOO^-$ nitration and, separately, the physical mechanism of Ca-ATPase stimulation by HNO oxidation of PLN.

For the nitration of the Ca-ATPase, we tested the hypothesis that nitration inhibits Ca^{2+} release and phosphoenzyme hydrolysis (step 5 and 6, **Figure 1-2**). This was accomplished using enzyme kinetic assays to test the effect of $ONOO^-$ on [Ca^{2+}]-dependent Ca^{2+} sensitivity of the Ca-ATPase and also tested individual steps 5 and 6 of the reaction cycle and their regulation by PLN. We also used electron paramagnetic resonance (EPR) spectroscopy to test the effect of $ONOO^-$ on protein-protein and protein-lipid interactions involving the Ca-ATPase and its regulation by PLN, as well as fluorescence spectroscopy to test the effect of $ONOO^-$ on Ca-ATPase conformational transitions and their regulation by PLN. For oxidation of PLN by HNO, we tested the hypothesis that HNO physically modifies PLN, in a manner that functionally uncouples PLN from the Ca-ATPase, thereby increasing Ca-ATPase enzyme activity. This was accomplished using the same kinetic and spectroscopic techniques as listed above. For this work, the baculovirus-insect cell expression system was utilized to produce samples containing the cardiac isoform of the Ca-ATPase expressed both in the absence or presence of PLN.

Aim 1: Determine the effect of $ONOO^-$ and HNO on Ca-ATPase activity and its regulation by PLN. We have measured ATPase activity and Ca^{2+} uptake activity of Ca-ATPase in the absence and presence of PLN, following

treatment with $ONOO^-$ and HNO. Dose-dependent studies were conducted first to find the optimal [$ONOO^-$] and [HNO] for Ca-ATPase inhibition and activation, as influenced by PLN, followed by [Ca^{2+}]-dependent activity assays to determine $ONOO^-$ and HNO effects on the function and regulation of Ca-ATPase by PLN.

Aim 2: Determine the effect of $ONOO^-$ and HNO on Ca-ATPase protein-protein interactions and its regulation by PLN. We have used conventional and saturation-transfer electron paramagnetic resonance spectroscopy of the Ca-ATPase covalently labeled with a maleimide spin label (MSL) to determine the effect of $ONOO^-$ and HNO on Ca-ATPase rotational mobility, as affected by PLN. We have used samples identical to those in Aim 1, to facilitate direct correlation of the kinetic and spectroscopic results.

Aim 3: Determine the effect of $ONOO^-$ and HNO on Ca-ATPase [Ca^{2+}]-dependent E2 to E1•Ca_2 conformational change. We have used fluorescence spectroscopy of the Ca-ATPase to determine the effect of $ONOO^-$ and HNO on [Ca^{2+}]-dependent Ca-ATPase conformational changes, as affected by PLN. We have used samples identical to those in Aim 1 to facilitate direct correlation of the kinetic and spectroscopic results.

Summary: Characterizing the effects of $ONOO^-$ on Ca^{2+} transport is an essential step in understanding the mechanism by which Ca-ATPase nitration of the cardiac Ca-ATPase leads to inhibition of Ca^{2+} uptake, and to determine the role, if any, of Ca-ATPase nitration in age-based loss of Ca^{2+} transport. Also, in order to

understand how the effects of HNO on Ca^{2+} transport leads to an increase in enzyme activity is essential to understanding how HNO may be used as a potential pharmaceutical therapy for congestive heart failure.

REFERENCES

ALLEN, R. G. 1998. Oxidative Stress and Superoxide Dismutase in Development, Aging, and Gene Regulation. *AGE,* 21**,** 47-76.

ALLEN, R. G. & BALIN, A. K. 1989. Oxidative Influence on Development and Differentiation: An Overview of a Free Radical Theory of Development. *Free Radical Biology and Medicine,* 6**,** 631-661.

ALLEN, R. G. & TRESINI, M. 2000. Oxidative Stress and Gene Regulation. *Free Radical Biology and Medicine,* 28**,** 463-499.

AUTRY, J. M. & JONES, L. R. 1997. Functional Co-Expression of the Canine Cardiac Ca2+ Pump and Phospholamban in Spodoptera frugiperda (Sf21) Cells Reveals New Insights on ATPase Regulation. *J. Biol. Chem.,* 272**,** 15872-15880.

AUTRY, J. M. & JONES, L. R. 1998. High-Level Co-expression of the Canine Cardiac Calcium Pump and Phospholamban in Sf21 Insect Cells. *Annals of the New York Academy of Sciences,* 853**,** 92-102.

BECKMAN, K. B. & AMES, B. N. 1998. The Free Radical Theory of Aging Matures. *Physiol. Rev.,* 78**,** 547-581.

BENJAMIN, I. J. & SCHNEIDER, M. D. 2005. Learning From Failure: Congestive Heart Failure in the Postgenomic Age. *the Journal of Clinical Investigation,* 115**,** 495-499.

BERS, D. M. 2002. Cardiac Excitation-Contraction Coupling. *Nature,* 415**,** 198-205.

BERS, D. M. 2008. Calcium Cycling and Signaling in Cardiac Myocytes. *Annual Review of Physiology,* 70**,** 23-49.

BIGELOW, D. J. & SQUIER, T. C. 2006. Coil-to-Helix Transition within Phospholamban Underlies Release of Ca-ATPase Inhibiton in Response to B-Adrenergic Signaling *Current Enzyme Inhibition,* 2**,** 19-27.

BOVERIS, A. & CHANCE, B. 1973. The Mitochondrial Generation of Hydrogen Peroxide. General Properties and Effect of Hyperbaric Oxygen. *Biochem. J,* 134**,** 707-716.

BRITTSAN, A. G. & KRANIAS, E. G. 2000. Phospholamban and Cardiac Contractile Function. *Journal of Molecular and Cellular Cardiology,* 32**,** 2131-2139.

CADENAS, E. & DAVIES, K. J. A. 2000. Mitochondrial Free Radical Generation, Oxidative Stress, and Aging. *Free Radical Biology and Medicine,* 29**,** 222-230.

CHIESI, M., ZURINI, M. & CARAFOLI, E. 1984. ATP Synthesis Catalyzed by the Purified Erythrocyte Ca-ATPase in the Absence of Calcium Gradients. *Biochemistry,* 23**,** 2595-2600.

CORNEA, R. L., AUTRY, J. M., CHEN, Z. & JONES, L. R. 2000. Reexamination of the Role of the Leucine/Isoleucine Zipper Residues of Phospholamban in Inhibition of the Ca2+ Pump of Cardiac Sarcoplasmic Reticulum. *The Journal of Biological Chemistry,* 275**,** 41487-41494.

CORNEA, R. L., JONES, L. R., AUTRY, J. M. & THOMAS, D. D. 1997. Mutation and Phosphorylation Change the Oligomeric Structure of Phospholamban in Lipid Bilayers. *Biochemistry,* 36**,** 2960-2967.

DAI, T., TIAN, Y., TOCCHETTI, C. G., KATORI, T., MURPHY, A. M., KASS, D. A., PAOLOCCI, N. & GAO, W. D. 2007. Nitroxyl Increases Force Development in Rat Cardiac Muscle. *The Journal of Physiology,* 580**,** 951-960.

DE MEIS, L. 1988. [13] Approaches to Studying the Mechanism of ATP Synthesis in Sarcoplasmic Reticulum. *In:* SIDNEY FLEISCHER, B. F. (ed.) *Methods in Enzymology*. Academic Press.

DODE, L., ANDERSEN, J. P., LESLIE, N., DHITAVAT, J., VILSEN, B. & HOVNANIAN, A. 2003. Dissection of the Functional Differences between Sarco(endo)plasmic Reticulum Ca2+-ATPase (SERCA) 1 and 2 Isoforms and Characterization of Darier Disease (SERCA2) Mutants by Steady-state and Transient Kinetic Analyses. *Journal of Biological Chemistry,* 278**,** 47877-47889.

EAST, M. J. 2000. Sarco(endo)plasmic Reticulum Calcium Pumps: Recent Advances in Our Understanding of Structure/Function and Biology. *Mol. Membr. Biol,* 17**,** 189-200.

EBASHI, S. 1976. Excitation-Contraction Coupling. *Annual Review of Physiology,* 38**,** 293-313.

ENDO, M. 1977. Calcium Release from the Sarcoplasmic Reticulum. *Physiol. Rev.,* 57**,** 71-108.

FEHER, J. J. & FABIATO, A. 1990. Cardiac Sarcoplasmic Reticulum: Calcium Uptake and Release. *Calcium and the Heart***,** 199-269.

FINKEL, T. & HOLBROOK, N. J. 2000. Oxidants, Oxidative Stress and the Biology of Ageing. *Nature,* 408**,** 239-247.

FRANK, K. F., BOLCK, B., ERDMANN, E. & SCHWINGER, R. H. G. 2003. Sarcoplasmic Reticulum Ca2+-ATPase Modulates Cardiac Contraction and Relaxation. *Cardiovasc Res,* 57**,** 20-27.

GARRISON, W. M. 1987. Reaction Mechanisms in Radiolysis of Peptides, Polypeptides, and Proteins. *Chem Rev,* 87**,** 381-398.

GARRISON, W. M., JAYKO, M. E. & BENNETT, W. 1962. Radiation-Induced Oxidation of Protein in Aqueous Solution. *Radiation Research* 16**,** 483-502.

GARRISON, W. M. & WEEDS, B. M. 1962. Radiation Chemistry of Compounds Containing the Peptide Bond. *Radiation Research***,** 341-352.

HAGHIGHI, K., SCHMIDT, A. G., HOIT, B. D., BRITTSAN, A. G., YATANI, A., LESTER, J. W., ZHAI, J., KIMURA, Y., DORN, G. W., II, MACLENNAN, D. H. & KRANIAS, E. G. 2001. Superinhibition of Sarcoplasmic Reticulum Function by Phospholamban Induces Cardiac Contractile Failure. *J. Biol. Chem.,* 276**,** 24145-24152.

HALLIWELL, B. 2007. Biochemistry of Oxidative Stress. *Biochemical Society Transactions* 35**,** 1146-1150.

HARMAN, D. 1956. Aging: A Theory Based on Free Radical and Radiation Chemistry. *J Gerontol,* 11**,** 298-300.

HARMAN, D. 1980. Free Radical Theory of Aging: Origin of Life, Evolution, and Aging. *AGE,* 3**,** 100-102.

INESI, G. 1987. Sequential Mechanism of Calcium Binding and Translocation in Sarcoplasmic Reticulum Adenosine Triphosphatase*. *Journal of Biological Chemistry,* 262**,** 16338-16342

INESI, G., KURZMACK, M., COAN, C. & LEWIS, D. 1980. Cooperative Calcium Binding and ATPase Activation in Sarcoplasmic Reticulum Vesicles. *The Journal of Biological Chemistry,* 255**,** 3025-3031.

JAMES, P., INUI, M., TADA, M., CHIESI, M. & CARAFOLI, E. 1989. Nature and Site of Phospholamban Regulation of the Ca2+ pump of Sarcoplasmic Reticulum *Nature,* 342**,** 90-92.

KATZ, A. M. 1993. Cardiac Ion Channels. *N Engl J Med,* 328**,** 1244-1251.

KIMURA, Y., KURZYDLOWSKI, K., TADA, M. & MACLENNAN, D. H. 1996. Phospholamban Regulates the Ca2+-ATPase Through Intramembrane Interactions. *Journal of Biological Chemistry,* 271**,** 21726-21731.

KIMURA, Y., KURZYDLOWSKI, K., TADA, M. & MACLENNAN, D. H. 1997. Phospholamban Inhibitory Function Is Activated by Depolymerization. *Journal of Biological Chemistry,* 272**,** 15061-15064.

KNYUSHKO, T. V., SHAROV, V. S., WILLIAMS, T. D., SCHONEICH, C. & BIGELOW, D. J. 2005. 3-Nitrotyrosine Modification of SERCA2a in the Aging Heart: A Distinct Signature of the Cellular Redox Environment. *Biochemistry,* 44**,** 13071-13081.

KOSS, K. L. & KRANIAS, E. G. 1996. Phospholamban: A Prominent Regulator of Myocardial Contractility. *Circ Res,* 79**,** 1059-1063.

KUHLBRANDT, W. 2004. Biology, Structure and Mechanism of P-type ATPases. *Nat Rev Mol Cell Biol,* 5**,** 282-295.

LAMBERTH, S., SCHMID, H., MUENCHBACH, M., VORHERR, T., KREBS, J., CARAFOLI, E. & GRIESINGER, C. 2000. NMR Solution Structure of Phospholamban. *Helvetica Chimica Acta,* 83**,** 2141-2152.

LAMMI-KEEFE, C. J., SWAN, P. B. & HEGARTY, P. V. J. 1984. Copper-zince and Manganese Superoxide Dismutase Acts in Cardiac and Skeletal Muscles During Aging in Male Rats. *Gerontology,* 30**,** 153-158.

LI, J., XIONG, Y., BIGELOW, D. J. & SQUIER, T. C. 2003. Phospholamban Binds in a Compact and Ordered Conformation to the Ca-ATPase†. *Biochemistry,* 43**,** 455-463.

MACLENNAN, D. H. & KRANIAS, E. G. 2003. Phospholamban: A Crucial Regulator of Cardiac Contractility. *Nat Rev Mol Cell Biol,* 4**,** 566-577.

MACLENNAN, D. H., RICE, W. J. & GREEN, N. M. 1997. The Mechanism of Ca^{2+} Transport by Sarco(endo)plasmic Reticulum Ca-ATPases. *J. Biol. Chem.,* 272**,** 28815-28828.

MAHANEY, J. E., ALBERS, R. W., WAGGONER, J. R., KUTCHAI, H. C. & FROEHLICH, J. P. 2005. Intermolecular Conformational Coupling and Free Energy Exchange Enhance the Catalytic Efficiency of Cardiac Muscle SERCA2a following the Relief of Phospholamban Inhibition *Biochemistry,* 44**,** 7713-7724.

MAHANEY, J. E., AUTRY, J. M. & JONES, L. R. 2000. Kinetic Studies of the Cardiac Ca-ATPase Expressed in Sf21 Cells: New Insights on Ca-ATPase Regulation by Phospholamban. *Biophysical Journal,* 78**,** 13061323.

MARTINDALE, J. L. & HOLBROOK, N. J. 2002. Cellular Response to Oxidative Stress: Signaling for Suicide and Survival. *Journal of Cellular Physiology,* 192**,** 1-15.

MARTONOSI, A., N. & PIKULA, S. 2003. The Structure of the Ca2+-ATPase of Sarcoplasmic Reticulum. *Acta Biochimica Polonica,* 50**,** 337-365.

MASUDA, H. & DE MEIS, L. 1973. Phosphorylation of the Sarcoplasmic Reticulum Membrane by Orthophosphate. Inhibition by Calcium Ions. *Biochemistry,* 12**,** 4581-4585.

MELDRUM, D. R., CLEVELAND, J. C., JR, SHERIDAN, B. C., ROWLAND, R. T., BANERJEE, A. & HARKEN, A. H. 1996. Cardiac Surgical Implications of Calcium Dyshomeostasis in the Heart. *Ann Thorac Surg,* 61**,** 1273-1280.

METCALFE, E. E., TRAASETH, N. J. & VEGLIA, G. 2005. Serine 16 Phosphorylation Induces an Order-to-Disorder Transition in Monomeric Phospholamban†. *Biochemistry,* 44**,** 4386-4396.

MINTZ, E. & GUILLAIN, F. 1997. Ca2+ Transport by the Sarcoplasmic Reticulum ATPase. *Biochimica et Biophysica Acta (BBA) - Bioenergetics,* 1318**,** 52-70.

MØLLER, J., OLESEN, C., JENSEN, A.-M. & NISSEN, P. 2005. The Structural Basis for Coupling of Ca2+ Transport to ATP Hydrolysis by the Sarcoplasmic Reticulum Ca2+-ATPase. *Journal of Bioenergetics and Biomembranes,* 37**,** 359-364.

MOLLER, J. V., OLESEN, C., JENSEN, A. L. & NISSEN, P. 2006. The Structural Basis for Coupling of Ca2+-Transport to ATP Hydrolysis by the Sarcoplasmic Reticulum Ca2+-ATPase *Journal of Bioenergetics and Biomembranes,* 37**,** 359-364.

MUSCARI, C., GIACCARI, A., GIORDANO, E., CLO, C., GUARNIERI, C. & CALDARERA, C. 1996. Role of Reactive Oxygen Species in Cardiovascular Aging. *Molecular and Cellular Biochemistry,* 160**,** 159-166.

OBARA, K., MIYASHITA, N., XU, C., TOYOSHIMA, I., SUGITA, Y., INESI, G. & TOYOSHIMA, C. 2005. Structural Role of Countertransport Revealed in Ca2+ Pump Crystal Structure in the Absence of Ca2+. *Proceedings of the National Academy of Sciences of the United States of America,* 102**,** 14489-14496.

OLESEN, C., PICARD, M., WINTHER, A.-M. L., GYRUP, C., MORTH, J. P., OXVIG, C., MOLLER, J. V. & NISSEN, P. 2007. The Structural Basis of Calcium Transport by the Calcium Pump. *Nature,* 450**,** 1036-1042.

PAOLOCCI, N., JACKSON, M. I., LOPEZ, B. E., MIRANDA, K., TOCCHETTI, C. G., WINK, D. A., HOBBS, A. J. & FUKUTO, J. M. 2007. The Pharmacology of Nitroxyl (HNO) and its Therapeutic Potential: Not Just the Janus Face of NO. *Pharmacology & Therapeutics,* 113**,** 442-458.

PEDERSEN, P. L. & CARAFOLI, E. 1987. Ion Motive ATPases. I. Ubiquity, Properties, and Significance to Cell Function. *Trends in Biochemical Sciences,* 12**,** 146-150.

POLLESELLO, P. & ANNILA, A. 2002. Structure of the 1-36 N-Terminal Fragment of Human Phospholamban Phosphorylated at Ser-16 and Thr-17. *Biophysical Journal,* 83**,** 484-490.

SANDLER, V. M. & BARBARA, J.-G. 1999. Calcium-Induced Calcium Release Contributes to Action Potential-Evoked Calcium Transients in Hippocampal CA1 Pyramidal Neurons. *J. Neurosci.,* 19**,** 4325-4336.

SCARBOROUGH, G. A. 1999. Structure and Function of the P-type ATPases. *Current Opinion in Cell Biology,* 11**,** 517-522.

SCHLEGEL, W., WINIGER, B. P., MOLLARD, P., VACHER, P., WUARIN, F., ZAHND, G. R., WOLLHEIM, C. B. & DUFY, B. 1987. Oscillations of Cytosolic Ca2+ in Pituitary Cells Due to Action Potentials. *Nature,* 329**,** 719-721.

SCHMIDT, A. G., EDES, I. & KRANIAS, E. G. 2001. Phospholamban: A Promising Therapeutic Target in Heart Failure. *Cardiovascular Drugs and Therapeutics,* 15**,** 387-396.

SCHMITT, J. P., KAMISAGO, M., ASAHI, M., LI, G. H., AHMAD, F., MENDE, U., KRANIAS, E. G., MACLENNAN, D. H., SEIDMAN, J. G. & SEIDMAN, C. E. 2003. Dilated Cardiomyopathy and Heart Failure Caused by a Mutation in Phospholamban. *Science,* 299**,** 1410-1413.

SIES, H. 1997. Oxidative Stress: Oxidants and Antioxidants. *Experimental Physiology,* 82**,** 291-295.

SIMMERMAN, H. K. B. & JONES, L. R. 1998. Phospholamban: Protein Structure, Mechanism of Action, and Role in Cardiac Function. *Physiological Reviews,* 78**,** 921-946.

SIMMERMAN, H. K. B., KOBAYASHI, Y. M., AUTRY, J. M. & JONES, L. R. 1996. A Leucine Zipper Stabilizes the Pentameric Membrane Domain of Phospholamban and Forms a Coiled-coil Pore Structure. *Journal of Biological Chemistry,* 271**,** 5941-5946.

SMALLWOOD, H. S., GALEVA, N. A., BARTLETT, R. K., URBAUER, R. J. B., WILLIAMS, T. D., URBAUER, J. L. & SQUIER, T. C. 2003. Selective Nitration of Tyr99 in Calmodulin as a Marker of Cellular Conditions of Oxidative Stress. *Chemical Research in Toxicology,* 16**,** 95-102.

SOHAL, R. S., MOCKETT, R. J. & ORR, W. C. 2002. Mechanisms of Aging: An Appraisal of the Oxidative Stress Hypothesis. *Free Radical Biology and Medicine,* 33**,** 575-586.

SOLARO, R. J. 2007. Nitroxyl Effects on Myocardium Provide New Insights into the Significance of Altered Myofilament Response to Calcium in the Regulation of Contractility. *The Journal of Physiology,* 580**,** 697-697.

SØRENSEN, T. L.-M., MØLLER, J. V. & NISSEN, P. 2004. Phosphoryl Transfer and Calcium Ion Occlusion in the Calcium Pump. *Science,* 304**,** 1672-1675.

SOUZA, J. M., DAIKHIN, E., YUDKOFF, M., RAMAN, C. S. & ISCHIROPOULOS, H. 1999. Factors Determining the Selectivity of Protein Tyrosine Nitration. *Archives of Biochemistry and Biophysics,* 371**,** 169-178.

STADTMAN, E. R. 2006. Protein Oxidation and Aging. *Free Radical Research,* 40**,** 1250-1258.

STERN, M. D. 1992. Theory of Excitation-Contraction Coupling in Cardiac Muscle. *Biophysical Journal,* 63**,** 497-517.

SUMIDA, M., WANG, T., MANDEL, F., SCHWARTZ, A., YOUNKIN, C. & FROEHLICH, J. P. 1980. The Ca2+-ATPase Partial Reactions in Cardiac and Skeletal Sarcoplasmic Reticulum *J. Biol. Chem.,* 255**,** 1497-1503.

TADA, M., YAMADA, M., OHMORI, F., KUZUYA, T., INUI, M. & ABE, H. 1980. Transient State Kinetics Studies of Ca2+-Dependent ATPase and Calcium Transport by Cardiac Sarcoplasmic Reticulum. *J. Biol. Chem.,* 255**,** 1985-1992.

TOCCHETTI, C. G., WANG, W., FROEHLICH, J. P., HUKE, S., AON, M. A., WILSON, G. M., DI BENEDETTO, G., O'ROURKE, B., GAO, W. D., WINK, D. A., TOSCANO, J. P., ZACCOLO, M., BERS, D. M., VALDIVIA, H. H., CHENG, H., KASS, D. A. & PAOLOCCI, N. 2007. Nitroxyl Improves Cellular Heart Function by Directly Enhancing Cardiac Sarcoplasmic Reticulum Ca2+ Cycling. *Circ Res,* 100**,** 96-104.

TOYOSHIMA, C. 2008. Structural Aspects of Ion Pumping by Ca2+-ATPase of Sarcoplasmic Reticulum. *Archives of Biochemistry and Biophysics,* 476**,** 3-11.

TOYOSHIMA, C. 2009. How Ca2+-ATPase Pumps Ions Across the Sarcoplasmic Reticulum Membrane. *Biochimica et Biophysica Acta (BBA) - Molecular Cell Research,* 1793**,** 941-946.

TOYOSHIMA, C. & INESI, G. 2004. Structural Basis of Ion Pumping by Ca^{2+}-ATPase of the Sarcoplasmic Reticulum. *Annual Review of Biochemistry,* 73**,** 269-292.

TOYOSHIMA, C. & MIZUTANI, T. 2004. Crystal Structure of the Calcium Pump with a bound ATP analogue. *Nature,* 430**,** 529-535.

TOYOSHIMA, C., NAKASAKO, M., NOMURA, H. & OGAWA, H. 2000. Crystal Structure of the Calcium Pump of Sarcoplasmic Reticulum at 2.6 [angst] Resolution. *Nature,* 405**,** 647-655.

TOYOSHIMA, C. & NOMURA, H. 2002. Structural Changes in the Calcium Pump Accompanying the Dissociation of Calcium. *Nature,* 418**,** 605-611.

TOYOSHIMA, C., NOMURA, H. & SUGITA, Y. 2003. Structural Basis of Ion Pumping by Ca2+-ATPase of Sarcoplasmic Reticulum. *FEBS Letters,* 555**,** 106-110.

TOYOSHIMA, C., NORIMATSU, Y., IWASAWA, S., TSUDA, T. & OGAWA, H. 2007. How Processing of Aspartylphosphate is Coupled to Lumenal Gating of the Ion Pathway in the Calcium Pump. *Proceedings of the National Academy of Sciences,* 104**,** 19831-19836.

VINER, R. I., FERRINGTON, D. A., WILLIAMS, T. D., BIGELOW, D. J. & SCHONEICH, C. 1999a. Protein Modification During Biological Aging: Selective Tyrosine Nitration of the SERCA2a Isoform of the Sarcoplasmic Reticulum Ca-ATPase in Skeletal Muscle. *Biochemical Journal,* 340**,** 657-669.

VINER, R. I., WILLIAMS, T. D. & SCHONEICH, C. 1999b. Peroxynitrite Modification of Protein Thiols: Oxidation, Nitrosylation, and S-Glutathiolation of Functionally Important Cysteine Residue(s) in the Sarcoplasmic Reticulum Ca-ATPase. *38,* 12408-12415.

VOSS, J., JONES, L. R. & THOMAS, D. D. 1994. The Physical Mechanism of Calcium Pump Regulation in the Heart. *Biophysical Journal,* 67**,** 190-195.

WAGGONER, J. R., HUFFMAN, J., FROELICH, J. P. & MAHANEY, J. E. 2007. Phospholamban Inhibits Ca-ATPase Conformational Changes Involving the E2 Intermediate. *Biochemistry,* 46**,** 1999-2009.

WALKER, C. A. & SPINALE, F. G. 1999. THE STRUCTURE AND FUNCTION OF THE CARDIAC MYOCYTE: A REVIEW OF FUNDAMENTAL CONCEPTS. *J Thorac Cardiovasc Surg,* 118**,** 375-382.

YANG, M. S., CHAN, H. W. & YU, L. C. 2006. Glutathione Peroxidase and Glutathione Reductase Activities are Partially Responsible for Determining the Susceptibility of Cells to Oxidative Stress. *Toxicology,* 226**,** 126-130.

ZHANG, H., BHARGAVA, K., KESZLER, A., FEIX, J., HOGG, N., JOSEPH, J. & KALYANARAMAN, B. 2003. Transmembrane Nitration of Hydrophobic Tyrosyl Peptides. *Journal of Biological Chemistry,* 278**,** 8969-8978.

ZHANG, L., KELLEY, J., SCHMEISSER, G., KOBAYASHI, Y. M. & JONES, L. R. 1997. Complex Formation between Junctin, Triadin, Calsequestrin, and the Ryanodine Receptor: PROTEINS OF THE CARDIAC JUNCTIONAL SARCOPLASMIC RETICULUM MEMBRANE. *Journal of Biological Chemistry,* 272**,** 23389-23397.

ZHANG, P., TOYOSHIMA, C., YONEKURA, K., GREEN, N. M. & STOKES, D. L. 1998. Structure of the Calcium Pump from Sarcoplasmic Reticulum at 8-A resolution. *Nature,* 392**,** 835-839.

Chapter 2

Physical Mechanism of Ca-ATPase Inhibition by Peroxynitrite

I was the sole contributor to this section.

Introduction

The free-radical theory of aging has promoted the hypothesis that increases in reactive oxygen species (ROS) may be responsible for age-related dysfunction (Harman, 1956, Waggoner et al., 2007, Waggoner and Kranias, 2005), which is a result of oxidative stress. Oxidative stress occurs when the concentration of ROS exceeds the cells ability to remove ROS and repair damage, which can lead to the oxidation of amino acid side chains (Squier, 2001), lipids, and nucleic acids (Berlett and Stadtman, 1997). For example, one important oxidized amino acid product is the formation of 3-nitrotyrosine (3-NY) in proteins which is the result of a nitrogen dioxide group added to the third carbon of the benzene ring on tyrosine. 3-NY is also one of the most commonly studied post-translational modifications in proteins, as it is an indicator of cell damage and inflammation (Barreiro et al., 2002, Souza et al., 2008). The modification, 3-NY, is formed by the reaction of peroxynitrite ($ONOO^-$) with tyrosine residues. Peroxynitrite is formed by the reactions of nitric oxide (NO) with superoxide ($O_2^{\bullet -}$). Peroxynitrite not only modifies tyrosine, but also reacts with methionine and cysteine residues (Viner et al., 1999b, Reiter et al., 2000, Beckman and Koppenol, 1996, Souza et al., 1999, Marla et al., 1997). One such protein modified by $ONOO^-$ is the sarco(endo)plasmic reticulum Ca-ATPase (SERCA) which plays a key role in Ca^{2+} cycling and is modified at specific tyrosine and cysteine residues through oxidation and nitrosylation from exposure to $ONOO^-$ (Viner et al., 1999b). This oxidation leads to an inhibition of enzyme activity, and as a result a decline in Ca^{2+} transport and decreased muscle function.

As oxidative stress increases, so do age-related issues. Age-based changes to the cardiovascular system can mimic changes that take place as a result of cardiovascular diseases, such as atherosclerosis and hypertension. It is known that age-based changes to the cardiovascular system, specifically Ca^{2+} transport, can affect cardiovascular function in ways that can increase susceptibility of aging individuals to cardiovascular diseases. This effect on Ca^{2+} transport in the aged heart is a result of an increased generation of ROS and the cell's inability to remove them (Lakatta and Sollott, 2002, Juhaszova et al., 2005). Age-based modifications can lead to inhibition of protein activity; however the molecular mechanisms by which this occurs are still unknown in several proteins. In that, SERCA2a has been identified as a protein modified by $ONOO^-$, we have studied the effects of $ONOO^-$-dependent 3-NY formation on SERCA2a activity and its regulation by phospholamban (PLN).

SERCA is a 100 kDa integral membrane enzyme found in the smooth, cardiac, and skeletal muscles that promotes muscle relaxation by utilizing ATP to sequester Ca^{2+} ions from the muscle cytosol into the sarcoplasmic reticulum (SR) lumen (MacLennan et al., 1997, East, 2000). In cardiac muscle, SERCA is regulated by a small integral membrane phosphoprotein, phospholamban (PLN), which works by decreasing SERCA's affinity for Ca^{2+} (Simmerman and Jones, 1998). Bigelow and colleagues have shown that the cardiac isoform, SERCA2a, shows a significant decrease in the rate of Ca^{2+} uptake with increasing age. In vivo studies in the Bigelow lab have shown that nitration occurs at Tyr-753 (Y753) in young adult skeletal muscle but that an additional 2 mol of nitrotyrosine are found at vicinal sites, Tyr-294 and Tyr-295 (Y294 and Y295),

which appears with aging and/or the appearance of higher concentrations of ROS. This nitration is accompanied by inhibition of SERCA2a (Knyushko et al., 2005, Viner et al., 1996). Y294 and Y295 are found in both the skeletal muscle isoform, SERCA1, and the cardiac muscle isoform, SERCA2a, which share 18 out of 24 tyrosine residues, including Y294 and Y295 (Viner et al., 1999b). Since these sites of nitration are shared between the two isoforms, it suggests a functional relevance to these sites, as well as its proximity to the Ca^{2+} binding domain. These residues are important for the E2 to E1 conformational transition, altering the configuration of the Ca^{2+} release site after Ca^{2+} entering the SR lumen. Y294 and Y295 are located within proximity to the negative charge of a glutamate carboxylate group of E785 (Smallwood et al., 2003, Zhang et al., 2003, Souza et al., 1999), in the E1 state; Y294 and Y295 are hydrogen-bonded to this residue. In the E2 state, these tyrosine residues are rotated away and these hydrogen bonds are disrupted. Peroxynitrite modification of these tyrosine residues would be expected to affect this structural change and enzyme function. Since PLN also affects the SERCA2a E2 to E1 conformational transition, it is possible that $ONOO^-$ modification may affect SERCA2a regulation by PLN, and vice versa, however this has not been tested. Y753 seems to have less effect on function because of its occurrence in young tissue. Despite this information, the exact mechanism of inhibition is unknown.

Therefore, in the present work, we have studied the mechanism by which nitration by $ONOO^-$ of SERCA2a inhibits SERCA2a activity and its regulation by PLN, using kinetic studies and biophysical techniques. For these studies, we have used our baculovirus insect cell expression system to express SERCA2a in the

absence and presence of co-expressed PLN and used electron paramagnetic resonance (EPR) spectroscopy and fluorescence spectroscopy to examine oligomeric and lipid interactions, as well as conformational changes. We found that increased exposure to $ONOO^-$ correlates with increased inhibition of Ca-ATPase activity, as seen in the aged heart (Knyushko et al., 2005), and the presence of PLN increases SERCA2a sensitivity to $ONOO^-$. The results of this study suggest $ONOO^-$ is an irreversible inhibitor of SERCA2a.

Materials and Methods:

Protein Expression, Isolation, and Characterization

Canine cardiac Ca-ATPase (the SERCA2a isoform) and canine PLN were coexpressed in High Five (HF) insect cells as reported elsewhere (Waggoner et al., 2004). Microsomes were harvested 48 h after the baculovirus infections and stored in small aliquots at -80˚C. Protein concentrations were determined by the method of biuret (Gornall et al., 1949) using bovine serum albumin (Sigma) as a standard. The amount of SERCA2a and PLN in the microsomes was quantified by gel electrophoresis and immuno-blotting, using methods described previously (Waggoner et al., 2004). Several different preparations of expressed SERCA2a with or without co-expressed PLN were used in these studies. The Ca-ATPase content of the microsomes was very carefully matched at 16% of the total protein by weight, and the relative proportion of Ca-ATPase to PLN co-expressed in the microsomes was between 1 and 2 mol of PLN/mol of Ca-ATPase (Waggoner et al., 2004). For all preparations, the Ca-ATPase was under full regulatory control by PLN when the two proteins were coexpressed, determined by assays of $[Ca^{2+}]$-

dependent ATPase and Ca^{2+}-uptake activity conducted in the presence and absence of anti-PLN antibody, as reported previously for these samples (Waggoner et al., 2004).

Peroxynitrite stock solutions (VWR) were stored at -80°C until use. The concentration of the stock solution was determined from the absorbance at 280 nm using $€_{280} = 5400\ M^{-1}\ cm^{-1}$. Serial [$ONOO^-$] dilutions were made in 0.1 N NaOH just prior to each experiment to provide the desired level of [$ONOO^-$] for each microsomal SERCA2a sample.

SERCA2a Inhibition and ATPase Assay Studies

[$ONOO^-$]-dependent inhibition of SERCA2a activity was measured colorimetrically using the malachite green-ammonium molybdate assay as previously described (Lanzetta et al., 1979). Insect cell microsomes containing SERCA2a ± PLN (1 mg/mL) were pre-incubated with serial concentrations of $ONOO^-$ for 10 min at room temperature. The $ONOO^-$-treated microsomes were diluted to 0.05 mg/mL protein in 50 mM 3-(N-morpholino)propanesufonic acid (MOPS) (pH 7.0), 3 mM $MgCl_2$, 100 mM KCl, 1 mM ethylenebis(oxyethylnenitrilo)tetraacetic acid (EGTA), and 0.7 mM $CaCl_2$ (ionized Ca^{2+} = 0.268 μM). To initiate the ATPase reaction, 5 mM MgATP was added to the incubation tubes at 37˚C. Samples were pre-treated with 20 μg of Ca^{2+} ionophore A23187/mg of total protein to prevent Ca^{2+} buildup within the microsomes during the assay. The [Ca^{2+}]-Dependent ATPase activity of SERCA2a in the High Five insect cell microsomes was measured colorimetrically at 37˚C using the malachite green-ammonium molybdate assay as described

above, using the 0-1.0 mM $CaCl_2$ to give a range of ionized [Ca^{2+}], as previously determined (Autry and Jones, 1997). Microsomes were pre-treated with $ONOO^-$ as described above.

Phosphoenzyme Decay

Radiometric EGTA-dependent phosphoenzyme (EP) decay assays were performed using insect cell microsomes containing SERCA2a ± PLN in the absence or presence of 100 μM $ONOO^-$. Incubation tubes, which for this experiment was the glass scintillation vial, contained 0.5 mg/mL total microsomal protein in 50 mM MOPS, 3 mM $MgCl_2$, 100 mM KCl, 1 mM EGTA, and 0.7 mM $CaCl_2$ at pH 7.0 (to match titration data). SERCA2a ± PLN was phosphorylated by adding 1 μM [γ-32P]ATP, at 0˚C for 10 seconds as described previously (Mahaney et al., 2000b). This addition was followed by the rapid addition of an EGTA chase solution (15 mM final) at 10 seconds, which chelated any free Ca^{2+} in the system and stopped subsequent SERCA2a phosphorylation. The reaction was allowed to proceed for variable times (0, 2, 3, 5, 7, 10, 15, 30, and 60 sec) before quenching with ice-cold 9% perchloric acid + 6 mM H_3PO_4, followed by vortexing. A zero-time sample was obtained by quenching the phosphorylation reaction at 10 seconds followed by the addition of an EGTA chase solution to the quenched samples. The samples were pelleted by centrifugation for 10 minutes at 3,000 rpm at 4˚C and then washed three times in 5% trichloroacidic, 6% polyphosphoric acid, 4 mM H_3PO_4, and 5 mM nonradioactive ATP to remove any unbound [γ-32p]ATP. The final pellets were dissolved in 1N NaOH and assayed by liquid scintillation counting.

Electrophoresis and Immunoblot Analysis

SERCA2a nitrotyrosine (NY) formation was detected using immunoblot analysis. Microsomes (2 mg/mL) were pre-treated with varying concentrations of $ONOO^-$ (to match titration data) and incubated for 10 minutes at room temperature. The treated samples were diluted to 1 mg/mL in a solution containing gel dissociation media (GDM) and 25 μg total protein was loaded per well onto a 12% acrylamide gel. The protein samples were transferred onto nitrocellulose membranes for immunodetection. The membranes were probed with 2A7-A1 and with anti-NY monoclonal antibodies for SERCA2a and nitrotyrosine detection, respectively. The membranes incubated with Horse-radish peroxidase (HRP) conjugated protein A and HRP protein A development buffer was used to detect NY and SERCA2a on membranes.

Spin labeling

The overall rotational mobility of the Ca-ATPase was measured by electron paramagnetic resonance (EPR) spectroscopy using the short-chain maleimide spin label, N-(1-oxyl-2,2,6,6-tetra-methyl-4-piperadinyl)maleimide (MSL), covalently bound to the ATPase, as previously described (Squier and Thomas, 1986b, Bigelow et al., 1986). Microsomes containing SERCA2a ± PLN (10 mg/mL) were first pre-treated with 100 μM N-ethylmaleimide (NEM) at a ratio of 1.0 mol NEM per mol of expressed SERCa2a to block fast-reacting thiols for 30 minutes on ice. After the 30 minute incubation, SERCA2a was then spin-labeled with 250 μM MSL for 1 hour on ice, at a ratio of 2.5 mols MSL per mol of expressed SERCA2a. Excess spin label was removed by two rounds of

centrifugation in ice cold 0.3 M sucrose and 20 mM MOPS (pH 7.0) buffer for 30 minutes at 30, 000 rpm (70000g), 4˚C, in a Beckman Ti45 rotor using a Beckman Optima LE-80K ultra centrifuge. The pellet, containing the MSL-labeled SERCA2a (henceforth denoted MSL-SERCa2a), was re-suspended in 0.3 M sucrose and 20 mM MOPS at pH 7.0 and stored on ice until use.

Lipid hydrocarbon chain rotational mobility was also measured by EPR using fatty acid spin labels, N-oxyl-4',4'-demethyloxazotidine derivatives of stearic acid, designated at 5- and 16-SASL (stearic acid spin label). The number designation indicates the position of the nitroxide group on the stearic acid chain. Spin labels were added to the microsomes at a ratio of less than 1 spin label per 200 phospholipids (Mahaney and Thomas, 1991).

EPR Spectroscopy

EPR spectra were obtained using a Bruker ER 200D spectrometer equipped with a Bruker ER 4102ST cavity. Submicrosecond rotational motion of spin labels was detected by conventional EPR (first harmonic absorption in phase, designated V1) using 100 kHz field modulation, a peak-to-peak amplitude of 2 gauss (G), and a microwave field amplitude of 0.032 G. Submillisecond rotational motion of spin labels was detected by saturation-transfer EPR (second harmonic absorption out of phase, designated V2') using a 50 kHz field modulation, with a modulation amplitude of 5.0 G, and a microwave field intensity of 0.25 G. Samples were contained in 50 μL glass capillaries. Sample temperature was controlled at 4˚C with a Bruker ER 4111VT variable temperature

controller. Spectra were digitized and stored on a computer and analyzed using the program EWWIN, written by Philip Morse (Scientific Software Solutions).

EPR Spectral Analysis

Conventional EPR spectra were analyzed for measuring the outer peak splitting parameter ($2T_{II}'$). ST-EPR spectra were analyzed using the H'/H line shape parameters (Squier and Thomas, 1986b). The effective rotational correlation time (τ_r) for spin-labeled SERCA2a in the various samples was determined from a standard curve constructed from an isotropically tumbling models system (Squier and Thomas, 1986b, Mahaney and Thomas, 1991). Fatty acid spin label EPR spectra were measured by evaluating the outer ($2T_{II}'$) and inner ($2T_{\perp}'$) spectral splitting, which are sensitive mainly to the rotational amplitude of hydrocarbon chain wobble relative to the membrane normal. The effective order parameter (S) was calculated from the splitting as described previously (Mahaney and Thomas, 1991).

Labeling of Ca-ATPase with FITC

SERCA2a and SERCA2a + PLN expressed in insect cell microsomes was labeled by florescein isothiocyanate (FITC) according to Birmachu and colleagues (Birmachu et al., 1989). A fresh stock of 5 mM FITC in N, N- dimethylformamide was prepared prior to each experiment from powder, using DMF as the solvent. The microsomes were incubated with FITC at a ratio of 0.9 mol FITC per mol of SERCA2a in a labeling buffer containing 60 mM Tris, 10 mM $MgCl_2$, and 200 mM KCl at a pH of 8.7 for 30 minutes at room temperature. BSA (1 mg/mL) was added to the solution and incubated for 20 minutes on ice to remove any

unbound label. Excess reagent and BSA were removed by pelleting the microsomes by centrifugation for 30 minutes at 30, 000 rpm, 4˚C, in a Beckman Coulter Ti45 rotor. The pellet, containing the FITC-labeled SERCA2a (henceforth denoted FITC-SERCA2a), was resusupended in 0.3 M sucrose and 20 mM MOPS.

Fluorescence Measurements

Measurements of the fluorescence intensity were performed at 25˚C using the Spectramax M5 microplate reader. Excitation and emission spectra of the FITC-SERCA2a showed optimal excitation and emission wavelengths of 490 nm and 505 nm, respectively.

To measure fluorescence intensity changes following a [Ca^{2+}]-jump, insect cell microsomes containing FITC-SERCA2a (~2.5 mg/mL) were suspended in a standard buffer (50 mM MOPS, 100 mM KCl, 3 mM $MgCl_2$, 0 mM $CaCl_2$, 1 mM EGTA, pH 7.0) designed to favor the Ca^{2+}-free E2 state initially. The addition of 1 mM Ca^{2+} to the standard buffer (final [Ca^{2+}] free ~ 100 μM) promoted the formation of the E1•Ca_2 conformation. The fluorescence intensity was measured by summing the total fluorescence emission (initial fluorescence intensity, F_0) and after (final fluorescence intensity, F) the respective additions. Fluorescence intensity changes were quantified as percent changes, according to the formula $100 \times (F-F_0)/F_0$.

Mutation

For the tyrosine mutant studies, the QuikChange XL Site-Directed Mutagenesis kit (Stratagene) was used using custom oligonucleotide primers

synthesized by Integrated DNA Technologies (San Jose, CA), and the cDNA of SERCA2a was inserted into the pFastBac™1 expression vector. In short, mutagenic primers were designed to bind the cDNA sequence selected for mutation. The mutagenic primers (125 ng each) were added to 5 μL of 10x reaction buffer, 10 ng of dsDNA template, 1 μL of dNTP mix, 3 μL of Quiksolution, and sterile, double-deionoized H_2O was added to a final volume of 50 μL. Next, 1 μL (2.5 units/μL) of P*fuTurbo* DNA polymerase were added and the mixture was incubated in the thermocycler as follows. An initial denaturing step of 1 min at 95˚C was followed by 18 cycles of 1) 50 seconds at 95˚C, 2) 50 seconds at 60˚C, and 3) 1 min/kb of plasmid length at 68˚C. Following completion, 1 μL of the restriction enzyme D*pn*I (10 units/μL) was added and the reaction was incubated at 37˚C for 1 hour in order to digest the parental strands. The mutant DNA was amplified using XL-10 Gold Ultracompetent *E. Coli* cells, and the mutant plasmids were isolated for sequence verification at the University of Georgia, Sequencing and Synthesis Facility. Once the mutations were verified, the mutant cDNA was introduced into DH10Bac™ *E. Coli* cells to produce a bacmid precursor for baculovirus production. The resulting bacmid was isolated and purified, and used to infect SF21 cells using the cellfectin reagent. After 3-5 days, mature baculovirus was isolated, and the viral titer was determined by rapid titer assay (Clontech).

Curve Fitting and Error Analysis

Experimental data were fitted using KFIT written by N.C. Millar, which was obtained originally from Dr. Carl Frieden. The best fits of the data were chosen on the basis of the minimization of the sum-of-squares error, χ^2.

Results

PLN increases SERCA2a sensitivity to $ONOO^-$

Knyushko and colleagues showed $ONOO^-$ inhibits SERCA2a activity in rat hearts; however the role of PLN in this inhibition is unknown. Therefore, we compared the enzyme activity of SERCA2a ± PLN in High Five insect cell microsome samples pre-treated with increasing [$ONOO^-$] (0, 10, 25, 50, 100, and 250 μM $ONOO^-$) to determine how PLN affects SERCA2a sensitivity to $ONOO^-$. In the presence of PLN, increasing [$ONOO^-$] progressively inhibited SERCA2a activity, reaching approximately 60% inhibition by 250 μM $ONOO^-$. These results are similar to published reports in native cardiac SR (Knyushko et al., 2005) showing our insect cell microsomes produce results similar in nature to cardiac SR vesicles. In contrast, the absence of PLN, $ONOO^-$ inhibited SERCA2a activity, but the maximal inhibition observed at 250 μM was only 40% on the overall activity (**Figure 2-2**). These results suggest the presence of PLN increased SERCA2a sensitivity to $ONOO^-$.

To test the role of Y294 and Y295 in the inhibition of SERCA2a by $ONOO^-$ we repeated the titrations using Y294F/Y295F-SERCA2a mutants. In one study, we found the substitution of Y294F/Y295F completely prevented inhibition by $ONOO^-$ where as in another preparation we found this substitution only

prevented the inhibition by approximately half (data not shown). These results suggest at a minimum that the sites Y294 and Y295 play a role in the $ONOO^-$ -dependent inhibition of SERCA2a. Additional studies are needed to better define the role of individual tyrosine residues in this inhibition mechanism.

Increasing nitrotyrosine formation correlated to a nitration-dependent loss of activity. In order to test this, we treated our samples with $ONOO^-$ and performed an immunoblot analysis to test for the presence of nitrotyrosine. Immunoblot analysis shows an increased formation of nitrotyrosine with incremental increases in the concentration of $ONOO^-$ added. Increased inhibition correlates with increased nitrotyrosine formation on SERCA2a, as determined by an anti-NY immunoblot (inset, **Figure 2-2**). Excess $ONOO^-$ appears to cause about 15% aggregation on the overall migration pattern of SERCA. $ONOO^-$ appears to only nitrate residues on SERCA (data not shown). A similar study was performed using the Y294F/Y295F–SERCA2a mutant but no nitrotyrosine bands could be resolved in the immunoblot (data not shown).

$ONOO^-$ has no effect on Ca-ATPase Ca^{2+} sensitivity

Since $ONOO^-$ inhibits ATPase maximal activity, we wanted to test the effect of $ONOO^-$ on SERCA2a ± PLN Ca^{2+} sensitivity. If $ONOO^-$ is altering Ca^{2+} binding dynamics, we should see a decrease in Ca^{2+} sensitivity. Therefore SERCA2a ± PLN in high five insect cell microsomes were treated with $ONOO^-$ in order to test the effect of nitration on the Ca^{2+} sensitivity of SERCA2a ATPase activity at the physiologically relevant $ONOO^-$ levels, 10 and 25 μM. Samples gave a typical sigmoidal shape. The presence of PLN shifts this curve to the right as

well documented. $ONOO^-$ did not affect the sigmoidal nature of the curve apart from affecting maximal activity (V_{max}). In the absence of PLN, SERCA2a V_{max} activity was inhibited by 30-50% but the $K_{0.5}$ value was not significantly changed. In the presence of PLN, SERCA2a V_{max} was inhibited by 40-55%, but again the $K_{0.5}$ did not change significantly. Apart from overall inhibition, treating SERCA2a with $ONOO^-$, either in the absence or presence of PLN, had no effect on the $[Ca^{2+}]$-dependent activity on either sample type (**Figure 2-3)**. For SERCA2a alone, SERCA2a + 10 μM $ONOO^-$, and 25 μM $ONOO^-$, the $K_{0.5}$ values were 0.14 ± 0.023, 0.18 ± 0.042, and 0.15 ± 0.016, respectively. For SERCA2a + PLN at the same concentrations, the $K_{0.5}$ values were 0.40 ± 0.023, 0.43 ± 0.031, and 0.48 ± 0.029. The $[Ca^{2+}]$-dependent activity data was the direct comparison of the curves. In the presence of PLN, the $[Ca^{2+}]$-dependent SERCA activity was shifted to the right, relative to SERCA2a in the absence of PLN, as well documented for this system (Waggoner et al., 2004), but treatment with $ONOO^-$ did not change the $K_{0.5}$ for SERCA2a in the absence or presence of PLN (**Figure 2-4**). These results indicated that while $ONOO^-$ inhibits SERCA2a activity, it does not affect the Ca^{2+} sensitivity of the enzyme.

SERCA2a tyrosine mutant Y294F/Y295F showed an attenuated inhibition at 10 μM $ONOO^-$. Samples were only inhibited by approximately 10% suggesting that the Y294F/ Y295F mutation is important in minimizing the effect of $ONOO^-$ on SERCA2a activity but is not responsible for completely abolishing it (**Figure 2-5**, **Figure 2-6**). Apart from the slight inhibition, treatment with $ONOO^-$ did not affect the $k_{0.5}$ showing no affect on the Ca^{2+} sensitivity of the enzyme.

$ONOO^-$ has no effect on the rate of enzyme dephosphorylation

SERCA2a dephosphorylation is the rate limiting step in the enzyme cycle (steps 5 and 6, **Figure 1-3**). To test for $ONOO^-$-dependent changes in the rate of phosphoenzyme decay, we measured the effect of $ONOO^-$ on the rate of this transition. For SERCA2a in the absence of PLN, the addition of 100 μM $ONOO^-$ inhibited the steady state level of the phosphoenzyme (40%), but did not alter the overall rate of dephosphorylation significantly (control = 0.2 ± 0.034 and $ONOO^-$-treated = 0.26 ± 0.032). For samples containing PLN, $ONOO^-$ also decreased the steady state phosphoenzyme level (37%) but also slightly inhibited the rate (data not shown).

$ONOO^-$ has no effect on the rotational mobility of SERCA2a

If $ONOO^-$ inhibits the enzyme such that we see an aggregation of protein in our immunoblots, then we should expect to see a change in the rotational mobility of the enzyme. Rotational mobility of MSL-SERCA2a conventional EPR studies measured the submicrosecond rotational motion of SERCA2a, both in the absence or presence of PLN. For both SERCA2a only and SERCA2a + PLN samples, MSL-labeled SERCA2a were dominated by a broad spectrum indicating a highly immobilized spin label bound to a slowly moving protein. $ONOO^-$ had no effect on the conventional spectrum, suggesting that $ONOO^-$ did not affect the physical environment of the label in its binding site within the protein. Because conventional EPR is sensitive to spin label motion on the nsec timescale and membrane proteins rotate on the μsec time scale, it is not possible to resolve difference in MSL-SERCA2a rotational mobility due to $ONOO^-$. Therefore, ST-

EPR was used to measure submillisecond rotational motion of MSL-SERCA2a. For the SERCA2a only samples, the MSL-labeled SERCA2a spectra were dominated by broad peaks that did not pass below the baseline. This was indicative of a spectrum of immobilized spin labels. In the presence of PLN, the MSL-labeled SERCA2a spectrum was dominated by peaks that were narrowed and did pass below the baseline, indicative of a much more mobile population of spin label, consistent with previous reports (Negash et al., 1996, Mahaney et al., 2003). Spectra were analyzed by line heights at well-defined positions in the spectrum, namely H″/H in the high field region. Previous studies on model systems have shown that L″ (corresponding line heights in the low field region) and H″ line heights change substantially with changing rotational mobility, whereas L and H do not, allowing these positions to be used as internal standards for L″ and H″, repeatedly. L″/L was not used because of spectral perturbations from weakly immobilized or more mobile spectral elements, which perturb the L″ peak. Using standard curves relating the line height motion to the rotational correlation time (τ_r). We determined the τ_r for SERCA2a alone as 63 μsec and for SERCA2a + PLN as 33 μsec. Treatment of the samples with 100 μM $ONOO^-$ and 500 μM $ONOO^-$ had no effect on the ST-EPR spectrum, suggesting that $ONOO^-$ did not alter SERCA2a rotational mobility.

$ONOO^-$ has no effect on lipid hydrocarbon chain dynamics

We performed EPR studies of the hydrocarbon chain rotational mobility in the lipid bilayer using stearic acid spin labels (5-SASL and 16-SASL) to test whether nitration of the membrane samples affects the bilayer lipid mobility.

Protein rotational motion is dependent, in part, on the viscosity of the lipid bilayer (Mahaney et al., 1992), which itself is dependent on lipid hydrocarbon mobility. Treatment with $ONOO^-$ had no significant effect on the 5-SASL or 16-SASL spectra, suggesting $ONOO^-$ treatment did not perturb the lipid bilayer.

$ONOO^-$ inhibits the Ca^{2+}-dependent conformational transition

If $ONOO^-$ affects ATPase maximal activity, then $ONOO^-$ should also inhibit the Ca^{2+}-dependent conformational transition. Therefore, to test the effects of $ONOO^-$ on SERCA2a [Ca^{2+}]-dependent conformational changes, we measured the effect of $ONOO^-$ on the SERCA2a E2 to E1•Ca_2 conformational transition. Fluorescence studies were performed on both sample types in the absence or presence of 100 uM $ONOO^-$. For FITC-SERCA2a in the absence of PLN, $ONOO^-$ treatment decreased amplitude of the E2 to E1•Ca_2 transition by approximately 40% (control = 10.80 % ± 1.80 and $ONOO^-$-treated = 6.26% ± 0.43). In the presence of PLN, $ONOO^-$ treatment decreased the amplitude of the E2 to E1•Ca_2 only slightly more greatly then in the absence of PLN (45% decrease in amplitude, control = 7.53% ± 1.11 and $ONOO^-$-treated = 4.11 ± 1.20). This suggests that PLN may slightly increase SERCA2a sensitivity to $ONOO^-$.

Discussion

$ONOO^-$ is a strong oxidant that is rapidly formed by the combination of NO and $O2^{\bullet-}$, which are both produced in several cell types, including cardiac muscle. $ONOO^-$ has a wide range of biological targets such as proteins, lipids, and nucleic acids. With this in mind, it has been reported that several SERCA2a tyrosine residues are modified in the presence of $ONOO^-$ with resulting inhibition

of Ca^{2+} transport activity. The proximity of the sarcoplasmic reticulum to the cellular mitochondria makes SERCA2a a susceptible target for $ONOO^-$ modification; the mitochondria produces $O2^{\cdot-}$ during oxidative phosphorylation, and cardiac endothelium produces NO as part of its signaling mechanism. However, the exact mechanism by which SERCA2a nitration leads to enzyme inhibition is unknown.

Previously, Knuyshko and colleagues (2005) studied the endogenous nitration of SERCA2a in young adult and senescent Fisher 344 rat hearts, and found an inhibition of SERCA2a activity of about 60% in the senescent heart relative to the young heart (Knyushko et al., 2005). With the aid of mass spectrometry, Knyushko and colleagues were able to show that SERCA2a tyrosine residues are selectively nitrated (Knyushko et al., 2005, Viner et al., 1996, Viner et al., 1999a, Sharov et al., 2006, Viner et al., 1999b, Schöneich and Sharov, 2006). In the young rat heart, it was found that one mol of nitrotyrosine was distributed over five tyrosine residues within SERCA2a, however within the senescent Fisher 344 hearts, an additional two mol of SERCA2a nitrotyrosines were found, residues Y294 and Y295 (Knyushko et al., 2005), suggesting these two tyrosine residues play a role in nitration-dependent enzyme inhibition. SERCA2a residue Y753 was found to be partially nitrated in young skeletal muscle, but fully nitrated in the senescent heart along with Y294 and Y295; giving rise to the possibility that nitration of Y753 is also important for loss of enzyme activity. Residues Y294 and Y295 are located within the Ca^{2+} binding and release domain on the luminal side of the M4 helix in the transmembrane, suggesting that oxidation of these residues might inhibit Ca^{2+} release, leading to a

prolonged Ca^{2+} transient and delayed muscle relaxation. $ONOO^-$ is lipid soluble and able to permeate the lipid membrane and modify the lipid soluble tyrosine residues 10-fold more greatly then those found in the aqueous environment (Zhang et al., 2003, Marla et al., 1997). Similarly, Y753 is located between the Ca^{2+} binding sites in the membrane and the site of phosphorylation in the P-domain of SERCA2a. Nitration of Y753 might lead to changes in Ca^{2+} dependent enzyme activation or changes in the phosphorylation kinetics of the enzyme.

To test these possibilities and their alternatives, we conducted more detailed studies on the effects of nitration on SERCA2a on the physical mechanism of Ca^{2+} transport activity and its regulation by PLN. We conducted our studies using SERCA2a expressed in High Five insect cells in order to conduct experiments of nitration on SERCA2a in the absence and presence of coexpressed PLN. Knyushko and colleagues reported that while $ONOO^-$ modifies primarily cysteine residues on SERCA1 in skeletal muscle, virtually no cysteine modification is present when SERCA2a in cardiac muscle is nitrated. Rather SERCA2a shows significant nitration on tyrosine, whereas SERCA1 shows very little nitration on tyrosine. SERCA1 and SERCA2a are 85% identical and greater than 90% homologous, suggesting that they would show similar nitration reactivity. The primary difference between the two proteins is the absence of PLN in skeletal muscle SR but presence of PLN in cardiac muscle SR. Waggoner and colleagues (2005) have shown that PLN binding to SERCA2a affects SERCA2a conformational dynamics, which may change side chain reactivity for SERCA2a. Conducting studies in the presence and absence of PLN allowed us to test whether PLN changes SERCA2a reactivity toward $ONOO^-$.

The results of our enzyme inhibition studies using insect cell microsomes agreed with the previous studies of Knyushko and colleagues (2005) where $ONOO^-$ treatment inhibited SERCA2a activity by ~ 60% in the presence of PLN. We found that the presence of PLN increased SERCA2a sensitivity to $ONOO^-$, because $ONOO^-$ only inhibited SERCA2a by 40% in the absence of PLN. However, our [Ca^{2+}]-dependent assays showed that $ONOO^-$ did not affect the Ca^{2+} sensitivity of the enzyme in the absence or presence of PLN, suggesting $ONOO^-$ did not inhibit enzyme activity by disrupting the Ca^{2+} binding kinetics. Likewise, $ONOO^-$ treatment had no significant effect on the rate of SERCA2a dephosphorylation in the absence of PLN, and only a slight inhibition of the rate of dephosphorylation in the presence of PLN, suggesting $ONOO^-$ treatment did not affect the rate-limiting step of the enzyme cycle. In contrast, $ONOO^-$ treatment decreased enzyme V_{max} while simultaneously inhibiting the steady-state level of phosphorylated SERCA2a. These results suggest that $ONOO^-$ may have irreversibly inhibited a fraction of SERCA2a in a dose-dependent manner, such that the remaining active enzyme units had the same Ca^{2+} sensitivity and rate of phosphoenzyme dephosphorylation. The classic test of irreversible enzyme inhibition would require constructing a plot of the enzyme V_{max} as a function of SERCA2a concentration at a series of [$ONOO^-$]. However, this was not possible for our samples. Our SERCA2a was membrane bound in the High Five insect cell microsomes, which themselves exhibit variability in enzyme content, making variation of [SERCA2a] difficult to quantify. But under the simple assumption of 1x, 2x, 3x, etc., concentration of microsomes, assays at these series of concentrations would be possible and comparable. However, we

found that $ONOO^-$ modification of SERCA2a depended on the concentration of microsomes in the test tube, and treatment of the microsomes with $ONOO^-$ was variable from one sample preparation to the next, making it difficult to quantify 1x, 2x, 3x, etc., amounts of $ONOO^-$ for such a plot. We are continuing to work on methodological advances to correct these problems so that we may construct such a plot and answer this irreversible inactivation question more definitively.

SERCA2a oligomeric interactions are important for optimal enzyme activity and that PLN disrupts these oligomeric interactions as part of its regulatory mechanism (Mahaney et al., 2003; Mahaney et al., 2005). Similarly, Mahaney and Thomas (1991) reported that agents that inactivate SERCA often cause the enzyme to form large protein aggregates. These inactive aggregates have greatly reduced rotational mobility compared to the more mobile, active SERCA units. Our anti-SERCA2a and anti-NY immunoblots indicated about a 15% of the 250 μM – 1000 μM $ONOO^-$ treated SERCA2a formed aggregates that were too large to enter the polyacrylamide gel during electrophoresis. Based on this finding, we expected our ST-EPR spectra to show that $ONOO^-$ treatment decreased SERCA2a rotational mobility. However, this was not the case. $ONOO^-$ treatment has no significant effect on the MSL-SERCA2a conventional or ST-EPR spectrum. We observed that the presence of PLN increased SERCA2a rotational mobility, as previously reported (Mahaney et al., 2003; Negash et al., 1996), indicating that our insect cell microsome samples were providing EPR data similar to that obtained using native cardiac SR vesicles, in agreement with previous comparative studies in the Mahaney laboratory (Southall and Mahaney, unpublished results). ST-EPR spectra reflect the average rotational mobility of

all spin-labeled species in the membrane, and while 15% of the $ONOO^-$ treated SERCA2a may have been large aggregates, this population of slow moving enzymes would not have a significant effect on the overall average rotational motion reported by the spectra. Therefore, we concluded that $ONOO^-$ had no significant effect on the rotational mobility of SERCA2a either in the presence or absence of PLN. This suggests that $ONOO^-$ inhibits SERCA2a without causing large scale aggregation of the enzyme.

Since Y294 and Y295 (and Y753) are located on helices that change conformation with Ca^{2+} binding (Toyoshima and Inesi, 2004), we proposed that SERCA2a nitration would most likely cause the enzyme to undergo the Ca^{2+}-dependent E2 to E1•Ca_2 conformational transition. Our [Ca^{2+}]-jump fluorescence experiments using FITC-SERCA2a indicated that $ONOO^-$ treatment inhibited the amplitude of this conformational transition, both in the presence and absence of co-expressed PLN. The presence of PLN (in the control, untreated microsomes) inhibited the amplitude of the E2 to E1•Ca_2 conformational transition, as previously reported by Waggoner and colleagues (2007). However, the $ONOO^-$-dependent decrease in the amplitude of the transition was greater in the presence of PLN compared to the absence of PLN, confirming the activity result that the presence of PLN increased SERCA2a sensitivity to $ONOO^-$. In that $ONOO^-$ treatment did not affect the [Ca^{2+}]-dependence of SERCA2a activity in the absence or presence of PLN, we interpreted this change in amplitude to reflect the decreased number of active enzymes following $ONOO^-$ treatment capable of undergoing the E2 to E1•Ca_2 conformational transition. Additional fluorescence studies are needed to confirm

(or refute) this interpretation, including using fluorescence probes that allow us to monitor other conformational changes in the enzyme, such as the probe 5-[2-[(2-Iodo-1-oxoethyl)amino]ethylamino]-1-naphthalenesulfonic acid (IAEDANS) (Waggoner et al., 2007).

Multiple attempts were made to use mass spectrometry to determine the exact sites of nitration on SERCA2a for our microsomal samples in collaboration with Dr. Rich Helm and Dr. Keith Ray. The main questions we sought to answer were (1) are the sites of nitration for our microsomal samples the same as those reported by Knyushko and colleagues (2005), and (2) does the presence of PLN change the sites of nitration, or perhaps the extent of nitration at the various sites? Due to the very limited amount of expressed SERCA2a in the insect cell microsomes compared to a large protein background and our inability to purify the expressed SERCA2a and obtain enough protein for mass spectrometric analysis, all mass spectrometry data was inconclusive. In that Bigelow's lab had previously reported that nitration of Y294 and Y295 as important for the $ONOO^-$-dependent inhibition of SERCA2a activity, we constructed SERCA2a containing phenylalanine at positions 294 and 295 in place of the tyrosine residues and treated these samples with $ONOO^-$ for activity and immunoblot analysis. These samples were active and showed a decreased sensitivity to $ONOO^-$ treatment. One preparation showed no $ONOO^-$-dependent inhibition up to 250 μM $ONOO^-$, whereas a second preparation showed about 50% less inhibition following $ONOO^-$ treatment up to 250 μM compared to the wild-type SERCA2a. While these results are equivocal, they do suggest that Y294/Y295 are important for the observed $ONOO^-$-dependent inhibition of SERCA2a in our microsomal samples.

The amount of expressed Y294F/Y295F-SERCA2a in our insect cell microsomes was too low to test for nitrated SERCA2a by the anti-NY antibody, though the anti-SERCA2a antibody clearly showed SERCA2a was present in the microsomes. We are continuing to improve our Y294F/Y295F-SERCA2a expression and isolation to allow for a more thorough test of the role of these specific tyrosine residues in the mechanism of SERCA2a inhibition by $ONOO^-$-dependent nitration.

In the Ca^{2+} bound E1 intermediate state, tyrosine residues 294 and 295 on the luminal end of M4 are hydrogen bonded with the proximal residue glutamate 785 on M5, which helps stabilize the configuration of the membrane helices that form the high affinity binding sites. In contrast, in the Ca^{2+} free E2 intermediate form, Y294/Y295 have rotated away from E785 and are no longer hydrogen bonded. Since residues in M4 and M5 make up the majority of residues that form the Ca^{2+} binding sites, any perturbation of the reversible hydrogen bonding between Y294/Y295 and E785 would be expected to affect enzyme activity. Ca-ATPase nitration at Y294 and Y295 by $ONOO^-$ would be such an example, where the increased negative charge would disrupt these conformation-dependent H-bonding interactions. Our overall results agree with the model that (Knyushko et al., 2005), nitration of Y294/Y295 disrupts specific conformational changes required for high affinity Ca^{2+} binding and translocation during the enzyme cycle leading to enzyme inhibition. However, we expected to observe changes in the $[Ca^{2+}]$-dependence of Ca-ATPase activity and a change in the rate of EP dephosphorylation, both of which are dependent on Ca^{2+} interaction at the high affinity Ca^{2+} transport sites. To reconcile this, we concluded that nitration at

Y294/Y295 completely inactivates the enzyme unit, rather than inhibiting Ca^{2+} transport by inhibiting specific steps in the enzyme cycle. By inhibiting enzyme units, the concentration of active enzyme in the sample decreases ($[E_T]$), which leads to a decrease in V_{max} without a change in the rate of the individual steps in the enzyme cycle for the enzymes that remain un-nitrated and active. This is consistent with a change in amplitude in the fluorescence experiment, which reflects a lower number of enzymes undergoing the E2 to E1•Ca_2 conformational transition after $ONOO^-$ treatment than before in the control, untreated sample. Finally, the results using the Y294F/Y295F double mutant confirm this conclusion, at least in part, by showing that much of the $ONOO^-$-dependent Ca-ATPase inhibition was avoided when residues at position 294 and 295 could not be nitrated.

Our observation that nitration of the Ca-ATPase inactivates the enzyme supports the model describing Ca-ATPase as sensor for nitrative stress in cardiac muscle. Nitration of the Ca-ATPase would decrease overall Ca-ATPase activity, slowing down cellular mechanics through the conservation of ATP, since the Ca-ATPase uses the majority of ATP produced in the muscle cell. Though this would result in extended calcium transients and slowed contraction and relaxation times, the reduced demand for ATP would slow ATP production by the mitochondria, reducing free radical generation, and allowing the cell's antioxidant defenses additional time to scavenge and destroy remaining radicals and repair cellular damage to proteins, lipids and nucleic acids. Presuming the presence of the as yet undiscovered denitrase enzyme, the Ca-ATPase could be reactivated by removal of the nitrate groups on the enzyme when the cell has

sufficiently recovered from the nitrative stress event. The cardiac Ca-ATPase is nitrated at lower levels as compared to skeletal muscle Ca-ATPase, suggesting the heart is better equipped in maintaining lower levels of nitration, possibly maintaining special repair mechanics. An interesting question that remains is why treatment of Ca-ATPase with $ONOO^-$ results in only partial inhibition, even at very high $ONOO^-$ levels. If $ONOO^-$ is truly an irreversible inactivator of Ca-ATPase, it would be expected to completely inhibit the enzyme at sufficiently high $ONOO^-$ levels. However we did not observe this behavior, nor did the Bigelow lab before us. It is possible that the enzyme has limited overall sensitivity to $ONOO^-$ due to its role as a reversible sensor for nitrative stress. Future work along these lines should help provide insight in both areas.

$ONOO^-$ is a dangerous free radical produced in increasing amounts during the biological aging process. Unfortunately, as we age, our antioxidant systems cannot keep up with the large amount of free radicals produced resulting in cellular damage. In the case of the Ca-ATPase, age-dependent nitration of SERCA2a leads to an inhibition of Ca^{2+} transport activity, which in turn slows the rate of cardiac muscle relaxation in preparation for the next heart beat. This functional effect mimics several cardiovascular diseases, and may well exacerbate the effects of these diseases, and vice versa. Understanding the mechanism of protein nitration and its effects on enzyme activity is an important step in finding solutions to this protein damage and inactivation, and therapeutic intervention to slow or even reverse the effects of cardiovascular disease.

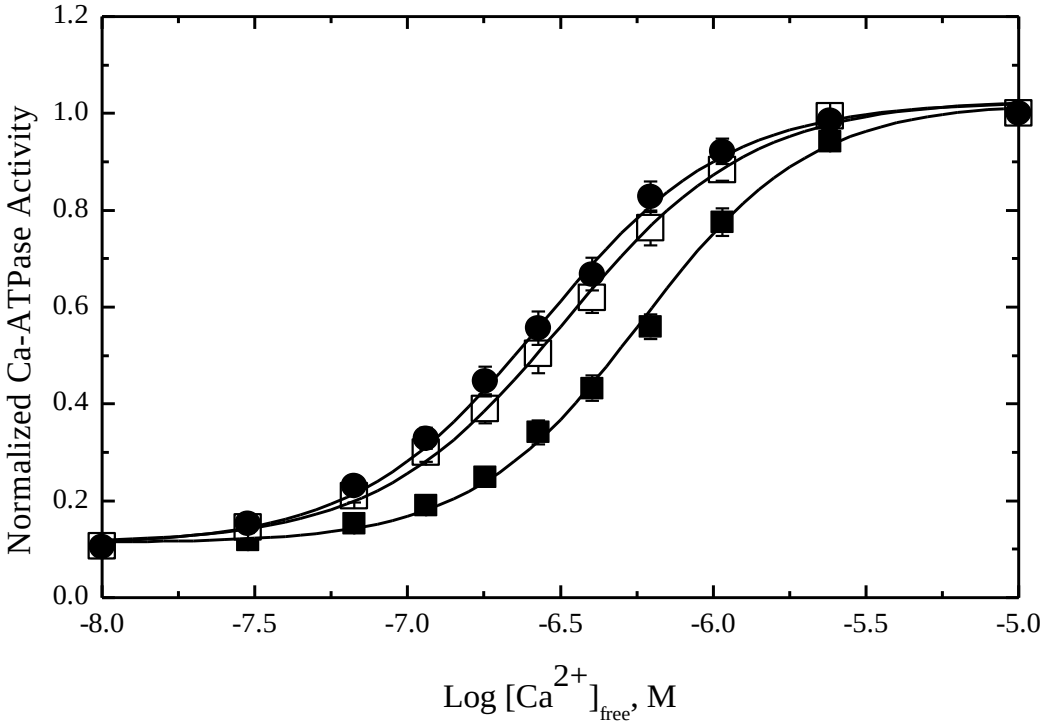

Figure 2-1. Effect of PLN on the [Ca^{2+}]-dependent Ca-ATPase activity of expressed SERCA2a in HF insect cell microsomes. HF microsomes (0.05 mg total protein/mL) containing SERCA2a alone (filled circles) or SERCA2a + PLN (filled squares) were assayed at 37˚C in a medium containing 50 mM MOPS, 3 mM Mg_2Cl, 100 mM KCl, 1 mM EGTA and 0-1.0 mM $CaCl_2$, pH 7.0, to give the desired ionized [Ca^{2+}], as previously determined (Waggoner et al., 2007). Each assay was initiated by the addition of 5 mM MgATP to the incubation tube. The microsomes were pretreated with 20 μg A23187 per mg protein in the incubation medium to prevent Ca^{2+} accumulation in the microsomes. The SERCA2a content of each sample was matched at 16%, which facilitated direct comparison of the activity data. To assess the inhibitory effect of PLN on Ca-ATPase activity, a SERCA2a + PLN sample was incubated for 20 min

on ice with anti-PLN monoclonal antibody, 2D12, at an antibody to protein weight ratio of 1:1 (Waggoner et al., 2004) prior to the assay (empty squares). Calcium-dependent SERCA2a ATPase and Ca^{2+} uptake activity data were fit to the Hill equation using the program KFIT to generate values for $K_{0.5}$ and V_{max}. Each curve in was normalized to its maximum value to more clearly demonstrate the effects of treating the SERCA2a + PLN sample (filled squares) with an anti-PLN monoclonal antibody (empty squares). Symbols represent the average of five repetitions, and error bars correspond to the standard error of the mean for each point.

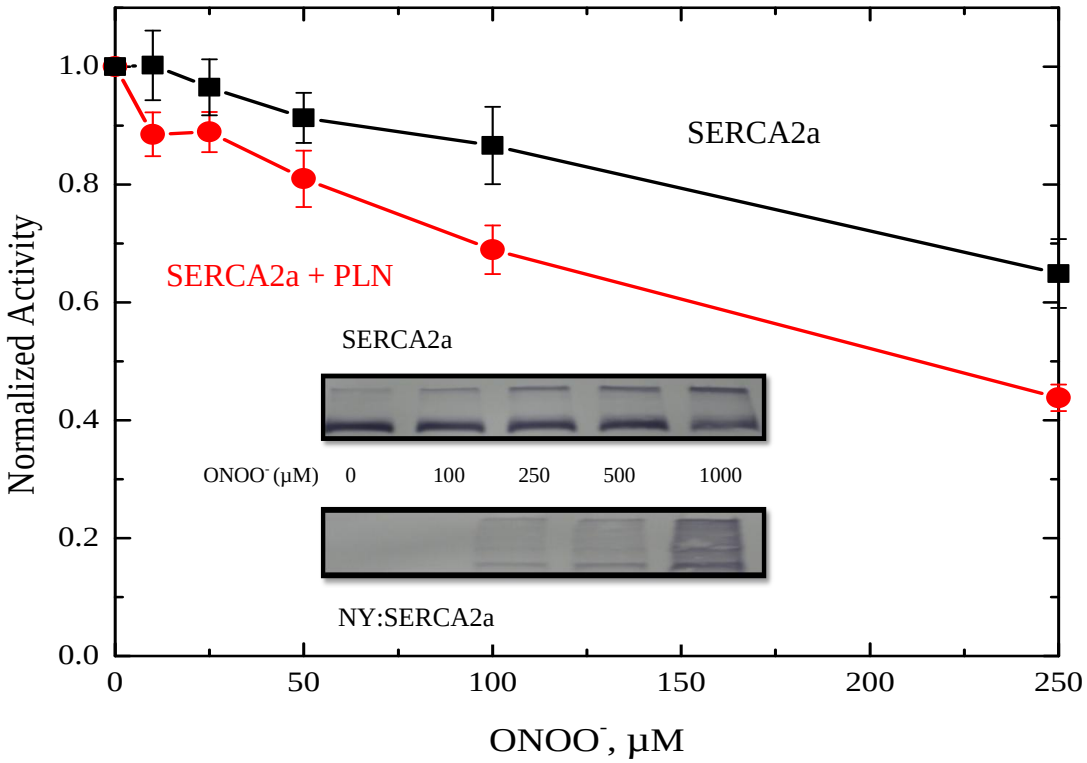

Figure 2-2. PLN increases [$ONOO^-$]-dependent inhibition of SERCA2a activity concomitant with nitrotyrosine formation. HF microsomes containing either SERCA2a expressed alone (squares) or SERCA2a coexpressed with PLN (circles) were suspended (1 mg total protein / ml) in 20 mM imidazole, pH 7.0, treated with the indicated concentrations of peroxynitrite ($ONOO^-$), and incubated for 15 min at room temperature. Ca-ATPase activity was measured at 37˚C at a saturating calcium concentration of 2.4 µM, as described in the text. Symbols represent the average of five repetitions, and error bars correspond to the standard error of the mean for each point. Inset: HF microsomes containing SERCA2a alone (2 mg total protein/mL) were pretreated with $ONOO^-$ at the

indicated levels for 15 min at room temperature, and the microsomal proteins were separated by SDS-PAGE and analyzed by immunoblot. The presence of SERCA2a was detected using anti-SERCA2a monoclonal antibody 2A7-A1 (top) and nitrotyrosine formation on SERCA2a was detected using anti-nitrotyrosine (NY) monoclonal antibody (bottom).

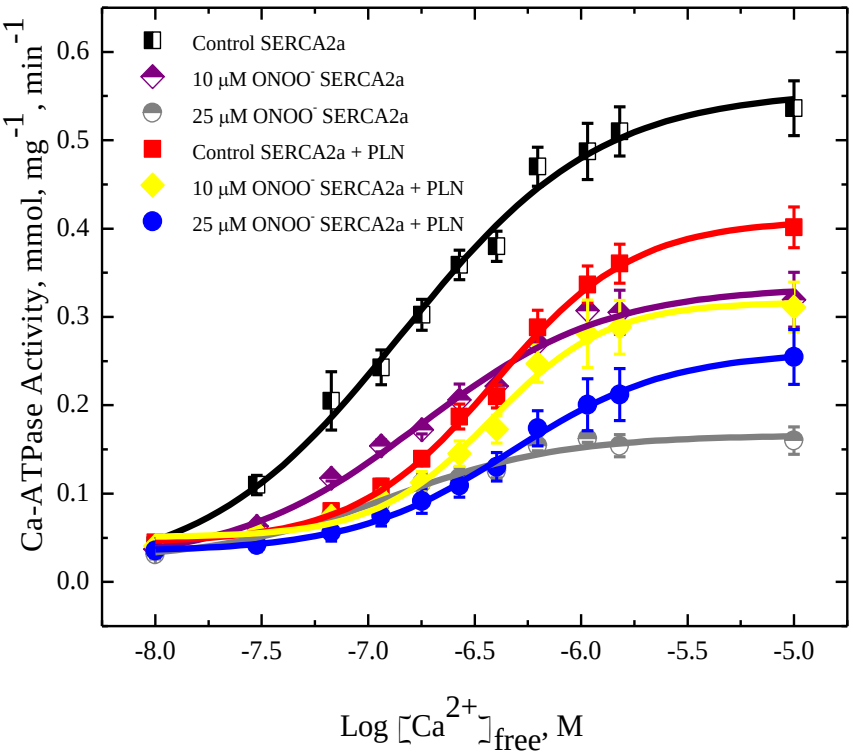

Figure 2-3. $ONOO^-$ inhibited SERCA2a maximal activity without changing the $[Ca^{2+}]$-dependence of SERCA2a ATPase activity in the absence or presence of PLN. HF microsomes containing SERCA2a alone (half-filled squares) or SERCA2a + PLN (filled squares) were suspended (0.2 mg total protein / ml) in 30 mM imidazole, pH 7.0, treated with either 0 (squares), 10 μM (diamonds) or 25 μM $ONOO^-$ (circles) and incubated at room temperature for 15 min, after which the $[Ca^{2+}]$-dependent ATPase activity was measured, as described in the text. Data were fit to the Hill equation using the fitting program KFIT (methods), which provided the V_{max}, the $K_{0.5}$ value, and the Hill coefficient for each sample. Symbols represent the average of five repetitions, and error bars correspond to the standard error of the mean for each point.

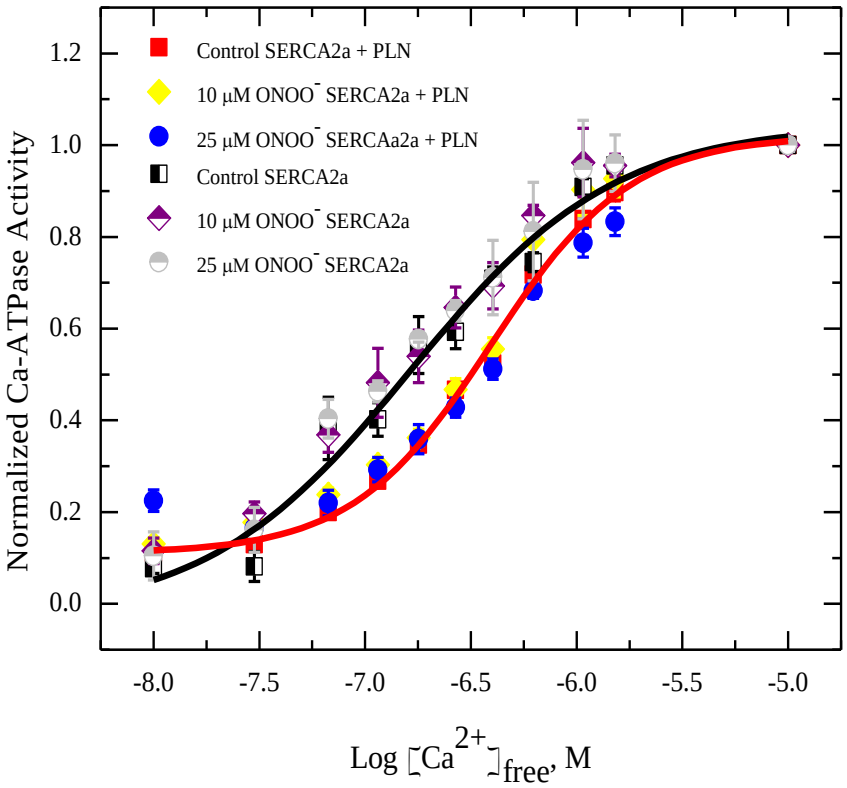

Figure 2-4. Normalized comparison of SERCA2a [Ca^{2+}]-dependent ATPase activity, as modified by PLN and $ONOO^-$. To better illustrate the effect of $ONOO^-$ on SERCA2a [Ca^{2+}]-dependent activity in the absence and presence of PLN, each data set in Figure 2-3 was normalized to the maximum value for that set. Symbols represent the average of five normalized data sets, and error bars correspond to the standard error of the mean for each point.

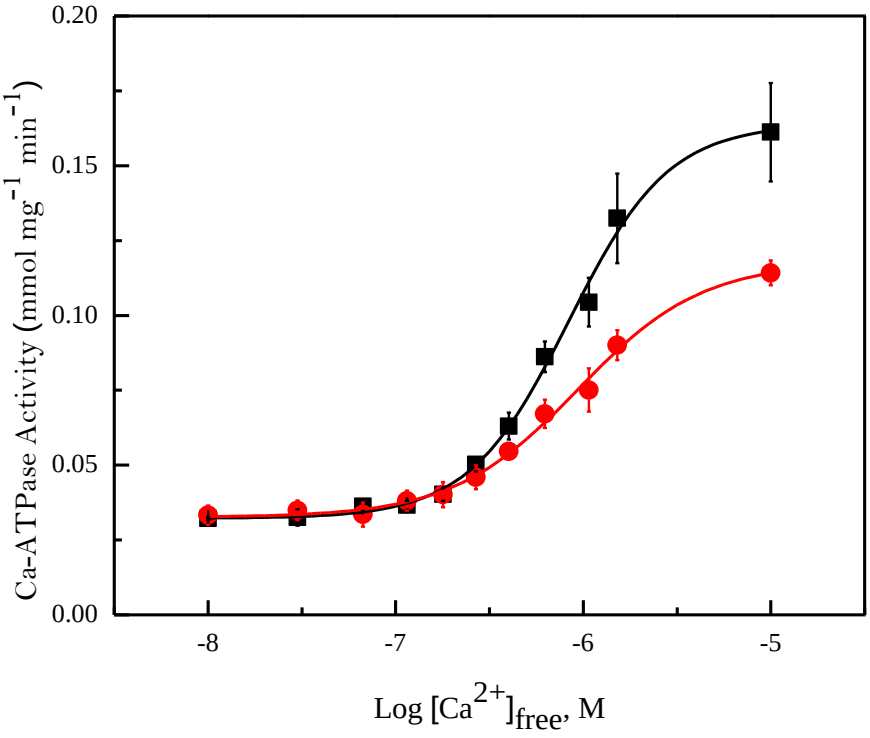

Figure 2-5. $ONOO^-$ inhibited the maximal activity of Y294F/Y295F-SERCA2a but did not affect the $[Ca^{2+}]$-dependence of Ca-ATPase activity. To test the role of SERCA2a tyrosine residues Y294 and Y295 in the mechanism of $ONOO^-$-dependent SERCA2a inhibition, the tyrosine double mutant Y294F/Y295F-SERCA2a was constructed and expressed in HF cells. HF microsomes containing Y294F/Y295F-SERCA2a were suspended (0.2 mg total protein / ml) in 30 mM imidazole, pH 7.0, treated with either 0 (squares) or 10 μM $ONOO^-$ (circles) and incubated at room temperature for 15 min, after which the $[Ca^{2+}]$-dependent ATPase activity was measured. Symbols represent the average of three repetitions, and error bars correspond to the standard error of the mean for each point.

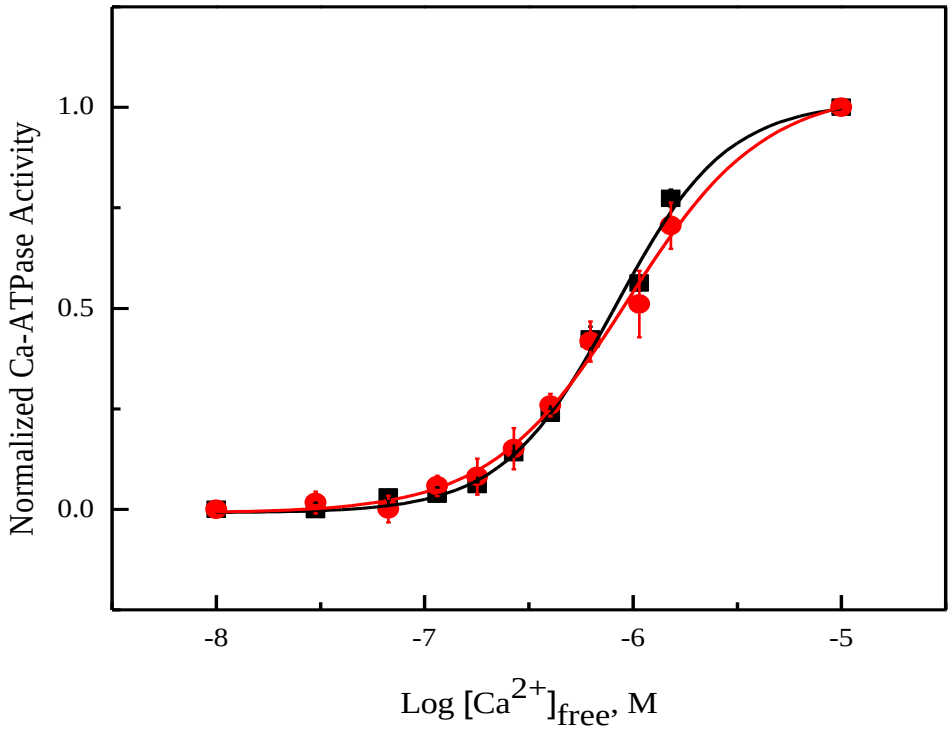

Figure 2-6. Normalized comparison of Y294F/Y295F-SERCA2a [Ca^{2+}]-dependent ATPase activity, as affected by $ONOO^-$. To better illustrate the effect of $ONOO^-$ on SERCA2a [Ca^{2+}]-dependent activity in the absence and presence of PLN, each data set in Figure 2-5 was normalized to the maximum value for that set. Symbols represent the average of three normalized data sets, and error bars correspond to the standard error of the mean for each point.

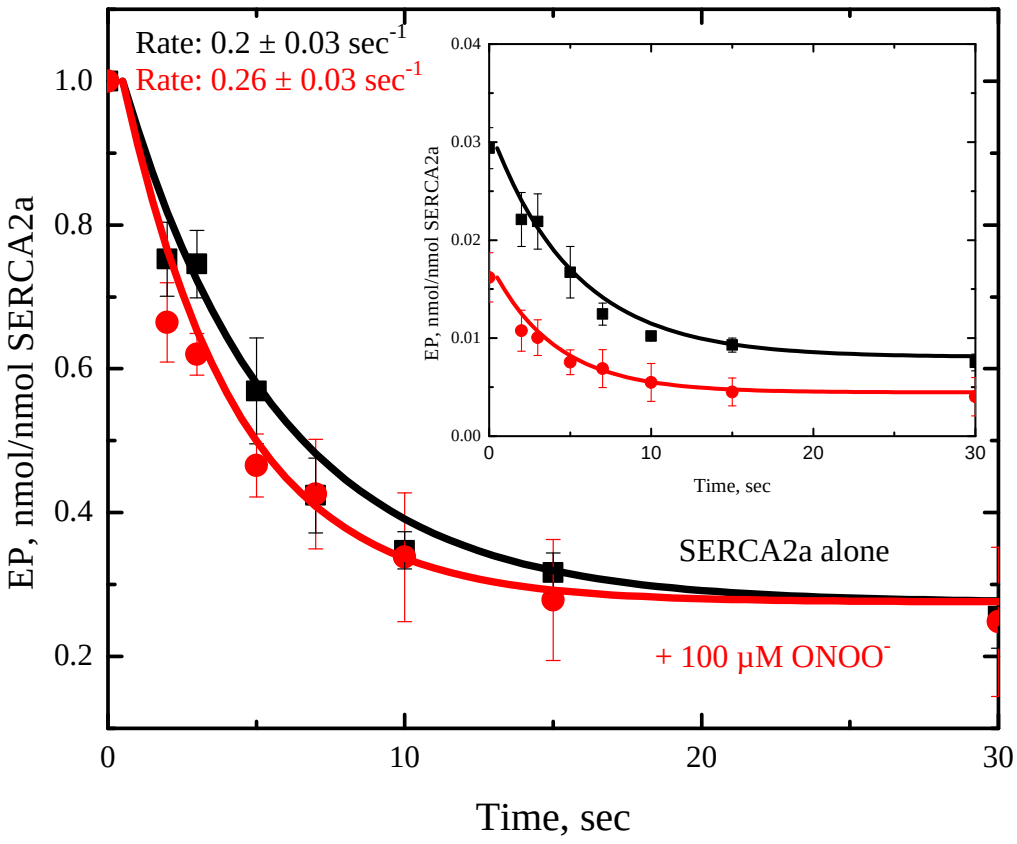

Figure 2-7. $ONOO^-$ did not significantly affect the rate of SERCA2a phosphoenzyme decay. HF microsomes containing SERCA2a alone were suspended (1 mg total protein / ml) in 30 mM imidazole, pH 7.0, treated with 0 (squares) or 100 µM (circles) $ONOO^-$ and incubated at room temperature for 15 minutes. The microsomes were diluted to 0.25 mg/ml in an ice cold solution of 50 mM MOPS, pH 7.0, 3 mM Mg_2Cl, 100 mM KCl, 1 mM EGTA and 0.7 mM $CaCl_2$ (ionized $[Ca^{2+}]$ 0.625 µM), and incubated on ice. The microsomal SERCA2a was phosphorylated by 10 µM [γ-^{32}P]ATP (final concentration) for 30 sec, after which 5 mM EGTA (final concentration) was added to the reaction

mixture to chelate the Ca^{2+} and halt subsequent EP formation. The time-dependent decay of radio-labeled SERCA2a phosphoenzyme (EP) was monitored at 0˚C by acid quenching the sample at serial times following EGTA addition as indicated. The quenched samples were processed as described in the text. The raw data (inset) were normalized (main panel) to the steady-state EP level at time zero for each sample, to facilitate direct comparison of the two time-courses. Symbols represent the average of three repetitions, and error bars correspond to the standard error of the mean for each point.

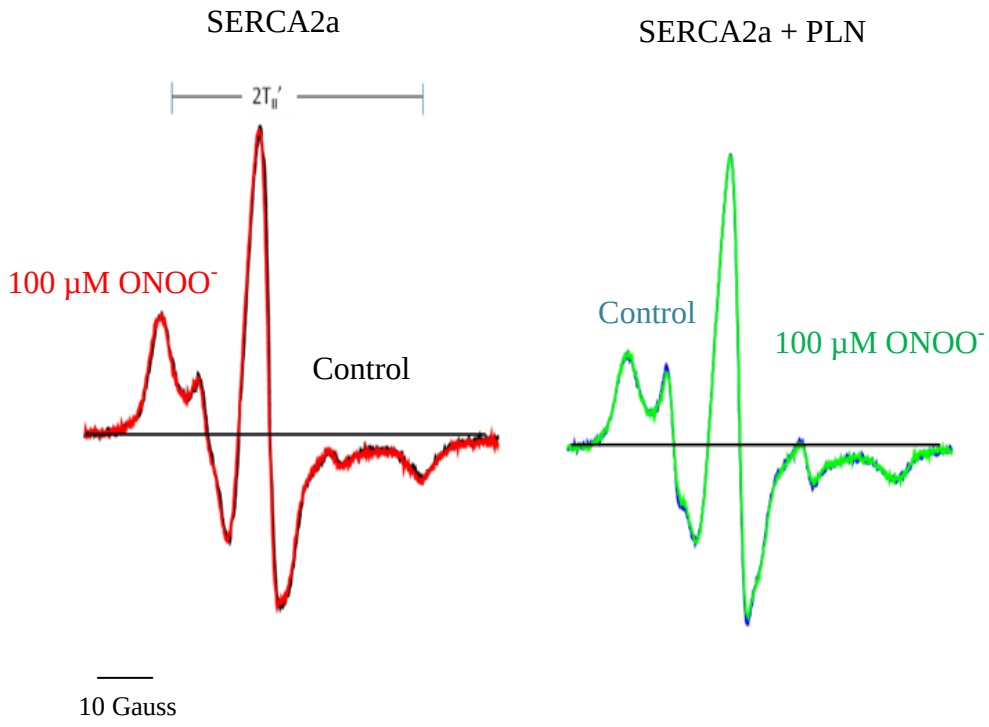

Figure 2-8. ONOO- had no effect on the conventional EPR spectrum of MSL-SERCA2a in HF microsomes. HF microsomes containing SERCA2a expressed alone (left, black and red) or SERCA2a + PLN (right, blue and green) were spin labeled with MSL as described in the text. The spin-labeled microsomes were treated with 0 (black and blue) or 100 µM $ONOO^-$ (red and green) and incubated for 15 min at room temperature, then prepared for EPR analysis. The spectra for each sample type are shown overlaid to facilitate comparison of $ONOO^-$ effects between the two samples. The conventional EPR spectra were analyzed by the outer splitting, $2T_{\parallel}'$, as defined in the figure. The experimental temperature was 4˚C.

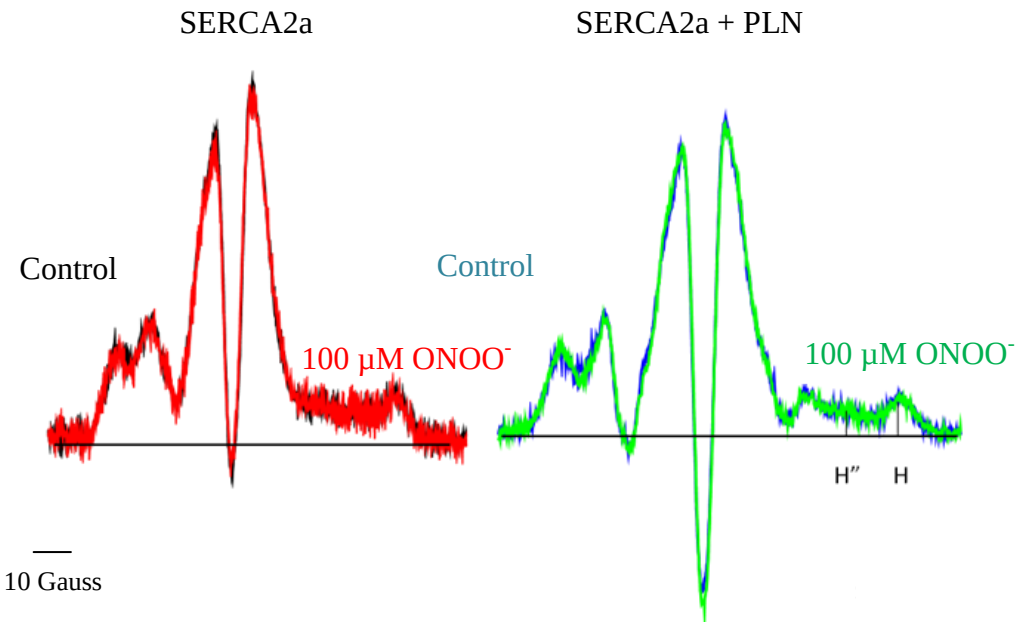

Figure 2-9. $ONOO^-$ had no effect on the ST-EPR spectrum of MSL-SERCA2a in HF microsomes. Using the same samples utilized in Figure 2-7, the saturation transfer EPR spectrum of MSL-SERCA2a at 4˚C in the absence (left, black and red) and presence (right, blue and green) of co-expressed PLN in HF microsomes treated with 0 (black and blue) or 100 µM (red and green) $ONOO^-$ was obtained as described in the text. ST-EPR spectra were analyzed by the high-field (H″/H) line-height ratio, which was used to determine the rotational correlation time for MSL-SERCA2a in each sample, based on standard curves constructed from a model system.

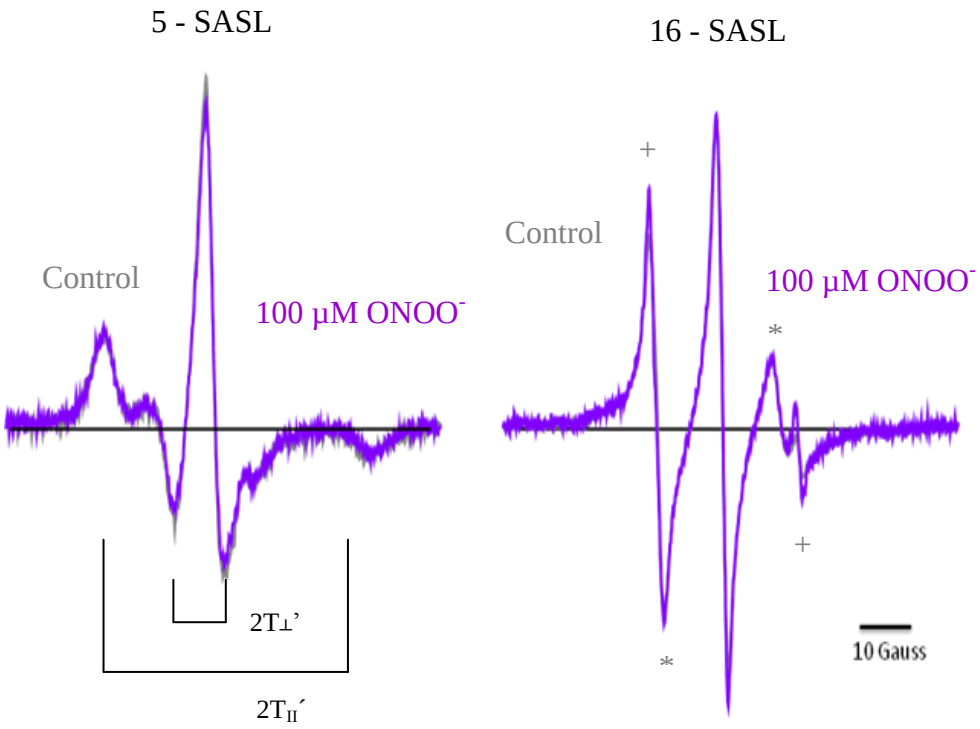

Figure 2-10. $ONOO^-$ had no effect on the conventional EPR spectra of 5-SASL and 16-SASL in HF microsomes. HF microsomes containing SERCA2a expressed alone were spin labeled with either 5-SASL (left) or 16-SASL (right) as described in Materials and Methods. The spin-labeled microsomes were treated with 0 (grey) or 100 µM (purple) $ONOO^-$, then prepared for EPR analysis. The spectra for each sample type are shown overlaid to facilitate comparison of $ONOO^-$ effects between the two samples. The EPR spectra were analyzed by the outer, $2T_{\parallel}'$ (larger bracket, 5-SASL, left and + signs, 16-SASL,

right) and inner $2T_{\perp}'$ (smaller bracket, 5-SASL, left and * signs, 16-SASL, right) splitting, which were used to determine the effective order parameter for the lipid hydrocarbon chains at each bilayer depth, as described in the text. The experimental temperature was 4˚C.

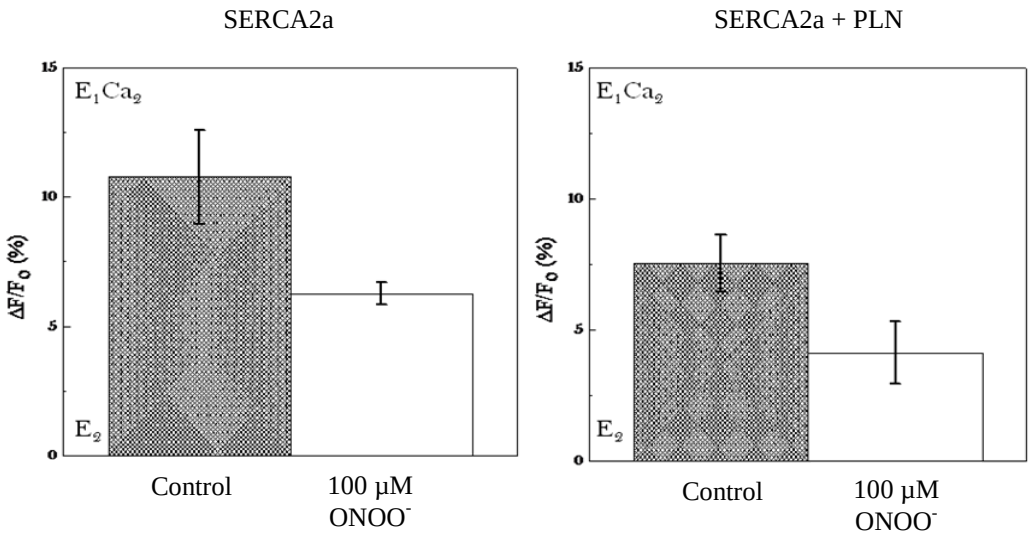

Figure 2-11. $ONOO^-$ inhibited the SERCA2a E2 to E1•Ca_2 conformational transition. HF insect cell microsomes containing SERCA2a expressed alone (left) or SERCA2a + PLN (right) were labeled with FITC as described in the text, then treated with 0 (dark grey) or 100 μM (light grey) $ONOO^-$ and incubated for 15 min at room temperature. The treated microsomes were suspended (0.35 mg total protein/mL) in 50 mM MOPS, pH 7.0, 3 mM Mg_2Cl, 100 mM KCl containing 1 mM EGTA without added Ca^{2+} ($[Ca^{2+}]_{free}$ ~ 0) to stabilize FITC-SERCA2a in the Ca^{2+}-free state. The steady state fluorescence intensity was recorded prior to and following the addition of 1 mM $CaCl_2$ (final $[Ca^{2+}]_{free}$ ~ 100 μM), and the $[Ca^{2+}]$-dependent change in fluorescence (ΔF) was divided by the initial fluorescence reading (F_o) and expressed as a percentage. Values represent the average of six independent experiments and error bars represent the standard error of the mean. The experimental temperature was 25˚C.

REFERENCES

AUTRY, J. M. & JONES, L. R. 1997. Functional Co-expression of the Canine Cardiac Ca2+ Pump and Phospholamban in Spodoptera frugiperda (Sf21) Cells Reveals New Insights on ATPase Regulation. *J. Biol. Chem.,* 272**,** 15872-15880.

BARREIRO, E., COMTOIS, A. S., GEA, J., LAUBACH, V. E. & HUSSAIN, S. N. A. 2002. Protein Tyrosine Nitration in the Ventilatory Muscles . Role of Nitric Oxide Synthases. *Am. J. Respir. Cell Mol. Biol.,* 26**,** 438-446.

BECKMAN, J. S. & KOPPENOL, W. H. 1996. Nitric Oxide, Superoxide, and Peroxynitrite: The Good, the Bad, and the Ugly. *The American Physiological Society*.

BERLETT, B. S. & STADTMAN, E. R. 1997. Protein Oxidation in Aging, Disease, and Oxidative Stress. *Journal of Biological Chemistry,* 272**,** 20313-20316.

BIGELOW, D. J., SQUIER, T. C. & THOMAS, D. D. 1986. Temperature Dependence of Rotational Dynamics of Protein and Lipid in Sarcoplasmic Reticulum Membranes. *Biochemistry,* 25**,** 194-202.

BIRMACHU, W., NISSWANDT, F. L. & THOMAS, D. D. 1989. Conformational Transitions in the Calcium Adenosine Triphosphatase Studied by Time-Resolved Fluorescence Resonance Energy Transfer. *Biochemistry,* 28**,** 3940-3947.

EAST, M. J. 2000. Sarco(endo)plasmic Reticulum Calcium Pumps: Recent Advances in Our Understanding of Structure/Function and Biology. *Mol. Membr. Biol,* 17**,** 189-200.

GORNALL, A. G., BARDAWILL, C., J. & DAVID, M., M. 1949. Determination of Serum Proteins by Means of the Biuret Reaction. *Journal of Biological Chemistry,* 177**,** 751-767.

HARMAN, D. 1956. Aging: A Theory Based on Free Radical and Radiation Chemistry. *J Gerontol,* 11**,** 298-300.

JUHASZOVA, M., RABUEL, C., ZOROV, D. B., LAKATTA, E. G. & SOLLOTT, S. J. 2005. Protection in the Aged Heart: Preventing the Heart-Break of Old Age? *Cardiovasc Res,* 66**,** 233-244.

KNYUSHKO, T. V., SHAROV, V. S., WILLIAMS, T. D., SCHONEICH, C. & BIGELOW, D. J. 2005. 3-Nitrotyrosine Modification of SERCA2a in the Aging Heart: A Distinct Signature of the Cellular Redox Environment. *Biochemistry,* 44**,** 13071-13081.

LAKATTA, E. G. & SOLLOTT, S. J. 2002. The "Heartbreak" of Older Age. *Mol. Interv.,* 2**,** 431-446.

LANZETTA, P. A., ALVAREZ, L. J., REINACH, P. S. & CANDIA, O. A. 1979. An Improved Assay for Nanomole Amounts of Inorganic Phosphate. *Analytical Biochemistry,* 100**,** 95-97.

MACLENNAN, D. H., RICE, W. J. & GREEN, N. M. 1997. The Mechanism of Ca^{2+} Transport by Sarco(endo)plasmic Reticulum Ca-ATPases. *J. Biol. Chem.,* 272**,** 28815-28828.

MAHANEY, J. E., ALBERS, R. W., KUTCHAI, H. & FROEHLICH, J. P. 2003. Phospholamban Controls Ca2+ Pump Oligomerization and Intersubunit Free Energy Exchange Leading to Activation of Cardiac Muscle SERCA2a. *N.Y. Acad. Sci,* 986**,** 1-3.

MAHANEY, J. E., AUTRY, J. M. & JONES, L. R. 2000. Kinetic Studies of the Cardiac Ca-ATPase Expressed in Sf21 Cells: New Insights on Ca-ATPase Regulation by Phospholamban. *Biophysical Journal,* 78**,** 1306-1323.

MAHANEY, J. E. & THOMAS, D. D. 1991. Effects of Melittin on Molecular Dynamics and Ca-ATPase Activity in Sarcoplasmic Reticulum Membranes: Electron Paramagnetic Resonance. *Biochemistry,* 30**,** 7171-7180.

MARLA, S. S., LEE, J. & GROVES, J. T. 1997. Peroxynitrite Rapidly Permeates Phospholipid Membranes. *Proceedings of the National Academy of Sciences of the United States of America,* 94**,** 14243-14248.
NEGASH, S., CHEN, L. T., BIGELOW, D. J. & SQUIER, T. C. 1996. Phosphorylation of Phospholamban by cAMP-Dependent Protein Kinase Enhances Interactions Between Ca-ATPase Polypeptide Chains in Cardiac Sarcoplasmic Reticulum Membranes. *Biochemistry,* 35**,** 11247-11259.
REITER, C. D., TENG, R.-J. & BECKMAN, J. S. 2000. Superoxide Reacts with Nitric Oxide to Nitrate Tyrosine at Physiological pH via Peroxynitrite. *J. Biol. Chem.,* 275**,** 32460-32466.
SCHÖNEICH, C. & SHAROV, V. S. 2006. Mass Spectrometry of Protein Modifications by Reactive Oxygen and Nitrogen Species. *Free Radical Biology and Medicine,* 41**,** 1507-1520.
SHAROV, V. S., DREMINA, E. S., GALEVA, N. A., WILLIAMS, T. D. & SCHONEICH, C. 2006. Quantitative Mapping of Oxidation-Sensitive Cysteine Residues in SERCA in vivo and in vitro by HPLC-Electrospray-Tandem MS: Selective Protein Oxidation During Biological Aging. *Biochemistry Journal,* 394**,** 605-615.
SIMMERMAN, H. K. B. & JONES, L. R. 1998. Phospholamban: Protein Structure, Mechanism of Action, and Role in Cardiac Function. *Physiological Reviews,* 78**,** 921-946.
SMALLWOOD, H. S., GALEVA, N. A., BARTLETT, R. K., URBAUER, R. J. B., WILLIAMS, T. D., URBAUER, J. L. & SQUIER, T. C. 2003. Selective Nitration of Tyr99 in Calmodulin as a Marker of Cellular Conditions of Oxidative Stress. *Chemical Research in Toxicology,* 16**,** 95-102.
SOUZA, J. M., DAIKHIN, E., YUDKOFF, M., RAMAN, C. S. & ISCHIROPOULOS, H. 1999. Factors Determining the Selectivity of Protein Tyrosine Nitration. *Archives of Biochemistry and Biophysics,* 371**,** 169-178.
SOUZA, J. M., PELUFFO, G. & RADI, R. 2008. Protein Tyrosine Nitration - Functional Alteration of Just a Biomarker. *Free Radical Biology and Medicine,* 45.
SQUIER, T. C. 2001. Oxidative Stress and Protein Aggregation During Biological Aging. *Experimental Gerontolgy,* 36**,** 1539-1550.
SQUIER, T. C. & THOMAS, D. D. 1986. Methodology for Increased Precision in Saturation Transfer Electron Paramagnetic Resonance Studies of Rotational Dynamics. 49**,** 921-935.
TOYOSHIMA, C. & INESI, G. 2004. Structural Basis of Ion Pumping by Ca^{2+}-ATPase of the Sarcoplasmic Reticulum. *Annual Review of Biochemistry,* 73**,** 269-292.
VINER, R. I., FERRINGTON, D. A., HUHMER, A. F. R., BIGELOW, D. J. & SCHONEICH, C. 1996. Accumulation of Nitrotyrosine on the SERCA2a Isoform of SR Ca-ATPase of Rat Skeletal Muscle During Aging: A Peroxynitrite-Mediated Process. *Federation of Biochemical Societies,* 379**,** 286-290.
VINER, R. I., FERRINGTON, D. A., WILLIAMS, T. D., BIGELOW, D. J. & SCHONEICH, C. 1999a. Protein Modification During Biological Aging: Selective Tyrosine Nitration of the SERCA2a Isoform of the Sarcoplasmic Reticulum Ca-ATPase in Skeletal Muscle. *Biochemical Journal,* 340**,** 657-669.
VINER, R. I., WILLIAMS, T. D. & SCHONEICH, C. 1999b. Peroxynitrite Modification of Protein Thiols: Oxidation, Nitrosylation, and S-Glutathiolation of Functionally Important Cysteine Residue(s) in the Sarcoplasmic Reticulum Ca-ATPase. *38,* 12408-12415.
WAGGONER, J. R., HUFFMAN, J., FROELICH, J. P. & MAHANEY, J. E. 2007. Phospholamban Inhibits Ca-ATPase Conformational Changes Involving the E2 Intermediate. *Biochemistry,* 46**,** 1999-2009.

WAGGONER, J. R., HUFFMAN, J., GRIFFITH, B. N., JONES, L. R. & MAHANEY, J. E. 2004. Improved Expression and Characterization of Ca^{2+}-ATPase and Phospholamban in High-Five Cells. *Protein Expression and Purification,* 34**,** 56-67.

WAGGONER, J. R. & KRANIAS, E. G. 2005. Role of Phospholamban in the Pathogenesis of Heart Failure. *Heart Failure Clinics,* 1**,** 207-218.

ZHANG, H., BHARGAVA, K., KESZLER, A., FEIX, J., HOGG, N., JOSEPH, J. & KALYANARAMAN, B. 2003. Transmembrane Nitration of Hydrophobic Tyrosyl Peptides. *Journal of Biological Chemistry,* 278**,** 8969-8978.

Chapter 3

Physical Mechanism of Ca-ATPase Stimulation by HNO

This study is part of a larger project in collaboration with Dr. Nazareno Paolocci's lab at The Johns Hopkins Medical Institutions. This study will be combined with physiological studies from the Paolocci lab in preparation of a larger manuscript for Circulation Research. The work presented here was contributed by me.

Introduction

Congestive heart failure (CHF) is the leading cause of mortality and morbidity worldwide (Tocchetti et al., 2007, Mahaney et al., 2003, Birmachu et al., 1989). The root of CHF is the weakened ability of the heart to cycle Ca^{2+}, which leads to a diminished ability to contract and relax. Organic nitrates such as nitroglycerin are widely used for the treatment of CHF because of their capacity to work as vasodilators. Conversely, these agents, as well as direct nitric oxide (NO), donors also influence cardiac contraction (Paolocci et al., 2003). Nitroxyl (HNO), the one electron reduction product of NO, has recently gained awareness as a potential pharmacological therapy in the treatment of heart failure. In particular, HNO has the ability to stimulate both cardiac contraction and relaxation (Paolocci et al., 2007). For this reason, HNO differs from other CHF therapies, suggesting its use as a cardiac enhancement agent for non-pathological uses (i.e. aging). Despite clinical studies showing that HNO improves cardiac muscle contraction and relaxation, the molecular mechanism by which HNO enhances contraction and relaxation is still not known. It is important to understand the effects of HNO at a molecular level to help evaluate HNO as a therapy for CHF.

HNO is the one-electron reduction product of NO (Paolocci et al., 2007), and *in vivo* leads to positive inotropy/lusitropy in both normal (Paolocci et al., 2001) and failing hearts (Paolocci et al., 2003). HNO reacts rapidly with thiols (-SH) and is believed to target critical reactive thiolates (RS-) in proteins without affecting the overall intracellular thiol content (Lopez et al., 2007). To date, direct effects of HNO on the Ca^{2+} release channel (the ryanodine receptor, RyR)

(Tocchetti et al., 2007), troponin C, the Ca-ATPase (Lancel et al., 2009), and phospholamban (PLN) have been reported, but the molecular details of these effects are not well understood. In terms of the Ca^{2+} release channel, HNO treatment increases the open probability of the channel, allowing more SR Ca^{2+} to enter the muscle cell cytoplasm to stimulate contraction (Tocchetti et al., 2007). HNO increases the Ca^{2+} sensitivity of the cardiac myofilaments, leading to increased force development during contraction without directly affecting myosin ATPase activity (Dai et al., 2007). For the Ca-ATPase, HNO stimulates Ca^{2+} uptake activity, potentially by uncoupling the regulatory protein, phospholamban from the Ca-ATPase (Froehlich et al., 2008), though one report suggests direct effects of HNO on the Ca-ATPase by stimulating S-glutathiolation of Cys-674 on the Ca-ATPase (Lancel et al., 2009). In each study, the central role of HNO-dependent thiol modification was demonstrated through the use of cysteine pre-blocking with N-ethyl maleimide (NEM), thiol modification reversibility by dithiothreitol (DTT) and the use of glutathione (GSH) as a HNO scavenger.

The molecular mechanism by which HNO affects Ca-ATPase is perhaps the best understood so far. Tochetti et al. (2007) reported HNO increases by 2-fold the rate of Ca^{2+} uptake in SR in mouse cardiac myocytes, without changing the maximum SR Ca^{2+} store achieved at the end of diastole. Using insect cell microsomes containing Ca-ATPase expressed in the absence and presence of PLN, Froehlich and colleagues (2008) showed that HNO increased by nearly 10-fold the rate of Ca-ATPase dephosphorylation (the rate-limiting step for enzyme turnover). However, these effects were only observed for Ca-ATPase in the presence of coexpressed PLN, not in its absence, suggesting that HNO modifies

the regulatory potency of PLN toward Ca-ATPase. To test the potential role of PLN cysteines in the mechanism of HNO action, Ca-ATPase was expressed with null-cysteine PLN in which the three native cysteine residues (Cys-36, Cys-41, and Cys-46) were replaced with alanine. For this sample, HNO had no effect on the rate of Ca-ATPase dephosphorylation. In this study, HNO activity was shown to be independent of the β-adrenergic PKA signaling pathway and that HNO functions completely differently than that of NO (Tocchetti et al., 2007).

While these studies suggest that HNO modification of PLN cysteine residues leads to increased Ca-ATPase Ca^{2+} transport activity, additional fundamental functional and physical studies are needed to better demonstrate the role of PLN in the mechanism of HNO stimulation of Ca-ATPase. Therefore, in the present study, we have used kinetic techniques to investigate the effects of HNO on PLN regulation of Ca-ATPase activity, and spectroscopic techniques to assess the effects of HNO on PLN regulation of Ca-ATPase conformational transitions and oligomeric protein-protein interactions. The functional and physical effects of PLN on Ca-ATPase have been well established in previous studies by us and others providing a good foundation for testing the effects of PLN on this system.

Material and Methods

Protein Expression, Isolation, and Characterization

Canine cardiac Ca-ATPase (the SERCA2a isoform) and canine PLN were coexpressed in High Five insect cells as reported elsewhere (Waggoner et al., 2004). Microsomes were harvested 48 h after the baculovirus infections and

stored in small aliquots at -80˚C. Protein concentrations were determined by the Biuret method (Gornall et al., 1949) using bovine serum albumin (Sigma) as a standard. The amount of SERCA2a and PLN in the microsomes was quantified by gel electrophoresis and immuno-blotting, using methods described previously (Waggoner et al., 2004). Several different preparations of expressed SERCA2a with or without co-expressed PLN were used in these studies. The Ca-ATPase content of the microsomes was very carefully matched at 16% of the total protein by weight, and the relative proportion of Ca-ATPase to PLN co-expressed in the microsomes was between 1 and 2 mol of PLN/mol of Ca-ATPase (Waggoner et al., 2004). For all preparations, the Ca-ATPase was under full regulatory control by PLN when the two proteins were coexpressed, determined by assays of [Ca^{2+}]-dependent ATPase and Ca^{2+}-uptake activity conducted in the presence and absence of anti-PLN antibody, as reported previously for these samples (Waggoner et al., 2004).

For these studies, the HNO donor Angeli's salt (AS) was used and was provided by Dr. John Toscano of Johns Hopkins University. Stock solutions of AS (100 mM in ice cold 10 mM NaOH) were freshly prepared before each experiment. Serial dilutions were made in ice cold 10 mM NaOH just prior to each experiment and used immediately to provide the desired level of [AS/HNO] for each microsomal SERCA2a sample. AS was added directly to the microsome suspension at the desired final concentration and allowed to incubate for 10-20 minutes at room temperature. The microsome samples were then diluted to the appropriate concentrations for each assay. Throughout this project, we noted that the method of addition of AS/HNO to the microsome samples had a direct

bearing on the results obtained. For examples, we initially used AS at 100x the final desired concentration, and added 1 μL of this stock to 99 μL of a 1 mg/mL solution of microsomes for the activity assays. However, we found that AS was primarily inhibitory toward the Ca-ATPase when added in this fashion, and we found no effects of AS/HNO on the coupling of PLN to Ca-ATPase. Specific control experiments using NaOH vehicle solution and AS-byproduct nitrite addition showed no effect on Ca-ATPase activity or regulation by PLN. We found differences in AS/HNO effects based on whether the AS stock solution was added to more dilute protein (0.2 mg/mL for enzyme assay) or more concentrated protein (10-15 mg/mL in preparation for spin labeling). We experimented with the temperature of the AS solution in 10 mM NaOH, using both room temperature and ice cold AS stocks, and again obtained different results based on the two methods of stock preparation. We also found that the age of the AS stock solution caused differences in our results, noting that freshly prepared, immediately used solutions provided the best consistency for results, whereas solutions that were only a few hours old on ice were not. After many such iterations and trial, we found that when we added a lower concentration of freshly prepared ice cold AS directly to the microsome sample, we obtained consistent results where AS/HNO was considerably less inhibitory toward the Ca-ATPase, and we began to observe reproducible uncoupling effects for PLN and the Ca-ATPase.

SERCA2a ATPase Assay Studies

[AS/HNO]-dependent activation of SERCA2a ATPase activity was measured colorimetrically using the malachite green-ammonium molybdate assay as previously described (Lanzetta et al., 1979). High Five microsomes containing SERCA2a ± PLN were pre-treated with AS/HNO and were incubated at room temperature for 10 minutes. The protein treated with the desired level of AS were suspended (0.05 mg/mL protein) in 50 mM 3-(N-morpholino)propanesufonic acid (MOPS), 3 mM $MgCl_2$, 100 mM KCl, 1 mM ethylenebis-(oxyethylnenitrilo)tetraacetic acid (EGTA), and 0.7 mM $CaCl_2$, pH 7.0, to give the desired ionized [Ca^{2+}]. To initiate the ATPase reaction 5 mM MgATP was added to the incubation tubes at 37˚C and phosphate (P_i) liberation was monitored over a 10 minute period. Samples were pre-treated with 20 μg of Ca^{2+} ionophore A23187/mg of total protein to prevent Ca^{2+} buildup within the microsomes during the assay. The [Ca^{2+}]-dependent ATPase activity of SERCA2a ± PLN in High Five insect cell microsomes pre-treated with 100 μM AS/HNO was measured colorimetrically at 37˚C using the malachite green-ammonium molybdate assay as described above, but the [Ca^{2+}] of the assay medium was varied from 0-1.0 mM $CaCl_2$ to give a range of ionized [Ca^{2+}], as previously determined (Autry and Jones, 1997).

Spin labeling

The overall rotational mobility of the Ca-ATPase was measured by electron paramagnetic resonance (EPR) spectroscopy using the short-chain maleimide spin label, N-(1-oxyl-2,2,6,6-tetra-methyl-4-piperadinyl)maleimide (MSL),

covalently bound to the ATPase as previously described (Squier and Thomas, 1986b, Bigelow et al., 1986). High Five microsomes containing SERCA2a ± PLN were first pre-treated with 100 μM AS for 20 minutes at room temperature. The sample was diluted to 2 mL in 250 mM sucrose buffer, 10 mM imidazole, at pH 7.0 (sucrose buffer) and spun in a microcentrifuge for 10 minutes at 4˚C at 13, 200 rpm to remove the AS reaction mixture. The pelleted samples were resuspended in the residual buffer then treated with N-ethylmaleimide (NEM) for 30 minutes on ice at a ratio of 1.0 mol NEM per mol of expressed SERCa2a to block fast-reacting thiols. After the 30 minute incubation, the microsomes were incubated with 250 μM MSL for 1 hour on ice, at a ratio of 2.5 mol MSL per mol of expressed SERCA2a. Excess spin label was removed by 2 rounds of centrifugation, where the microsomes were diluted into cold 0.3 M sucrose and 20 mM MOPS, pH 7.0, for 30 min at 30, 000 rpm (70000g), 4˚C, in a Beckman Ti45 rotor using a Beckman Optima LE-80K ultra centrifuge. The pellet, containing the MSL-labeled SERCA2a (henceforth denoted MSL-SERCA2a), was re-suspended in 0.3 M sucrose and 20 mM MOPS at pH 7.0 and stored on ice until use.

A few methods of treating the microsomes with AS prior to EPR were attempted here as well. Treatment of AS/HNO after pre-blocking with NEM and spin-labeling with MSL led to a near total loss of intensity in the EPR spectrum. It is possible that HNO chemically reacted with the bound MSL spin label, destroying the nitroxide functionality, or that HNO, being a cysteine modifier, displaced the bound MSL from the Ca-ATPase at Cys-344. Therefore, we adopted

the method of using ice cold AS/HNO added directly to the microsomes and incubated for 10-20 minutes at room temperature, followed by pelleting the treated microsomes by table-top centrifugation to remove any excess AS/HNO prior to the spin labeling procedure.

EPR Spectroscopy:

EPR spectra were obtained using a Bruker ER 200D spectrometer equipped with a Bruker ER 4102ST cavity. Submicrosecond rotational motion of spin labels was detected by conventional EPR (first harmonic absorption in phase, designated V1) using 100 kHz field modulation, a peak-to-peak amplitude of 2 gauss (G), and a microwave field amplitude of 0.032 G. Submillisecond rotational motion of spin labels was detected by saturation-transfer EPR (second harmonic absorption out of phase, designated V2') using a 50 kHz field modulation, with a modulation amplitude of 5.0 G, and a microwave field intensity of 0.25 G. Samples were contained in 50 μL glass capillaries. Sample temperature was controlled at 4˚C with a Bruker ER 4111VT variable temperature controller. Spectra were digitized and stored on a PC and analyzed using the program EWWIN, written by Philip Morse (Scientific Software Solutions).

EPR Spectral Analysis

MSL-SERCA2a and MSL-SERCA2a + PLN in High Five insect cell microsome conventional spectra were analyzed by the outer splitting parameter ($2T_{II}'$). ST-EPR spectra were analyzed by line shape parameter (Squier and Thomas, 1986b), which provided the effective rotational correlation time (τ_r) for

spin-labeled SERCA2a, which was determined from a standard curve constructed from an isotropically tumbling models system (Squier and Thomas, 1986b, Mahaney and Thomas, 1991).

Labeling of Ca-ATPase with FITC

SERCA2a and SERCA2a + PLN expressed in insect cell microsomes were labeled by florescein isothiocyanate (FITC) according to Birmachu and colleagues (1989). A fresh stock of 5 mM FITC in N, N- dimethylformamide was prepared prior to each experiment. The microsomes were incubated with FITC at a ratio of 0.9 mol FITC per mol of SERCA2a in a labeling buffer containing 60 mM Tris, 10 mM $MgCl_2$, and 200 mM KCl at a pH of 8.7 for 30 min at room temperature. BSA (1 mg/mL) was added to the solution and incubated for 20 minutes on ice to remove any unbound label. Excess reagent and BSA were removed by pelleting the microsomes by centrifugation for 30 min at 30, 000 rpm, 4˚C, in a Beckman Coulter Ti45 rotor. The pellet, containing the FITC-labeled SERCA2a (henceforth denoted FITC-SERCA2a), was resusupended in 0.3 M sucrose and 20 mM MOPS. High Five microsomes were pre-treated with 100 μM AS/HNO prior to addition of the FITC and washed for 10 minutes, at 4˚C at 13, 200 rpm.

Fluorescence Measurements

Measurements of the fluorescence intensity were performed at 25˚C using the Spectramax M5 microplate reader. Excitation and emission spectra of the FITC-SERCA2a showed optimal excitation and emission wavelengths of 490 nm and 505 nm, respectively.

To measure fluorescence intensity changes following a [Ca^{2+}]-jump, insect cell microsomes containing FITC-SERCA2a (~2.5 mg/mL) were suspended in a standard buffer (50 mM MOPS, 100 mM KCl, 3 mM $MgCl_2$, 0 mM $CaCl_2$, 1 mM EGTA, pH 7.0) designed to favor the Ca-free E2 state initially. The addition of 1 mM Ca^{2+} to the standard buffer (final [Ca^{2+}] free ~ 100 μM) promoted the formation of the E1•Ca_2 conformation. The fluorescence intensity was measured by summing the total fluorescence emission (initial fluorescence intensity, F_o) and after (final fluorescence intensity, F) the respective additions. Fluorescence intensity changes were quantified as percent changes, according to the formula 100 x ($F-F_o/F_o$).

Curve Fitting and Error Analysis

Experimental data were fitted using KFIT written by N.C. Millar, which was kindly provided by Dr. Carl Frieden. The best fits of the data were chosen on the basis of the minimization of the sum-of-squares error, χ^2.

Results

HNO stimulates Ca-ATPase activity in (High Five microsomes) in the presence of PLN

The High Five (HF) insect cell microsomes containing expressed SERCA2a without PLN and SERCA2a + PLN used for this study were produced and characterized, as previously described (Waggoner et al., 2004). The microsomes contained approximately 16% SERCA2a by weight total protein, and SERCA2a co-expressed with PLN (approximately 1% PLN by weight total protein) was

under the full regulatory control of PLN. **Figure 3-1** shows the [Ca^{2+}]-dependent ATPase activity for the expressed samples at 37˚C. The data are shown normalized to their respective activity maximum to better demonstrate the effects of PLN on SERCA2a activity. In the absence of PLN, the SERCA2a activity curve (**Figure 3-1**, empty squares) was shifted to the left ($\Delta K_{0.5}$ = 300 nM) relative to SERCA2a + PLN (**Figure 3-1**, empty circles). Pre-treatment of the SERCA2a + PLN sample with anti-PLN antibody 2D12 (**Figure 3-1**, filled circles) increased the apparent Ca^{2+} affinity of the enzyme compared to that of SERCA2a in the absence of PLN.

To determine the effect of AS/HNO on SERCA2a activity and its regulation by PLN, HF microsomes containing SERCA2a alone or co-expressed with PLN were incubated with varying levels of AS/HNO for 20 minutes at room temperature, followed by ATPase activity assay by the inorganic phosphate (P_i) liberation assay (Lanzetta et al., 1979, Waggoner et al., 2004). As shown in **Figure 3-2**, AS/HNO treatment of HF microsomes containing SERCA2a co-expressed with PLN increased SERCA2a activity up to 100 μM AS/HNO, followed by a decline in activity at higher AS/HNO levels. In contrast, in the absence of PLN, SERCA2a activity was slightly but not statistically significantly inhibited by AS/HNO treatment over the same [AS] range. To further probe the effect of HNO on SERCA2a regulation by PLN, we conducted [Ca^{2+}]-dependent SERCA2a ATPase assays in the absence and presence of co-expressed PLN. For these experiments, we used 100 μM AS treatment, which provided the greatest stimulation of SERCA2a activity (**Figure 3-2**), and matches the level of AS used in our previous kinetics studies using HF insect cell microsomes (Froehlich et al.,

2008). **Figure 3-4** shows that treating HF microsomes containing SERCA2a + PLN with AS/HNO resulted in a leftward shift in the SERCA2a [Ca^{2+}]-dependent activity curve ($K_{0.5}$ = 480 nM) relative to untreated microsomes containing SERCA2a + PLN ($K_{0.5}$ = 180 nM) similar to the effect observed when PLN is uncoupled from SERCA2a by treatment with anti-PLN monoclonal antibody, 2D12 (**Figure 3-1**). In contrast, the [Ca^{2+}]-dependent activity curve of SERCA2a in the absence of PLN showed no change following treatment with 100 μM AS ($K_{0.5}$ = 340 nM). These activity results are consistent with the WT and PLN knockout myocyte studies, which showed that HNO stimulation of SERCA2a activity is PLN-dependent. These results extend this conclusion by showing HNO stimulates SERCA2a activity specifically by functionally uncoupling PLN from SERCA2a.

HNO increases Ca-ATPase conformational flexibility in the presence of PLN

We next used fluorescence spectroscopy of SERCA2a covalently labeled with FITC (FITC-SERCA2a) to study the effect of AS/HNO on the [Ca^{2+}]-dependent conformational flexibility of SERCA2a. FITC binds to a single lysine residue on SERCA2a (Lys-514) and inactivates the enzyme by blocking ATP access to the catalytic site on the enzyme. However, the enzyme is still active and sensitive to high affinity Ca^{2+} binding, and undergoes the [Ca^{2+}]-dependent conformational changes associated with transition from the Ca^{2+} free E2 intermediate to the Ca^{2+}-bound E1•Ca_2 intermediate (Birmachu et al., 1989). Therefore, FITC-SERCA2a in the absence (SERCA2a alone) or presence of PLN

(SERCA2a + PLN) was incubated in a Ca^{2+}-free buffer containing 5 mM EGTA to stabilize the enzyme in the Ca^{2+}-free E2 state, and the fluorescence emission intensity of the FITC-SERCA2a was recorded before and after a medium [Ca^{2+}] jump to 5 mM Ca^{2+} (resulting free Ca^{2+} 15 μM) to promote formation of the Ca^{2+}-bound E1•Ca_2 intermediate. For HF microsomes containing SERCA2a without PLN, the fluorescence intensity increased 7.8 ± 1.3 % upon the addition of Ca^{2+}, and treatment of the sample with 100 μM AS/HNO had little effect on this change (8.7 ± 1.0%). In the presence of PLN, the amplitude of the [Ca^{2+}]-dependent E2 to E1•Ca_2 conformational change was inhibited (6.0 ± 0.7 %) relative to SERCA2a in the absence of PLN, as reported previously (Waggoner et al., 2007). However, unlike SERCA2a in the absence of PLN, treatment of the FITC-SERCA2a + PLN sample resulted in a 3.7-fold change in the amplitude of the [Ca^{2+}]-dependent E2 to E1•Ca_2 conformational change (22.4 ± 3.35%). The results indicated that HNO treatment substantially increased the conformational flexibility of SERCA2a while in the presence of PLN. Because there was no significant effect of AS/HNO on SERCA2a alone, the results suggest that AS/HNO treatment uncouples PLN from SERCA2a, removing PLN inhibition of SERCA2a [Ca^{2+}]-dependent conformational changes. Control gels testing FITC binding to the Ca-ATPase showed AS/HNO had no effect on FITC binding to SERCA2a (data not shown).

HNO promotes SERCA2a oligomeric rearrangements

To further test whether HNO physically uncouples PLN from SERCA2a, we used saturation transfer-EPR (ST-EPR) to measure the effect of HNO on

SERCA2a rotational mobility in the absence and presence of PLN. For these studies, we used the maleimide spin label (MSL), which covalently binds to SERCA2a predominantly at Cys-344 (Negash et al., 1996). The conventional EPR spectrum of MSL-SERCA2a in the presence of PLN was consistent with a spin-label strongly immobilized by SERCA2a undergoing microsecond timescale motion in the microsomal membrane (Squier and Thomas, 1986). Treatment of the microsomes with AS had no significant effect on the conventional EPR spectrum (**Figure 3-8**), indicating AS/HNO had no effect on the motion of the spin label in its micro-environment on SERCA2a. The corresponding ST-EPR spectrum of MSL-SERCA2a in the presence of PLN (SERCA2a + PLN) (**Figure 3-9**) indicated the rotational correlation time (τ_r) for SERCA2a was approximately 75 μsec, which was similar to previous measurements of SERCA2a rotational mobility (Negash et al., 1996, Southall et al., unpublished). Treatment of the sample with 100 μM AS produced clear changes in the ST-EPR spectrum, and increased the rotational correlation time to 250 μsec. This indicates that AS/HNO treatment significantly decreased the global rotational mobility of SERCA2a in the presence of PLN, consistent with AS/HNO uncoupling PLN from SERCA2a (Negash et al., 1996). In addition, the ST-EPR spectral changes are consistent with AS/HNO-dependent changes in SERCA2a conformational flexibility in the presence of PLN, as described above (**Figure 3-6**). The results suggest that AS/HNO treatment uncouples PLN from SERCA2a, allowing the enzyme to more readily undergo Ca^{2+}-dependent conformational transitions concomitant with increased SERCA2a activity.

Discussion

Previous studies on the effects of AS/HNO on Ca-ATPase activity have provided evidence that HNO stimulates Ca-ATPase activity by uncoupling regulatory PLN from the Ca-ATPase, but little information is available about the physical mechanism for this effect. Mahaney and colleagues (2005) reported that PLN inhibits Ca-ATPase Ca^{2+} sensitivity by disrupting SERCA2a oligomeric interactions important for enzyme dephosphorylation and subsequent high affinity Ca^{2+} binding necessary to activate the enzyme for ATP-dependent phosphorylation. In support of this finding, Waggoner and colleagues (2007) used fluorescence spectroscopy to show PLN inhibits the Ca^{2+}-dependent E2 to E1•Ca_2 conformational transition. Likewise, Southall and colleagues (unpublished results) showed regulatory PLN decreases SERCA2a rotational motion by decreasing the average cross-sectional area (i.e., oligomeric size) of the rotating unit. Therefore, if AS/HNO uncouples PLN from SERCA2a, we expected to observe HNO-dependent increases in Ca^{2+} sensitivity for Ca-ATPase activity, enhanced Ca^{2+}-dependent conformational transitions and changes in SERCA2a oligomeric interactions in the presence of PLN compared to untreated SERCA2a + PLN microsomes. Froehlich and colleagues (2008) demonstrated that AS/HNO treatment of SERCA2a + PLN microsomes increased the rate of SERCA2a dephosphorylation similar to microsomes containing only SERCA2a. Our activity studies showed that AS/HNO treatment increased Ca-ATPase Ca^{2+} sensitivity in the presence of PLN, mimicking the effects of PLN phosphorylation or treatment of PLN with an anti-PLN monoclonal antibody, thereby removing its regulatory influence on the Ca-ATPase. Likewise, we found that AS/HNO

treatment of SERCA2a + PLN microsomes increased the amplitude (i.e., shifted the poise) of the E2 to E1•Ca_2 conformational transition toward the high affinity E1•Ca_2 intermediate state, consistent with uncoupling PLN from the Ca-ATPase. In contrast, however, our ST-EPR results did not provide clear evidence for an HNO-dependent change in Ca-ATPase rotational mobility in the presence versus absence of PLN. Nevertheless, there were pronounced changes in the ST-EPR following HNO treatment consistent with increased domain motion, typical of increased conformational flexibility.

For our activity studies and fluorescence measurements, we added AS/HNO directly to the microsome samples prior to measurement. In the case of the enzyme assays, no physical manipulation of the sample was needed. The AS/HNO was allowed to react (complete within the 20 minute incubation period) and the enzyme activity was measured. For the fluorescence studies, the microsomes were first labeled with FITC, which involved incubation on ice, followed by a single centrifugation to remove the labeling buffer from the microsomes. Specific control experiments (Waggoner et al., 2007, Southall et al., unpublished) have shown that this physical manipulation of the microsomes has no significant effect on the enzyme activity of the microsomes. In contrast, the spin labeling procedure required more extensive physical manipulation of the sample. Due to a loss of EPR signal intensity that resulted from adding AS to MSL-Ca-ATPase, we had to treat the native microsomes with AS first, followed by a centrifugation step, then treat with NEM and MSL to spin label the enzyme. This was followed by two high speed centrifugation steps to completely remove unbound spin label. Apart from AS/HNO effects, Southall and colleagues

(unpublished results) found that the Ca-ATPase activity of the microsomes declined steadily with increased centrifugation such that as much as half the enzyme activity would be lost after three centrifugation steps. This is most likely due to physical damage to the labile microsomal membranes, as evidenced in our St-EPR spectra. Negash et al., (1996) and Mahaney et al. (2003) reported that the rotational correlation time (τ_R) for the Ca-ATPase in native cardiac SR vesicles and insect cell microsomes, respectively, was approximately 80-100 μsec, consistent with our result. Visible differences in our SERCA2a spectra suggest the physical manipulation of our microsomes resulted in an observable change in the predicted spectra, and thus prevented a proper evaluation of HNO-dependent changes in Ca-ATPase rotational motion. We continue to refine the spin-labeling procedure and test alternative methods for removing unbound spin label that do not require the harsh conditions of centrifugation. For example, subsequent spin-labeling will utilize dialysis to remove AS reaction by products and unbound NEM and MSL. We have avoided dialysis in the past because of the time required for sample preparation compared to the relatively quick centrifugation step, and because we have always had very good success with centrifugation using native SR vesicles. As such, we will also now process our FITC-treated samples by dialysis and carry out activity studies on microsomes treated similarly, to ensure more faithful comparison of the activity and spectroscopy data.

A chief concern for these experiments was variability of the experimental results during the early phases of this project. One consideration was the redox state of the protein cysteines in our microsomes following their preparation from insect cells. Any modification of sulfydryl groups would be expected to change

the cysteine reactivity pattern of AS/HNO, and we suspected this might have contributed to the variability we found in our activity results while we were working out the method for adding AS to the microsomes. To explore this possibility, we treated our microsomes with 40 mM DTT (Simmerman and Jones, 1998) prior to our activity studies, but found that this made no difference in the activity of the native microsomes. Likewise, the presence of DTT in our sample buffer and gels in our electrophoresis experiments made no difference in the migration pattern of the microsomal protein. We also tried adding DTT to the buffers used in the cell microsome preparation protocol, but saw no significant difference in protein yield or resulting activity. We, therefore, concluded that the cysteine redox state in our microsomes was not a major contributor to the variability of our results in the early phase of this project. Rather, we suspect that the variability of AS addition to our samples may have been a major factor, since we used high and low microsome protein concentrations and a wide variety of AS concentrations for the various experiments. As a second order reaction, the relative amount of HNO and protein sulfhydryls is a relevant concern for reproducible HNO reactivity. While we did not solve this problem explicitly, we did find an AS treatment protocol that increased dramatically the experimental reproducibility and provided consistency between the various types of experiments utilized in this project.

Very few sulfhydryl targets of HNO action have been positively identified, and the Mahaney Laboratory's investigation of HNO effects on PLN's three cysteine residues has the potential to provide important new insight into the molecular mechanism of HNO action at the amino acid side chain level. While

not focused on PLN sulfhydryls directly, the present study provides an important foundation for the PLN cysteine study by showing in greater detail that HNO stimulation of Ca-ATPase activity is dependent, at least in part, on the physical uncoupling of PLN from the Ca-ATPase. This provided the "proof of concept" needed to take the next logical step of investigating the role of each PLN cysteine residue in the HNO mechanism.

Our collaborator, Dr. Nazareno Paolocci, at the Johns Hopkins Medical Institutions, has continued his physiological studies of HNO, by comparing directly the effects of cardiac myocytes from PLN knock-out mice to those from wild-type mice. His results show that while HNO has substantial effects on Ca^{2+} release, contractility, Ca^{2+} uptake and myocyte relaxation in normal myocytes, HNO has virtually no effect on these parameters in myocytes from the PLN knockout mouse, confirming for the first time at the cellular level the central role of PLN in the mechanism of HNO stimulation of myocyte contractility. Our molecular level studies using isolated microsomes containing Ca-ATPase in the absence and presence of PLN complement nicely the cellular physiological studies in Paolocci's laboratory, and our results will be combined in a joint manuscript upon the completion of both studies.

A significant drawback of using Angeli's salt as an HNO donor for CHF therapy is its relatively short half life at 37˚C and neutral pH (~ 2.5 min) (Cheong et al., 2005). This would limit AS/HNO from reaching all tissues and target proteins. Therefore, one of the current areas of HNO research is to develop novel HNO donors with much longer half-lives. Future studies for this project will involve using these novel HNO donors in similar studies described here to help

characterize the utility of these new donors, such as studies using the "blue compound" described in Appendix A. Likewise, HNO will react with any free sulfhydryl or thiolate, which creates a specificity problem. Current research is focused on using improved drug delivery techniques to localize the novel HNO donor to its target tissue to increase the likelihood that HNO will be produced and react at the site where it is needed. Future studies for the present project will include studies of sulfhydryl reactivity on a variety of SR proteins to determine the specificity of HNO reactivity and the effects of non-specific sulfhydryl reactivity.

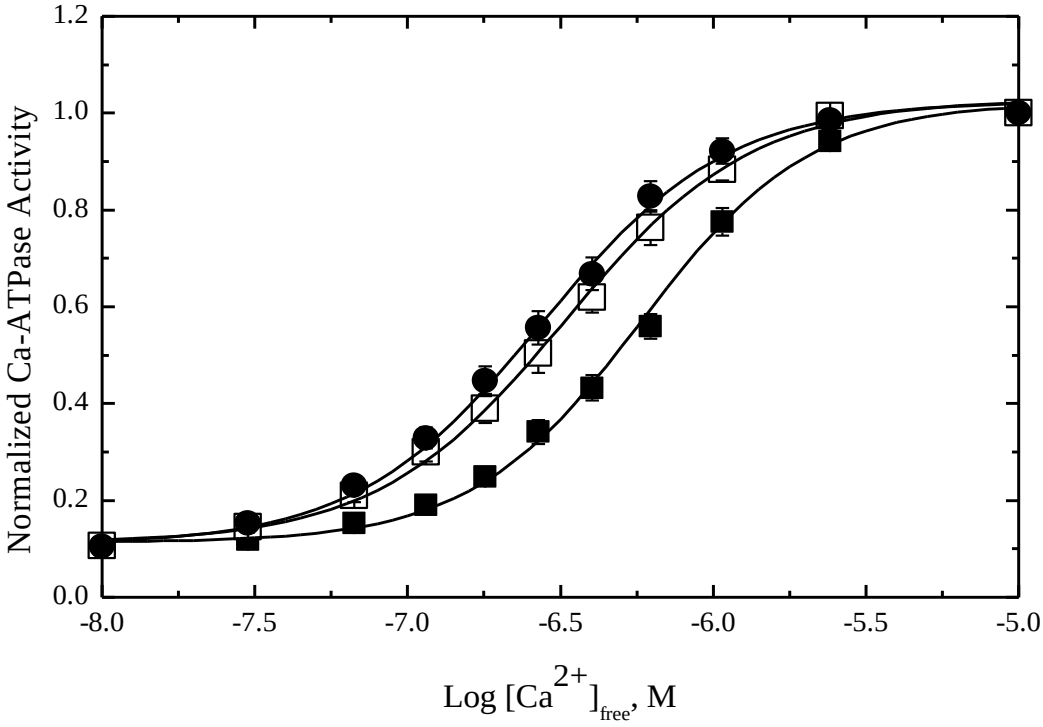

Figure 3-1. Effect of PLN on the [Ca^{2+}]-dependent Ca-ATPase activity of expressed SERCA2a in HF insect cell microsomes. HF microsomes (0.05 mg total protein / ml) containing SERCA2a alone (filled circles) or SERCA2a + PLN (filled squares) were assayed at 37˚C in a medium containing 50 mM MOPS, 3 mM Mg_2Cl, 100 mM KCl, 1 mM EGTA, pH 7.0, and 0-1.0 mM $CaCl_2$, to give the desired ionized [Ca^{2+}], as previously determined (Waggoner et al., 2007). Each assay was initiated by the addition of 5 mM MgATP to the incubation tube. The microsomes were pretreated with 20 μg A23187 per mg protein in the incubation medium to prevent Ca^{2+} accumulation in the microsomes. The SERCA2a content of each sample was matched at 16%, which facilitated direct comparison of the activity data. To assess the inhibitory effect of PLN on Ca-ATPase activity, a SERCA2a + PLN sample was incubated for 20 min

on ice with anti-PLN monoclonal antibody 2D12 at an antibody to protein weight ratio of 1:1 (Waggoner et al., 2004) prior to assay (empty squares). Calcium-dependent SERCA2a ATPase and Ca^{2+} uptake activity data were fit to the Hill equation using the program KFIT to generate values for $K_{0.5}$ and V_{max}. Each curve was normalized to its maximum value to more clearly demonstrate the effects of treating the SERCA2a + PLN sample (filled squares) with an anti-PLN monoclonal antibody (empty squares). Symbols represent the average of five repetitions, and error bars correspond to the standard error of the mean for each point.

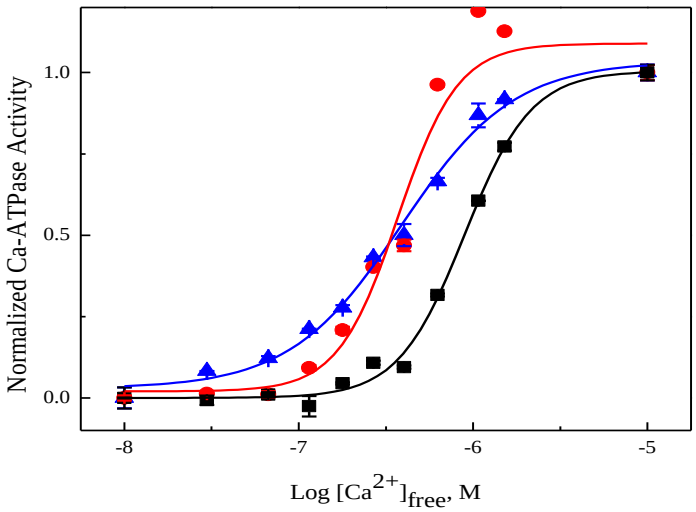

Figure 3-2. AS/HNO functionally uncoupled PLN from SERCA2a in native cardiac vesicles. Native cardiac SR vesicles were suspended (0.2 mg total protein/ml) in 250 mM sucrose and 10 mM imidazole, pH 7.0, treated with either 100 μM AS/HNO (circles) or anti-PLN monoclonal antibody 2D12 (triangles) and incubated at room temperature for 15 min. Untreated control vesicles (squares) were treated identically but had no additions. [Ca^{2+}]-dependent ATPase activity was assayed and analyzed as described in Figure 3-1. Each curve is shown normalized to its maximum value to facilitate direct comparison of the three curves. In this experiment, 100 μM AS/HNO inhibited slightly the maximum ATPase activity at saturating [Ca^{2+}], such that when the AS/HNO treated curve was normalized to its maximum value, the background activity at low [Ca^{2+}] appeared to be elevated compared to the other samples. However, in the raw activity data, the background activity for all three samples was nearly identical. Symbols represent the average of three repetitions, and error bars correspond to the standard error of the mean for each point.

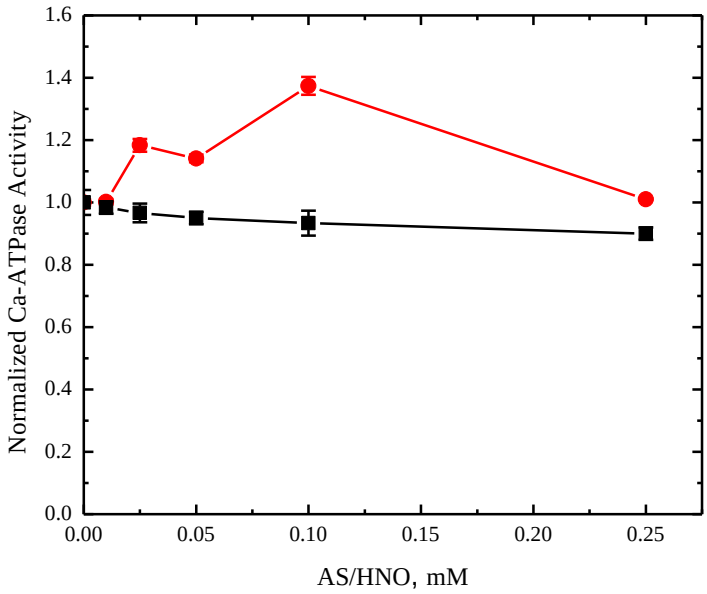

Figure 3-3. AS/HNO increased SERCA2a activity in the presence of PLN. HF microsomes containing either SERCA2a alone (squares) or SERCA2a+PLN (circles) were suspended (1 mg total protein / ml) in 250 mM sucrose, 10 mM imidazole, pH 7.0, treated with the indicated concentrations of Angeli's salt (AS/HNO) and incubated for 20 min at room temperature. Steady-state SERCA2a ATPase activity was measured at 37˚C at a saturating calcium concentration of 2.4 μM using colorimetric phosphate assay, as described in the text. Symbols represent the average of three repetitions, and error bars correspond to the standard error of the mean for each point.

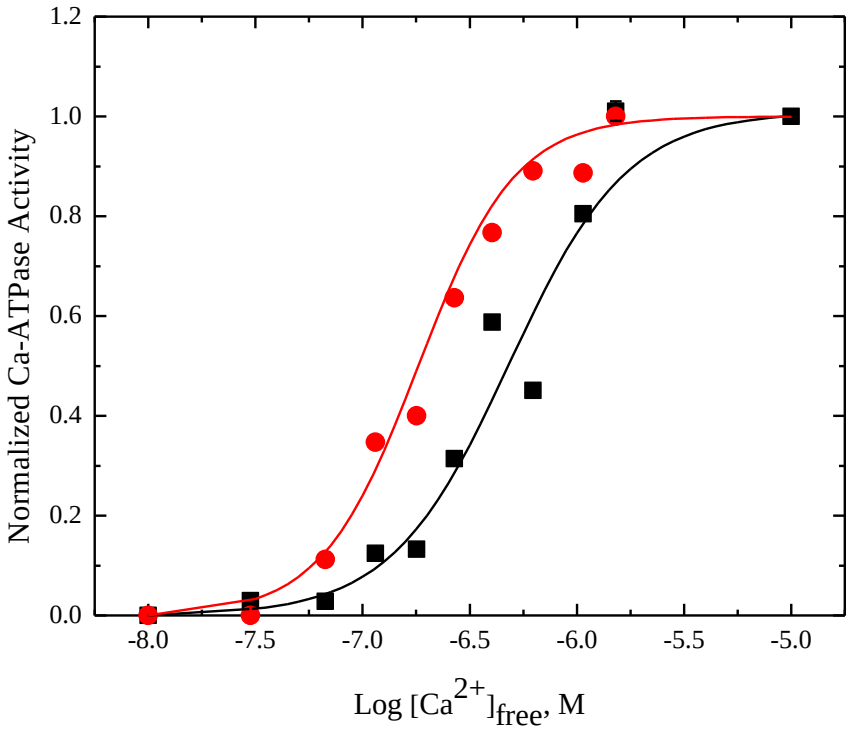

Figure 3-4. AS/HNO functionally uncoupled PLN from SERCA2a in HF microsome vesicles. HF microsomes containing SERCA2a coexpressed with PLN were suspended (0.2 mg total protein / ml) in 250 mM sucrose and 10 mM imidazole, pH 7.0, treated with either 0 (squares) or 100 μM AS/HNO (circles) and incubated at room temperature for 10 min. [Ca^{2+}]-dependent ATPase activity was assayed and analyzed as described in Figure 3-1. Treatment with 100 μM AS/HNO slightly inhibited the maximal activity of the SERCA2a + PLN sample. Therefore, the data are shown normalized to their respective maximums to better illustrate the AS/HNO-dependent shift in the [Ca^{2+}]-dependent activity curve. Symbols are the average of duplicate experiments and the error bars, which are smaller than the symbols, represent the high/low values for each point.

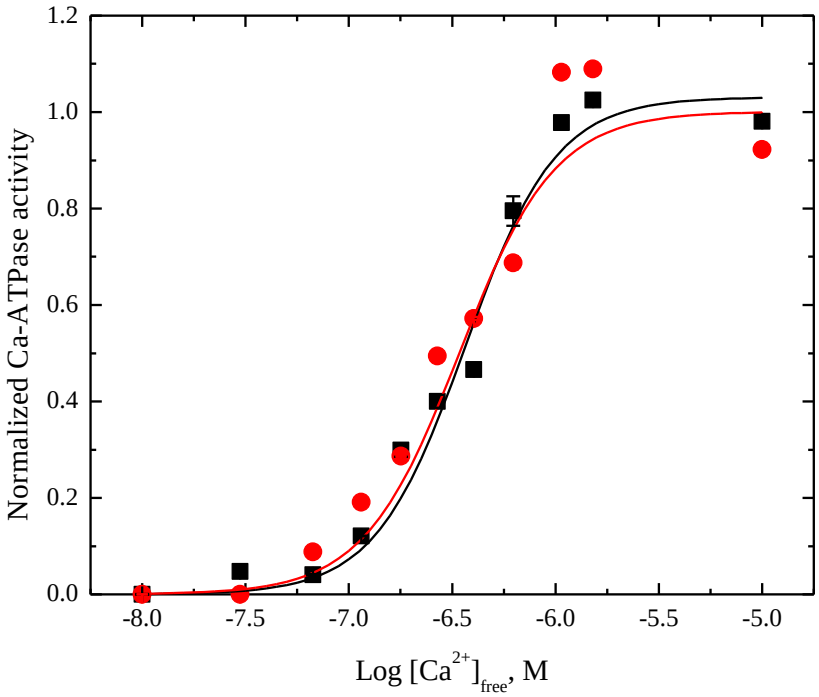

Figure 3-5. AS/HNO had little effect on SERCA2a activity in the absence of PLN. HF microsomes containing SERCA2a expressed were suspended (0.2 mg total protein / ml) in 250 mM sucrose and 10 mM imidazole, pH 7.0, treated with either 0 (squares) or 100 μM AS/HNO (circles) and incubated at room temperature for 10 min. [Ca^{2+}]-dependent ATPase activity was assayed and analyzed as described in Figure 3-1. Treatment with 100 μM AS/HNO slightly inhibited the maximal activity of the SERCA2a + PLN sample. Therefore, the data are shown normalized to their respective maximums to better illustrate the AS/HNO-dependent shift in the [Ca^{2+}]-dependent activity curve. Symbols are the average of duplicate experiments and the error bars, which are generally smaller than the symbols, represent the high/low values for each point.

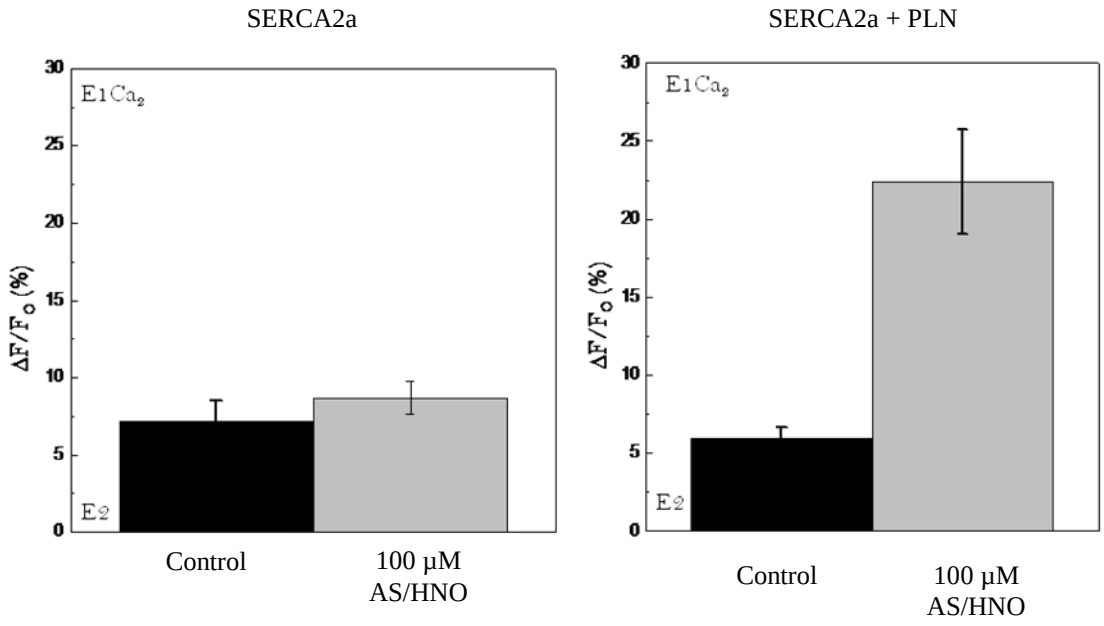

Figure 3-6. AS/HNO increased the amplitude of the SERCA2a E2 to E1•Ca_2 conformational transition in the presence of PLN. HF insect cell microsomes containing SERCA2a expressed alone (left) or SERCA2a + PLN (right) were labeled with FITC as described in the text, and treated with 0 (black) or 100 µM (grey) AS/HNO for 10 minutes at room temperature. The treated microsomes were suspended (0.35 mg total protein / ml) in 50 mM MOPS, pH 7.0, 3 mM Mg_2Cl, 100 mM KCl containing 1 mM EGTA without added Ca^{2+} ($[Ca^{2+}]_{free}$ ~ 0) to stabilize FITC-SERCA2a in the Ca^{2+}-free state The steady state fluorescence intensity was recorded prior to and following the addition of 1 mM Ca^{2+} (final $[Ca^{2+}]_{free}$ ~ 100 µM), and the $[Ca^{2+}]$-dependent change in fluorescence (ΔF) was divided by the initial fluorescence reading (F_o) and expressed as a percentage. Values represent the average of six independent experiments and error bars represent the standard error of the mean.

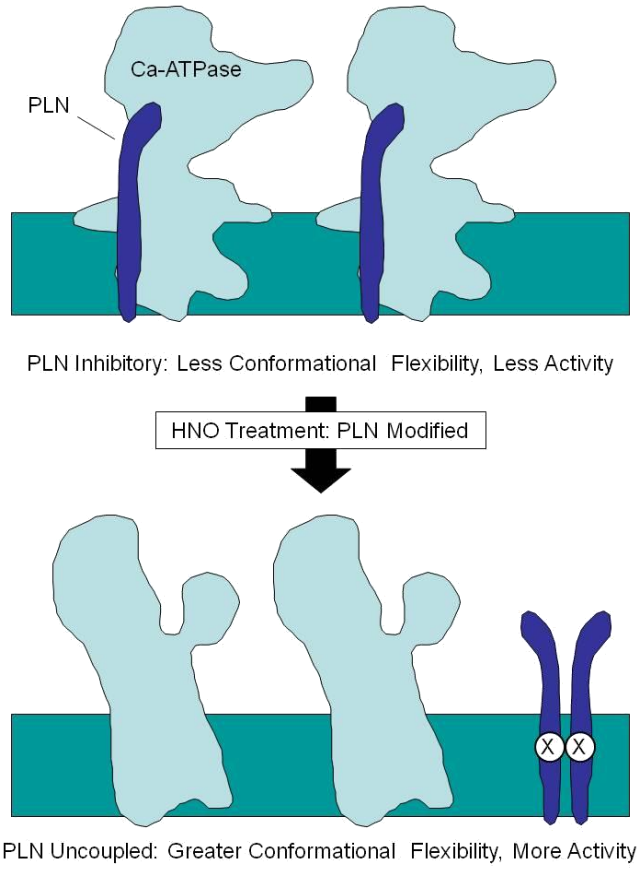

Figure 3-7. Model for the effect of AS/HNO on SERCA2a conformational flexibility, as modified by PLN. PLN decreases Ca-ATPase conformational flexibility concomitant with inhibition of Ca-ATPase activity (Waggoner et al., 2007). AS/HNO treatment results in increased Ca-ATPase activity in a PLN-dependent manner (Figs. 3-3, 3-4, and 3.5), which may result from PLN transmembrane sulfhydryl modification (Froehlich et al., 2008). We propose that AS/HNO modification of PLN physically uncouples PLN from SERCA2a, substantially increasing the Ca^{2+}-dependent conformational flexibility of SERCA2a.

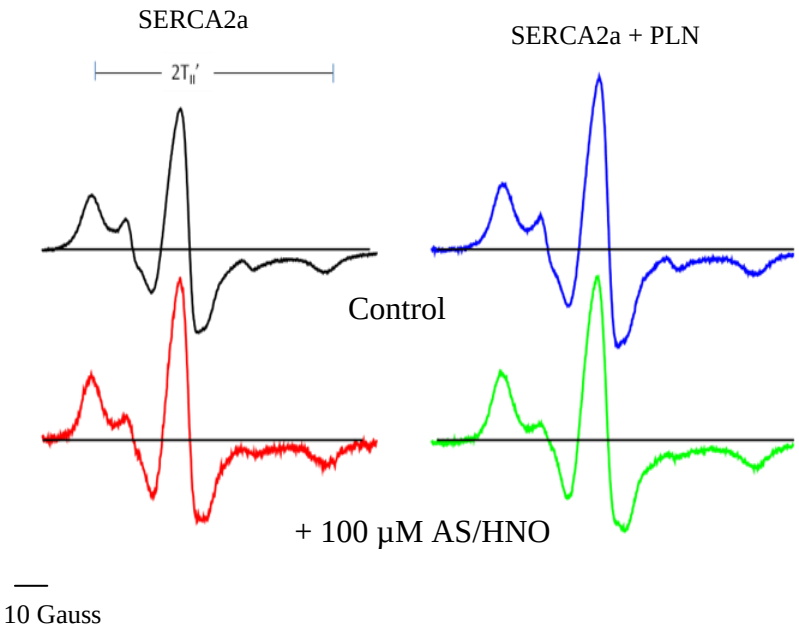

Figure 3-8. AS/HNO had no effect on the conventional EPR spectrum of MSL-SERCA2a in the absence or presence of PLN. HF microsomes containing SERCA2a expressed alone (left) or SERCA2a + PLN (right) were pre-treated with 0 or 100 µM AS for 10 minutes at room temperature, washed to remove the AS reaction buffer, then covalently spin labeled with MSL as described in the text. The final washed pellet of HF microsomes containing MSL-SERCA2a (~40 mg/ml total protein) was drawn by gentle suction into a 50 µl capillary tube in preparation for EPR analysis. The EPR spectra were analyzed by the outer splitting, $2T_{\parallel}'$, as defined in the figure. The experimental temperature was 4˚C.

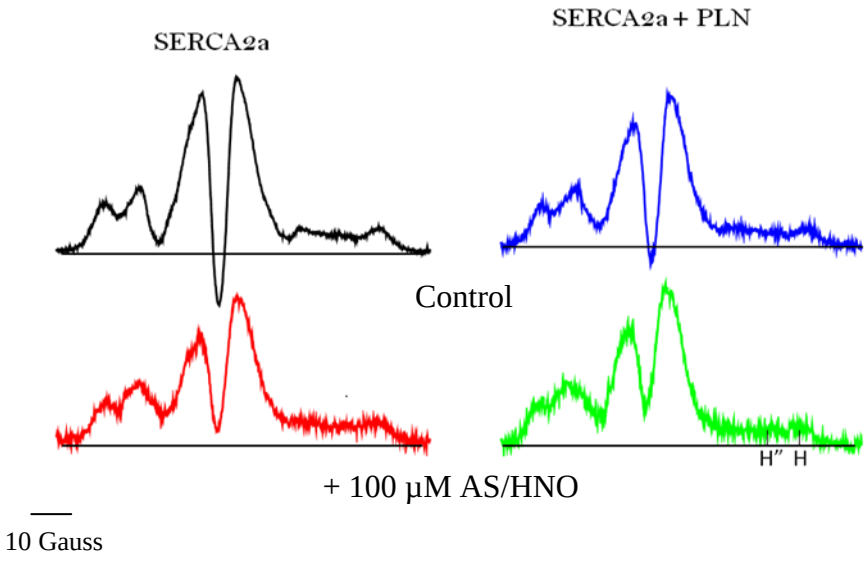

Figure 3-9. AS/HNO increased MSL-SERCA2a rotational mobility in the presence of PLN. Using the samples utilized in Figure 3-8, the saturation transfer EPR spectrum of MSL-SERCA2a at 4˚C in the absence (left) and presence (right) of coexpressed PLN in HF microsomes pre-treated with 0 (top) or 100 µM (bottom) AS/HNO was obtained as described in the text. ST-EPR spectra were analyzed by the high-field (H″/H) line-height ratio, which was used to determine the rotational correlation time for MSL-SERCA2a in each sample, based on standard curves constructed from a model system.

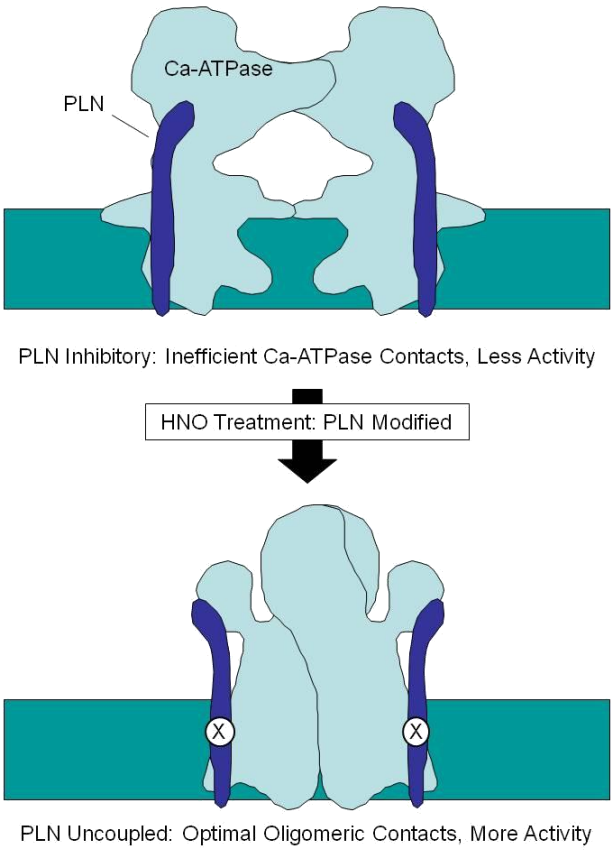

Figure 3-10. Model for the effect of AS/HNO on SERCA2a oligomeric interactions, as modified by PLN. PLN inhibits Ca-ATPase oligomeric interactions (Negash et al., 1996) important for optimal Ca-ATPase conformational flexibility (Waggoner et al., 2007) and activity (Mahaney et al., 2005). AS/HNO treatment increases the amplitude of the [Ca^{2+}]-dependent E2 to E1•Ca_2 conformational transition (Fig. 3-6) and increases Ca-ATPase activity in a PLN-dependent manner (Figs. 3-3, 3-4 and 3.5), which may result from PLN transmembrane sulfhydryl modification (Froehlich et al., 2008). We propose that AS/HNO treatment of PLN uncouples PLN from Ca-ATPase, allowing it to form preferred oligomeric contacts, similar to PLN phosphorylation (Negash et al., 1996), concomitant with increasing Ca-ATPase activity.

REFERENCES

AUTRY, J. M. & JONES, L. R. 1997. Functional Co-expression of the Canine Cardiac Ca2+ Pump and Phospholamban in Spodoptera frugiperda (Sf21) Cells Reveals New Insights on ATPase Regulation. *J. Biol. Chem.,* 272**,** 15872-15880.

BIGELOW, D. J., SQUIER, T. C. & THOMAS, D. D. 1986. Temperature Dependence of Rotational Dynamics of Protein and Lipid in Sarcoplasmic Reticulum Membranes. *Biochemistry,* 25**,** 194-202.

BIRMACHU, W., NISSWANDT, F. L. & THOMAS, D. D. 1989. Conformational Transitions in the Calcium Adenosine Triphosphatase Studied by Time-Resolved Fluorescence Resonance Energy Transfer. *Biochemistry,* 28**,** 3940-3947.

CHEONG, E., TUMBEV, V., ABRAMSON, J., SALAMA, G. & STOYANOVSKY, D. A. 2005. Nitroxyl Triggers Ca2+ Release from Skeletal and Cardiac Sarcoplasmic Reticulum by Oxidizing Ryanodine Receptors. *Cell Calcium,* 37**,** 87-96.

DAI, T., TIAN, Y., TOCCHETTI, C. G., KATORI, T., MURPHY, A. M., KASS, D. A., PAOLOCCI, N. & GAO, W. D. 2007. Nitroxyl Increases Force Development in Rat Cardiac Muscle. *The Journal of Physiology,* 580**,** 951-960.

FROEHLICH, J. P., MAHANEY, J. E., KECELI, G., PAVLOS, C. M., GOLDSTEIN, R., REDWOOD, A. J., SUMBILLA, C., LEE, D. I., TOCCHETTI, C. G., KASS, D. A., PAOLOCCI, N. & TOSCANO, J. P. 2008. Phospholamban Thiols Play a Central Role in Activation of the Cardiac Muscle Sarcoplasmic Reticulum Calcium Pump by Nitroxyl&#x2020. *Biochemistry,* 47**,** 13150-13152.

GORNALL, A. G., BARDAWILL, C., J. & DAVID, M., M. 1949. Determination of Serum Proteins by Means of the Biuret Reaction. *Journal of Biological Chemistry,* 177**,** 751-767.

LANCEL, S., ZHANG, J., EVANGELISTA, A., TRUCILLA, M. P., TONG, X. Y., SIWIK, D. A., COHEN, R. A. & COLUCCI, W. S. 2009. Nitroxyl Activates SERCA in Cardiac Myocytes via S-Glutathiolation of Cysteine 674. *Circulation Research,* 104.

LANZETTA, P. A., ALVAREZ, L. J., REINACH, P. S. & CANDIA, O. A. 1979. An Improved Assay for Nanomole Amounts of Inorganic Phosphate. *Analytical Biochemistry,* 100**,** 95-97.

LOPEZ, B. E., WINK, D. A. & FUKUTO, J. M. 2007. The Inhibition of Glyceraldehyde-3-Phosphate Dehydrogenase by Nitroxyl (HNO). *Archives of Biochemistry and Biophysics,* 465**,** 430-436.

MAHANEY, J. E., ALBERS, R. W., KUTCHAI, H. & FROEHLICH, J. P. 2003. Phospholamban controls Ca2+ Pump Oligomerization and Intersubunit Free Energy Exchange Leading to Activation of Cardiac Muscle SERCA2a. *N.Y. Acad. Sci,* 986**,** 1-3.

MAHANEY, J. E. & THOMAS, D. D. 1991. Effects of Melittin on Molecular Dynamics and Ca-ATPase Activity in Sarcoplasmic Reticulum Membranes: Electron Paramagnetic Resonance. *Biochemistry,* 30**,** 7171-7180.

NEGASH, S., CHEN, L. T., BIGELOW, D. J. & SQUIER, T. C. 1996. Phosphorylation of Phospholamban by cAMP-Dependent Protein Kinase Enhances Interactions Between Ca-ATPase Polypeptide Chains in Cardiac Sarcoplasmic Reticulum Membranes. *Biochemistry,* 35**,** 11247-11259.

PAOLOCCI, N., JACKSON, M. I., LOPEZ, B. E., MIRANDA, K., TOCCHETTI, C. G., WINK, D. A., HOBBS, A. J. & FUKUTO, J. M. 2007. The Pharmacology of Nitroxyl (HNO) and its Therapeutic Potential: Not Just the Janus Face of NO. *Pharmacology & Therapeutics,* 113**,** 442-458.

PAOLOCCI, N., KATORI, T., CHAMPION, H. C., ST. JOHN, M. E., MIRANDA, K. M., FUKUTO, J. M., WINK, D. A. & KASS, D. A. 2003. Positive Inotropic and Lusitropic Effects of HNO/NO– In Failing Hearts: Independence from β-Adrenergic Signaling. *Proceedings of the National Academy of Sciences of the United States of America,* 100**,** 5537-5542.

PAOLOCCI, N., SAAVEDRA, W. F., MIRANDA, K. M., MARTIGNANI, C., ISODA, T., HARE, J. M., ESPEY, M. G., FUKUTO, J. M., FEELISCH, M., WINK, D. A. & KASS, D. A. 2001. Nitroxyl Anion Exerts Redox-Sensitive Positive Cardiac Inotropy in vivo by Calcitonin Gene-Related Peptide Signaling. *Proceedings of the National Academy of Sciences of the United States of America,* 98**,** 10463-10468.

SIMMERMAN, H. K. B. & JONES, L. R. 1998. Phospholamban: Protein Structure, Mechanism of Action, and Role in Cardiac Function. *Physiological Reviews,* 78**,** 921-946.

SOUTHALL, J., HUFFMAN, J., SIVAKUMARAN, V. & MAHANEY, J. E. unpublished.

SQUIER, T. C. & THOMAS, D. D. 1986. Methodology for Increased Precision in Saturation Transfer Electron Paramagnetic Resonance Studies of Rotational Dynamics. 49**,** 921-935.

TOCCHETTI, C. G., WANG, W., FROEHLICH, J. P., HUKE, S., AON, M. A., WILSON, G. M., DI BENEDETTO, G., O'ROURKE, B., GAO, W. D., WINK, D. A., TOSCANO, J. P., ZACCOLO, M., BERS, D. M., VALDIVIA, H. H., CHENG, H., KASS, D. A. & PAOLOCCI, N. 2007. Nitroxyl Improves Cellular Heart Function by Directly Enhancing Cardiac Sarcoplasmic Reticulum Ca2+ Cycling. *Circ Res,* 100**,** 96-104.

WAGGONER, J. R., HUFFMAN, J., FROELICH, J. P. & MAHANEY, J. E. 2007. Phospholamban Inhibits Ca-ATPase Conformational Changes Involving the E2 Intermediate. *Biochemistry,* 46**,** 1999-2009.

WAGGONER, J. R., HUFFMAN, J., GRIFFITH, B. N., JONES, L. R. & MAHANEY, J. E. 2004. Improved Expression and Characterization of Ca^{2+}-ATPase and Phospholamban in High-Five Cells. *Protein Expression and Purification,* 34**,** 56-67.

Chapter 4

Preliminary Investigation of 1-nitosocyclohexyl acetate as a potential HNO donor, and its role in the physical mechanism of Ca-ATPase stimulation

This work is a starting point for future studies using second generation HNO donors. I was the major contributor to this section.

Introduction

With HNO emerging as important constituent of NO biochemistry and as a potential pharmaceutical therapy for congestive heart failure, it has become important to identify new HNO donors with improved biological and pharmacological properties. Angeli's salt (AS) is currently the most popular HNO donor in the literature; however AS has a very short half-life of ~2.5 min at room temperature at a pH of 7.2 (Paolocci et al., 2007, Mahaney et al., 2005, Paolocci et al., 2003), suggesting it would have only limited utility as a general donor throughout the body after administration. With this in mind, finding a new HNO donor with a longer half-life has become one of the primary goals for using HNO as a cardiotherapy. Several research groups have initiated an investigation of other C-nitroso compounds (Shafiullah and Ali, 1979, Sha et al., 2006, Xu et al., 2000, King and Nagasawa, 1999, Gubelt and Warkentin, 1969, Lown, 1966, Zhutov et al., 2003), known as acyloxy nitroso compounds (called the "blue compound," because of its bright blue color). Bruce King's group at Wake Forest University has initiated an investigation specifically looking into these acyloxy nitroso compounds as HNO donors. One of the most promising candidates is 1-nitrosocyclohexyl acetate (NCA) (Sha et al., 2006), derived from cyclohexane, which is a blue oil that is produced by the oxidation of a cyclohexanone oxime and contains a tetra-acetate group. The hydrolysis of the acyl portion of these compounds generates an unstable intermediate that decomposes to HNO and the corresponding ketone (Sha et al., 2006). The oxidation of cyclohexanone oxime with lead tetra-acetate gives NCA in a 52% yield (Lown, 1966, Sha et al., 2006). This compound generates small amounts of NO and HNO.

As mentioned previously, HNO is the one-electron reduction product of NO (Paolocci et al., 2007), and *in vivo* leads to positive inotropy/lusitropy in both normal (Paolocci et al., 2001) and failing hearts (Paolocci et al., 2003). HNO reacts rapidly with thiols (-SH) and is believed to target critical reactive thiolates (RS-) in proteins without affecting the overall intracellular thiol content (Lopez et al., 2007). How exactly HNO performs is not well understood. For the Ca-ATPase, HNO derived from AS stimulates Ca^{2+} uptake activity, potentially by uncoupling the regulatory protein phospholamban from the Ca-ATPase (Froehlich et al., 2008), though one report suggests direct effects of HNO on the Ca-ATPase by stimulating S-glutathiolation of Cys-674 in the Ca-ATPase (Lancel et al., 2009).

While NCA may have improved properties as a HNO donor, it is important to determine whether NCA/HNO affects Ca-ATPase activity and its regulation by PLN the same as AS/HNO. Additional functional and physical studies are needed to better demonstrate utility of this compound and, more generally, newer second and third generation HNO donors. Therefore, we have carried out preliminary EPR and fluorescence studies similar to those described for AS/HNO in Chapter 3, as a first step in characterizing the action of NCA on cardiac cellular membranes.

Materials and Methods

Spin labeling

The overall rotational mobility of the Ca-ATPase was measured by electron paramagnetic resonance (EPR) spectroscopy using the short-chain maleimide spin label, N-(1-oxyl-2,2,6,6-tetra-methyl-4-piperadinyl)maleimide (MSL), covalently bound to the ATPase as previously described (Squier and Thomas, 1986b, Bigelow et al., 1986), using the optimized labeling protocol developed in the AS/HNO study. High Five microsomes containing SERCA2a ± PLN were first pre-treated with 100 μM NCA for 40 minutes at room temperature. The sample was diluted to 2 mL in 250 mM sucrose buffer, 10 mM imidazole, at pH 7.0 (sucrose buffer) and spun in a microcentrifuge for 10 minutes at 4˚C at 13, 200 rpm to remove the NCA/HNO reaction mixture; this was done twice since the half life of the NCA/HNO is much longer than that of AS. The pelleted samples were resuspended in the residual buffer then treated with N-ethylmaleimide (NEM) for 30 minutes on ice at a ratio of 1.0 mol NEM per mol of expressed SERCa2a to block fast-reacting thiols. After the 30 minute incubation, the microsomes were incubated with 250 μM MSL for 1 hour on ice, at a ratio of 2.5 mol MSL per mol of expressed SERCA2a. Excess spin label was removed by 2 rounds of centrifugation, where the microsomes were diluted into cold 0.3 M sucrose and 20 mM MOPS, pH 7.0, for 30 min at 30, 000 rpm (70000g), 4˚C, in a Beckman Ti45 rotor using a Beckman Optima LE-80K ultra centrifuge. The pellet, containing the MSL-labeled SERCA2a (henceforth denoted MSL-SERCA2a), was re-suspended in 0.3 M sucrose and 20 mM MOPS at pH 7.0 and stored on ice until use.

EPR Spectroscopy

EPR spectra were obtained using a Bruker ER 200D spectrometer equipped with a Bruker ER 4102ST cavity. Submicrosecond rotational motion of spin labels was detected by conventional EPR (first harmonic absorption in phase, designated V1) using 100 kHz field modulation, a peak-to-peak amplitude of 2 gauss (G), and a microwave field amplitude of 0.032 G. Submillisecond rotational motion of spin labels was detected by saturation-transfer EPR (second harmonic absorption out of phase, designated V2') using a 50 kHz field modulation, with a modulation amplitude of 5.0 G, and a microwave field intensity of 0.25 G. Samples were contained in 50 μL glass capillaries. Sample temperature was controlled at 4˚C with a Bruker ER 4111VT variable temperature controller. Spectra were digitized and stored on a computer and analyzed using the program EWWIN, written by Philip Morse (Scientific Software Solutions).

EPR Spectral Analysis

MSL-SERCA2a and MSL-SERCA2a + PLN in High Five insect cell microsome conventional spectra were analyzed by the outer splitting parameter ($2T_{II}'$). ST-EPR spectra were analyzed by line shape parameter (Squier and Thomas, 1986b), which provided the effective rotational correlation time (τ_r) for spin-labeled SERCA2a, which was determined from a standard curve constructed from an isotropically tumbling models system (Squier and Thomas, 1986b, Mahaney and Thomas, 1991). Fatty acid spin label EPR spectra were measured by evaluating out ($2T_{II}'$) and inner ($2T_{\perp}'$) spectral splitting, which were used to

determine the effective order parameter (S) for lipid hydrocardon chain mobility at the 5-and 16-carbon positions (Mahaney and Thomas, 1991).

Labeling of Ca-ATPase with FITC

SERCA2a and SERCA2a + PLN expressed in insect cell microsomes were labeled by florescein isothiocyanate (FITC) according to Birmachu and colleagues (1989). A fresh stock of 5 mM FITC in N, N- dimethylformamide (DMF) was prepared prior to each experiment. The microsomes were incubated with FITC at a ratio of 0.9 mol FITC per mol of SERCA2a in a labeling buffer containing 60 mM Tris, 10 mM $MgCl_2$, and 200 mM KCl at a pH of 8.7 for 30 min at room temperature. BSA (1 mg/mL) was added to the solution and incubated for 20 minutes on ice to remove any unbound label. Excess reagent and BSA were removed by pelleting the microsomes by centrifugation for 30 min at 30, 000 rpm, 4˚C, in a Beckman Coulter Ti45 rotor. The pellet, containing the FITC-labeled SERCA2a (henceforth denoted FITC-SERCA2a), was resusupended in 0.3 M sucrose and 20 mM MOPS. High Five microsomes were pre-treated with 100 μM NCA/HNO prior to addition of the FITC and washed for 10 minutes, at 4 ◦C at 13, 200 rpm.

Fluorescence Measurements

Measurements of the fluorescence intensity were performed at 25˚C using the Spectramax M5 microplate reader. The excitation and emission wavelengths for the FITC-SERCA2a were 490 nm and 505 nm, respectively.

To measure fluorescence intensity changes following a $[Ca^{2+}]$-jump, insect cell microsomes containing FITC-SERCA2a (~2.5 mg/mL) were suspended in a

standard buffer (50 mM MOPS, 100 mM KCl, 3 mM $MgCl_2$, 0 mM $CaCl_2$, 1 mM EGTA, pH 7.0) designed to favor the Ca^{2+}-free E2 state initially. The addition of 1 mM Ca^{2+} to the standard buffer (final [Ca^{2+}] free ~ 100 μM) promoted the formation of the E1•Ca_2 conformation. The fluorescence intensity was measured by summing the total fluorescence emission (initial fluorescence intensity, F_0) and after (final fluorescence intensity, F) the respective additions. Fluorescence intensity changes were quantified as percent changes, according to the formula 100 x ($F-F_0/F_0$).

Results

HNO increases Ca-ATPase conformational flexibility in the presence of PLN

We used fluorescence spectroscopy of SERCA2a covalently labeled with FITC (FITC-SERCA2a) to study the effect of HNO on the [Ca^{2+}]-dependent conformational flexibility of SERCA2a. FITC binds to a single lysine residue on SERCA2a (Lys-514) and inactivates the enzyme by blocking ATP access to the catalytic site on the enzyme. However, the enzyme is still active and sensitive to high affinity Ca^{2+} binding, and undergoes the [Ca^{2+}]-dependent conformational changes associated with transition from the Ca^{2+} free E2 intermediate to the Ca^{2+}-bound E1•Ca_2 intermediate (Birmachu et al., 1989). Therefore, FITC-SERCA2a in the absence or presence of PLN was incubated in a Ca^{2+}-free buffer containing 1 mM EGTA to stabilize the enzyme in the Ca^{2+}-free E2 state, and the fluorescence emission intensity of the FITC-SERCA2a was recorded before and after a medium [Ca^{2+}] jump to 1 mM Ca^{2+} (resulting free Ca^{2+} 100 μM) to

promote formation of the Ca^{2+}-bound $E1{\bullet}Ca_2$ intermediate. For HF microsomes containing SERCA2a without PLN, the calcium jump changed the fluorescence intensity by 17.8 ± 1.8 % for the control, untreated microsomes, whereas treatment with 100 μM NCA/HNO resulted in a smaller change of 13.1 ± 1.12%. Nevertheless, the presence of PLN inhibited the amplitude of the $[Ca^{2+}]$-dependent E2 to $E1{\bullet}Ca_2$ conformational change (3.23 ± 1.16 %) relative to SERCA2a in the absence of PLN, as reported previously (Waggoner et al., 2007). However, treatment of the FITC-SERCA2a + PLN sample resulted in a 2.6-fold increase (8.27 ± 0.85 %) in the amplitude of the $[Ca^{2+}]$-dependent E2 to $E1{\bullet}Ca_2$ conformational change. The results indicated that NCA/HNO treatment increased the conformational flexibility of SERCA2a in the presence of PLN, consistent with the results using AS/HNO.

HNO has little effect on Ca-ATPase global rotational mobility

To further test whether HNO physically uncouples PLN from SERCA2a, we used saturation transfer-EPR to measure the effect of HNO on SERCA2a rotational mobility in the absence and presence of PLN. For these studies, we used the maleimide spin label (MSL), which covalently binds to SERCA2a predominantly at Cys-344 (Negash et al., 1996). The conventional EPR spectrum of MSL-SERCA2a in the presence of PLN was consistent with a spin-label strongly immobilized by SERCA2a undergoing microsecond timescale motion in the microsomal membrane (Squier and Thomas, 1986a). Treatment of the microsomes with AS had no significant effect on the conventional EPR spectrum (**Figure 4-2**), indicating HNO had no effect of the motion of the spin label in its

micro-environment on SERCA2a. The corresponding ST-EPR spectrum of MSL-SERCA2a in the presence of PLN (**Figure 4-3**) indicated the rotational correlation time (τ_r) for SERCA2a was approximately 23 μsec.

Discussion

Angeli's salt has been the most commonly used HNO donor for studies in the literature. However, the half-life of HNO production by AS under physiological conditions (37˚C, pH 7.4) is so short (1-2 minutes) that AS itself could not be considered a competent HNO donor for *in vivo* use. Therefore, one major goal in HNO research is to develop novel HNO donors with significantly longer half-lives, to ensure the donor can adequately move throughout the entire circulation system on the time-scale of HNO release, so that HNO may reach the intended target tissues. One such novel HNO donor is NCA, which has a half life of approximately 8 minutes, suggesting it would have improved performance in HNO delivery throughout the body. Studies on the effects of HNO on intact cardiac myocytes indicate that Ca^{2+} uptake activity and myocyte relation are significantly increased by HNO, and HNO generated by NCA appears to have the same effects as HNO generated by AS (Tian et al., 2007), suggesting a similar physical mechanism for HNO-dependent activation of cardiac myocyte function. However, it remains to be determined whether NCA/HNO has the same molecular level effects on the myocyte as AS/HNO. Therefore, we carried out a series of preliminary fluorescence and EPR studies to test the effects of NCA/HNO on the Ca-ATPase/PLN system for comparison with our AS spectroscopic studies. If NCA/HNO affects PLN in a manner similar to AS/HNO,

we should obtain spectroscopic results using NCA that are similar to those obtained using AS.

Our fluorescence studies indicated treatment with NCA caused a slight but significant inhibition of Ca-ATPase conformational flexibility in the absence of PLN, which was similar to that observed in our preliminary studies with AS/HNO. After optimization of the AS/HNO treatment procedures, we found that AS/HNO did not significantly inhibit SERCA2a in the absence of PLN. We think optimization of the NCA treatment protocol will also eliminate the inhibition observed in the fluorescence study. This inhibition could be due to the longer half-life of NCA. We may need to add additional washes of the microsomes to more completely remove the reaction mixture from our system, in order to guarantee the HNO reaction is extinguished prior to fluorescence labeling and measurement.

Unlike AS/HNO, NCA/HNO treatment did not significantly affect the global rotational mobility of SERCA2a in the absence of PLN suggesting that NCA-derived HNO may not affect Ca-ATPase oligomeric interactions in the same way as AS/HNO. However, we noted that the intensity of the NCA/HNO-treated spectra was very much weaker than the control, untreated spectra, suggesting a significantly reduced level of spin-labeled Ca-ATPase in the NCA/HNO-treated spectra compared to the control spectra. It is possible that residual NCA/HNO remained in the spin-labeling incubation mixture after the initial washing steps to remove unreacted NCA from the microsomes, resulting in degradation of the MSL itself or preventing MSL reaction with Ca-ATPase. This was not observed for AS/HNO, perhaps because of the much shorter half-life of AS compared to

NCA. Additional washes and even longer incubation times may be needed to eradicate any residual HNO from the system when using NCA. This serves as a starting point for the spin-labeling optimization experiments that are needed to resolve this issue. Therefore, the present EPR results using NCA/HNO must be considered equivocal until more definitive results are obtained.

The initial spectroscopic studies presented here provide a plausible foundation for continued studies testing the effects of NCA on the Ca-ATPase/PLN system to help determine the suitability of NCA as an HNO donor. In addition to more detailed spectroscopic studies, we need to carry out a variety of pre-steady state kinetics and steady-state activity studies on the effects of NCA on Ca-ATPase activity, as affected by PLN, correlating the physical and functional effects of NCA. If NCA is found to be a viable candidate in use as a HNO donor functioning in a manner similar to AS, then additional studies on NCA/HNO effects on PLN's three cysteine residues would be the next logical step after elucidating the mechanism by which NCA is working on the Ca-ATPase, as well as continuing work on HNO reactivity with sulfhydryl groups on Ca-ATPase and on other microsomal (and SR) proteins.

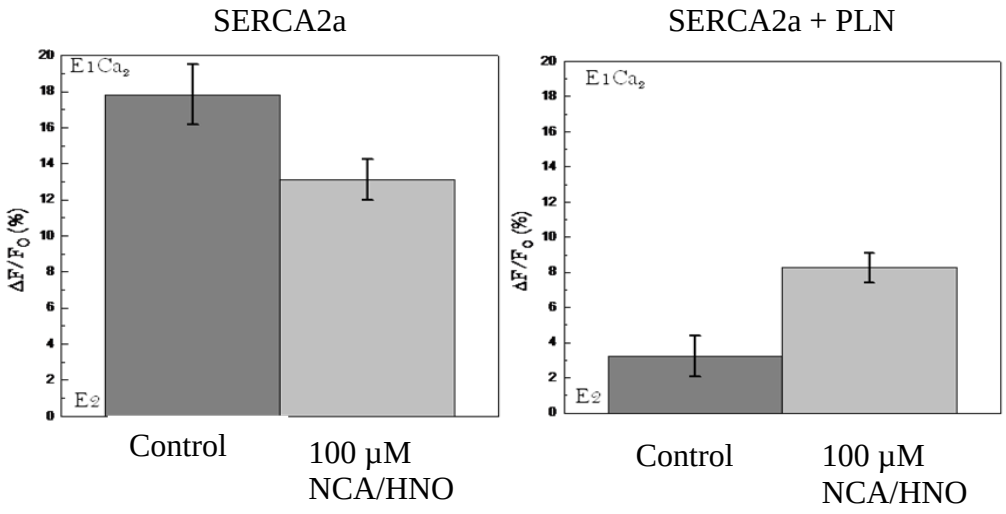

Figure 4-1. NCA/HNO alters the amplitude of the SERCA2a E2 to E1•Ca_2 conformational transition in the presence of PLN. HF insect cell microsomes containing SERCA2a expressed alone (left) or SERCA2a + PLN (right) were labeled with FITC as described in the text. The labeled microsomes were treated with 0 (dark grey) or 100 µM (light grey) NCA for 10 minutes at room temperature and centrifuged to remove the NCA reaction mixture. The treated microsomes were resuspended (0.35 mg total protein / ml) in 50 mM MOPS, pH 7.0, 3 mM Mg_2Cl, 100 mM KCl containing 1 mM EGTA without added Ca^{2+} ($[Ca^{2+}]_{free}$ ~ 0) to stabilize FITC-SERCA2a in the Ca^{2+}-free E2 intermediate state. The steady state fluorescence intensity was recorded prior to and following the addition of 1 mM Ca^{2+} (final $[Ca^{2+}]_{free}$ ~ 100 µM) and the $[Ca^{2+}]$-dependent change in fluorescence (ΔF) was divided by the initial fluorescence reading (F_o) and expressed as a percentage. Values represent the average of five independent experiments and error bars represent the standard error of the mean. The experimental temperature was 25˚C.

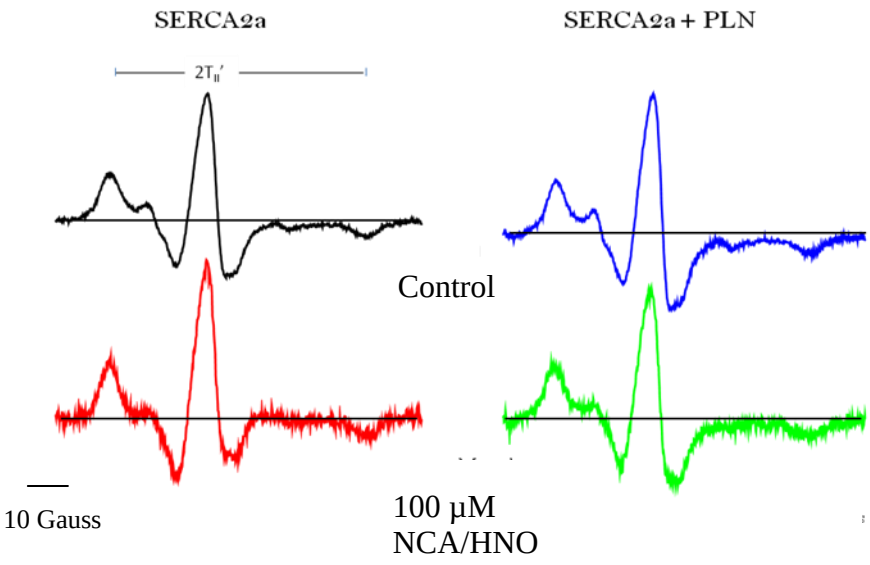

Figure 4-2. NCA/HNO had only minor effects on the conventional EPR spectrum of MSL-SERCA2a in the absence or presence of PLN. HF microsomes containing SERCA2a expressed alone (left) or SERCA2a + PLN (right) were pre-treated with 0 (top) or 100 µM (bottom) NCA for 10 minutes at room temperature, washed to remove the NCA reaction buffer, then covalently spin labeled with MSL as described in the text. The final washed pellet of HF microsomes containing MSL-SERCA2a (~40 mg/ml total protein) was drawn by gentle suction into a 50 µl capillary tube in preparation for EPR analysis. The EPR spectra were analyzed by the outer splitting, $2T_{\parallel}'$, as defined in the figure. The experimental temperature was 4˚C.

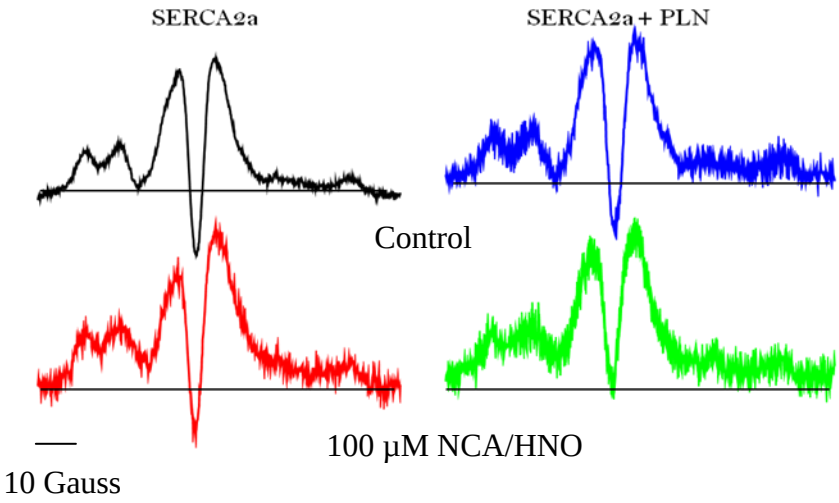

Figure 4-3. NCA/HNO increased MSL-SERCA2a rotational mobility in the presence of PLN. Using the samples utilized in Figure 3-8, the saturation transfer EPR spectrum of MSL-SERCA2a at 4˚C in the absence (left) and presence (right) of coexpressed PLN in HF microsomes pre-treated with 0 (top) or 100 μM (bottom) NCA/HNO was obtained as described in the text. The low signal-to-noise ratio in the ST-EPR spectra overall prevented analysis by the high-field (H″/H) line-height ratio, which is the standard means for determination of the rotational correlation time for MSL-SERCA2a in each sample, based on standard curves constructed from a model system. Qualitatively, the spectrum for both NCA/HNO-treated samples showed signs of decreased MSL-SERCA2a rotational mobility compared to control, untreated microsomes, based on the increased line-height of peaks throughout the spectrum.

REFERENCES

BIGELOW, D. J., SQUIER, T. C. & THOMAS, D. D. 1986. Temperature of Rotational Dynamics of Protein and Lipid in Sarcoplasmic Reticulum Membranes. *Biochemistry,* 25**,** 194-202.

BIRMACHU, W., NISSWANDT, F. L. & THOMAS, D. D. 1989. Conformational Transitions in the Calcium Adenosine Triphosphatase Studied by Time-Resolved Fluorescence Resonance Energy Transfer. *Biochemistry,* 28**,** 3940-3947.

CHEONG, E., TUMBEV, V., ABRAMSON, J., SALAMA, G. & STOYANOVSKY, D. A. 2005. Nitroxyl Triggers Ca2+ Release from Skeletal and Cardiac Sarcoplasmic Reticulum by Oxidizing Ryanodine Receptors. *Cell Calcium,* 37**,** 87-96.

FROEHLICH, J. P., MAHANEY, J. E., KECELI, G., PAVLOS, C. M., GOLDSTEIN, R., REDWOOD, A. J., SUMBILLA, C., LEE, D. I., TOCCHETTI, C. G., KASS, D. A., PAOLOCCI, N. & TOSCANO, J. P. 2008. Phospholamban Thiols Play a Central Role in Activation of the Cardiac Muscle Sarcoplasmic Reticulum Calcium Pump by Nitroxyl&#x2020. *Biochemistry,* 47**,** 13150-13152.

GUBELT, G., B. & WARKENTIN, J. 1969. Oxidation with Lead Tetraacetate. IV. Cyclization of Phenylhydrazones of Levulinic Acid, Levulinanilide, 5-Ketohexanoic Acid, 4-keto-1-pentanol, and of Levulinic Acid Oxime. *Canadian Journal of Chemistry,* 47**,** 3983-3987.

KING, S. B. & NAGASAWA, H. T. 1999. [22] Chemical Approaches Toward Generation of Nitroxyl. *In:* LESTER, P. (ed.) *Methods in Enzymology*. Academic Press.

LANCEL, S., ZHANG, J., EVANGELISTA, A., TRUCILLA, M. P., TONG, X. Y., SIWIK, D. A., COHEN, R. A. & COLUCCI, W. S. 2009. Nitroxyl Activates SERCA in Cardiac Myocytes via S-Glutathiolation of Cysteine 674. *Circulation Research,* 104.

LOPEZ, B. E., WINK, D. A. & FUKUTO, J. M. 2007. The Inhibition of Glyceraldehyde-3-Phosphate Dehydrogenase by Nitroxyl (HNO). *Archives of Biochemistry and Biophysics,* 465**,** 430-436.

LOWN, J. W. 1966. The Reaction of Lead Tetra-Acetate with Oximes. Part I. Alicyclic and Aliphatic Oximes. *J. Chem. Soc. B.,*.

MAHANEY, J. E., ALBERS, R. W., WAGGONER, J. R., KUTCHAI, H. C. & FROEHLICH, J. P. 2005. Intermolecular Conformational Coupling and Free Energy Exchange Enhance the Catalytic Efficiency of Cardiac Muscle SERCA2a following the Relief of Phospholamban Inhibition *Biochemistry,* 44**,** 7713-7724.

MAHANEY, J. E. & THOMAS, D. D. 1991. Effects of Melittin on Molecular Dynamics and Ca-ATPase Activity in Sarcoplasmic Reticulum Membranes: Electron Paramagnetic Resonance. *Biochemistry,* 30**,** 7171-7180.

NEGASH, S., CHEN, L. T., BIGELOW, D. J. & SQUIER, T. C. 1996. Phosphorylation of Phospholamban by cAMP-Dependent Protein Kinase Enhances Interactions Between Ca-ATPase Polypeptide Chains in Cardiac Sarcoplasmic Reticulum Membranes. *Biochemistry,* 35**,** 11247-11259.

PAOLOCCI, N., JACKSON, M. I., LOPEZ, B. E., MIRANDA, K., TOCCHETTI, C. G., WINK, D. A., HOBBS, A. J. & FUKUTO, J. M. 2007. The Pharmacology of Nitroxyl (HNO) and its Therapeutic Potential: Not Just the Janus Face of NO. *Pharmacology & Therapeutics,* 113**,** 442-458.

PAOLOCCI, N., KATORI, T., CHAMPION, H. C., ST. JOHN, M. E., MIRANDA, K. M., FUKUTO, J. M., WINK, D. A. & KASS, D. A. 2003. Positive Inotropic and lusitropic Effects of HNO/NO– In Failing Hearts: Independence from β-adrenergic Signaling. *Proceedings of the National Academy of Sciences of the United States of America,* 100**,** 5537-5542.

PAOLOCCI, N., SAAVEDRA, W. F., MIRANDA, K. M., MARTIGNANI, C., ISODA, T., HARE, J. M., ESPEY, M. G., FUKUTO, J. M., FEELISCH, M., WINK, D. A. & KASS, D. A. 2001. Nitroxyl Anion Exerts Redox-Sensitive Positive Cardiac Inotropy in vivo by Calcitonin Gene-Related Peptide Signaling. *Proceedings of the National Academy of Sciences of the United States of America,* 98**,** 10463-10468.

SHA, X., ISBELL, T. S., PATEL, R. P., DAY, C. S. & KING, S. B. 2006. Hydrolysis of Acyloxy Nitroso Compounds Yields Nitroxyl (HNO). *Journal of the American Chemical Society,* 128**,** 9687-9692.

SHAFIULLAH, D. & ALI, H. 1979. A Convenient Synthesis of Steroidal Nitrosoacetates and Nitroacetates. *Synthesis* 1979**,** 124-126.

SOUTHALL, J., HUFFMAN, J., SIVAKUMARAN, V. & MAHANEY, J. E. unpublished.

SQUIER, T. C. & THOMAS, D. D. 1986a. Methodology for Increased Precision in Saturation Transfer Electron Paramagnetic Resonance Studies of Rotational Dynamics. 49**,** 921-935.

SQUIER, T. C. & THOMAS, D. D. 1986b. Methodology for Increased Precision in Saturation Transfer Electron Paramagnetic Resonance Studies of Rotational Dynamics. *Biophysical Journal,* 49**,** 921-935.

WAGGONER, J. R., HUFFMAN, J., FROELICH, J. P. & MAHANEY, J. E. 2007. Phospholamban Inhibits Ca-ATPase Conformational Changes Involving the E2 Intermediate. *Biochemistry,* 46**,** 1999-2009.

XU, Y., ALAVANJA, M.-M., JOHNSON, V. L., YASAKI, G. & KING, S. B. 2000. Production of Nitroxyl (HNO) at Biologically Relevant Temperatures from the Retro-Diels-Alder Reaction of N-hydroxyurea-derived acyl nitroso-9,10-dimethylanthracene cyclo Adducts. *Tetrahedron Letters,* 41**,** 4265-4269.

ZHUTOV, E. V., SKORNYAKOV, Y. V., PROSKURINA, M. V. & ZEFIROV, N. S. 2003. p-Bromo(diacetoxyiodo)benzene, an Efficient Oxidant for Conversion of Oximes into Nitroso Compounds. *Russian Journal of Organic Chemistry,* 39**,** 1672-1673.

Chapter 5

Future Directions

This sections lays out the future directions for each project.

The body of work described in this dissertation will lead to three peer-reviewed publications. The Angeli's salt HNO study is complete and will become part of a larger collaborative manuscript with the Paolocci laboratory at Johns Hopkins Medical Institutions to be submitted to *Circulation Research* (Tocchetti and Sivakumaran, co-first authors). The NCA/HNO work is in its preliminary stages and significant work remains to bring this to manuscript readiness. However, at that time, these preliminary studies will merit co-authorship on that manuscript as well. The ONOO- project is also complete and will be a self-contained manuscript submitted to *Biochemistry* (Sivakumaran first author). This latter manuscript will include long-time protein nitration collaborators Diana Bigelow and Tom Squier at the Pacific Northwest National Laboratories. In both cases, however, there are still unanswered questions and major project objectives remain. There are still several things that need to be done in order to definitely elucidate the molecular mechanisms by which these two oxidizing agents affect the function of the Ca-ATPase.

Nitration of the Ca-ATPase by $ONOO^-$

Our results indicate that $ONOO^-$ inhibits Ca-ATPase activity by inhibited decreasing the fraction of active enzyme units by an irreversible inhibition mechanism. Several details still need to be reconciled though. Our studies have not fully verified that we are nitrating the same residues as in the endogenous system (Y294 and Y295). Several attempts were made to use mass spectrometry to determine if Y294 and Y295 are the exact sites of nitration on SERCA2a. Our microsomal samples contained very small amounts of expressed SERCA2a as

compared to the endogenous samples which were used by the Bigelow lab, which prevented successful mass spectrometry determinations. One of our highest priorities will be to express and purify the Ca-ATPase in sufficient amounts to determine nitration sites by mass spectrometry.

We also need to determine more definitively whether or not residues mutation of Y294 and Y295 to phenylalanine removes inhibition of the Ca-ATPase by ONOO-. To date, the literature suggests Y294/Y295 are critically important residues involved in the mechanism of inhibition of the Ca-ATPase. As such, we would expected that mutation of Y294/Y295 to phenylalanine would ablate or at least significantly reduce ONOO- inhibition of the enzyme. Our results showed these mutations only reduced about half the observed inhibition, suggesting other sites besides Y294/Y295 are nitrated and contribute to enzyme inhibition. Our data suggests nitration results in an inactivation of a fraction of enzyme units, rather than modifying the reaction rates of key steps in the enzyme cycle. Based on the location of Y294/Y295, we would expect the latter. Therefore, it is possible that the other sites nitrated by $ONOO^-$ may be the cause of the inactivation, as opposed to nitration at Y294/Y295. Additional studies using Ca-ATPase tyrosine mutants are needed to better resolve this question.

Finally, our results showing ONOO- inhibition of Ca-ATPase supports the proposal that Ca-ATPase may function as a sensor for cell oxidative stress, with nitration of the Ca-ATPase being a reversible inhibitor. A major condition for this function would be the presence of a denitrase enzyme, which could remove nitrate groups on the enzyme. Future studies testing the role of Ca-ATPase as a

sensor for cell stress should focus on whether ONOO- is a true irreversible inactivator of Ca-ATPase or perhaps a reversible inhibitor (via denitrase activity).

Oxidation of PLN by HNO

Several studies have suggested that HNO stimulates Ca-ATPase activity by uncoupling PLN from the Ca-ATPase. Our data supports this model for HNO action. Likewise, previous studies have suggested HNO uncouples PLN from Ca-ATPase by modifying specifically one or more PLN cysteine residues. However we have yet to establish which cysteine residue(s) are modified by HNO. Studies are underway using PLN single, double and triple cysteine mutants to determine the structural basis for HNO modification of PLN. Likewise, Ca-ATPase contains several cysteine residues in the vicinity of the PLN binding site. It is possible that HNO modifies one or more Ca-ATPase cysteine residues, thereby changing Ca-ATPase affinity for PLN with concomitant increase in Ca-ATPase activity. Future studies will examine Ca-ATPase cysteines in parallel with PLN cysteines. This is an important extension of the current work. Future studies should focus on the specificity of HNO for cysteine targets. HNO could possibly react with any free thiol or thiolate present, but in practical application, only some cysteines are modified. As we gain a better understanding of the structureal and environmental conditions that facilitate HNO reaction with cysteines, we can focus on more efficient and targeted methods of drug delivery to localize HNO donors to its intended cysteine targets.

Our studies demonstrated clearly that different methods for AS treatment of microsomal samples yielded significantly different results. This variability

between the experimental results made it difficult to know which data were truly representative of HNO effects and which were plagued by experimental artifact. Several HNO treatment methods were attempted until one AS treatment protocol was found that increased the reproducibility between experimental results. Future work should focus on understanding why different treatment protocols lead to different experimental results, including a consideration of which cysteine residue(s) is altered in each case, which will provide a better understanding and (hopefully) support that HNO stimulation of the Ca-ATPase is dependent on the functional uncoupling of PLN from the Ca-ATPase.

Another critical focus for this work will be to test and characterize the effects of novel long half-life HNO donors on the Ca-ATPase-PLN system. We have initiated this type of study using the HNO donor NCA, which in preliminary studies appeared to operate consistently with Angeli's salt. However, a much wider range of study is needed to fully characterize NCA, including Ca-ATPase kinetics studies and spectroscopic measurements of Ca-ATPase conformational transitions and oligomeric protein interactions.

In the next stage of my career, I will be continuing these studies in the laboratory of our collaborator, Dr. Nazareno Paolocci, using physiological methods of studying HNO effects of cardiac myocytes, in order to more clearly correlate the biochemical data with the physiological studies underway in the laboratory and in the literature.

Chapter 6

Appendix

The results in this section did not easily fit into the main dissertation work. This work does, however, serve as a reference and starting point for future studies.

Appendix A

The Induction of Heat Shock Protein 70 at Specific Hypothermic Intervals in an Isolated and Perfused Rat Heart Model – Implications for Cardiac Transplantation

This work is part of a collaborative effort between the Mahaney Lab and the Wyeth Lab. I served as an aid with the biochemical assays in this project and was a major contributor to this section.

Introduction

Human cardiac transplantation has limitations. The current time span from obtaining a donor heart to transplantation into the recipient patient is limited to approximately 4 hours, since there is increasing ischemic injury suffered to explanted hearts as the time window increases to implantation. Likewise, the conditions of heart storage on ice during transportation contribute to this tissue damage. With such a limited time span, the recipient of this organ is limited by geography relative to the donor, which limits the availability of hearts for transplant patients. Transportation and implantation harmfully affect the time a heart remains suitable for implantation. This work is a preliminary study designed to develop an alternative to current methods. Current methodology involves using a hypothermic solution kept at 4˚C and maintaining the heart with a high extra-cellular potassium concentration. This prolonged exposure to the cold and ischemia leads to an increased chance of myocardial injury which narrows the heart viability to around 4 hours from explantation to implantation. Our goal is to help find better storage and transport conditions for explanted hearts that might extend the time window for transport and transplantation.

Cardiac ischemia following explantation of the heart can lead to widespread cell death through apoptosis. Likewise, temperature variation from donor to storage to patient can also damage cells and denature proteins. Heat shock proteins (HSP), a class of protein whose expression increases when cells are exposed to stressors, such as elevated or lowered temperatures, are partially responsible for cellular survival (Lindquist and Craig, 1988). HSPs are found within all living cells. They serve as chaperones during protein production,

correcting any problems with misfolding and protein damage while moving to the outer membrane. HSPs can also help prevent cellular death; but this mechanism is unknown. HSPs can be induced by changes in temperature, ischemia, hypoxia, and free radical damage (Schmitt et al., 2002, Kukreja and Hess, 2000, Hutter et al., 1994, Arnaud et al., 2002). HSP70, specifically, has been found to be induced by a change in the normothermic conditions of myocytes. Alternatively, caspases are a class of proteases that are essential to roles for apoptosis, and also increase in expression and activity when cells are exposed to stressors (Degterev et al., 2003). As such, monitoring caspase expression and activity during cell stress is a common method for assessing cell status during the stress state.

The goal of this study was to test the feasibility of using a continuous forward perfusion of the myocardium with an oxygenated buffer and using a more moderate hypothermic temperature to help with cell survival and cardiac viability. We monitored HSP70 and caspase expression in the perfused hearts as a function of time during the cooling and re-warming of explanted hearts to test this regimen. Our hypothesis was that HSP70 expression will be greatest at 27˚C, at a point where we would observe the least amount to myocardial injury. The specific aim of the project was:

Aim: To correlate myocardial cellular injury and HSP70 expression with temperature changes in explanted rat hearts perfused with an oxygenated buffer. Rat hearts were explanted and mounted on a Langendorf perfusion apparatus, and temperature changes were made over a program time interval after which the hearts were flash frozen for biochemical analysis. A

caspase colorimetric assay kit was utilized in order to quantify the degree of myocardial injury and apoptosis using an antibody detection system. A HSP70 ELISA assay was utilized in order to determine the expression levels of HSP70 at the various temperatures. **The goal was to determine the degree of cooling for explanted rat heart perfused with an oxygenated buffer that would induce the greatest increase in the production of protective HSP70 while minimizing the expression of caspases.**

Materials and Methods

In this study, 20 Sprague-Dawley rat hearts were individually cannulated on a Langendorff apparatus, stabilized at a specific target temperature by a circulating waterbath, and then perfused for 30 min with Krebs-Henseleit buffer (D-glucose, 2.0 g/L; magnesium sulfate (anhydrous), 0.141 g/L; potassium phosphate monobasic, 0.16 g/L; potassium chloride, 0.35 g/L; sodium chloride, 6.9 g/L). Following perfusion, hearts were flash frozen in liquid nitrogen and stored at -80 ˚C until the time to test for myocardial injury. This work was carried out by Dr. Wyeth's laboratory worker, Eric Taylor, D. O., VCOM medical student.

For our contribution to the project, hearts were individually thawed and weighed, then diced and minced with a scalpel blade and placed into individual conical tubes containing 5 mLs of assay diluents from the rat total HSP70 immunoassay kit. Each heart was homogenized into a crude myocardial homogenate using a Potter-Elvehjem manual homogenizer. Protein concentration was determined by the biuret method (Gornall et al., 1949). Homogenates were stored at -80˚C between uses.

For each homogenate, we quantified caspase and HSP70 expression using the caspase-1/ICE colorimetric Assay Kit from Biovision (Catalog number K111-100) and the human/mouse/rat total HSP70 immunoassay kit from R&D Systems (Catalog number SUV1663). Both kits used employed an ELISA immunoblot-based assay, using an antibody detection method to quantitate expression levels. The caspase-1/ICE colorimetric assay measured the activity of caspases that recognize the sequence YVAD (Biovision). The assay used spectrophotometric detection of the chromophore *p*-nitroanilide (*p*NA) after cleavage of the labeled substrate YVAD-*p*NA, using 400 nM of visible light. The absorbance values were compared against control absorbance values to calculate the fold difference in caspase expression. The HSP70 assay quantified HSP70 using an antibody specific for HSP70 that had been pre-coated onto a microplate. HSP70 present in the homogenate bound to the immobilized antibody. After washing, a biotinylated detection antibody which recognizes HSP70 was used for detection using a standard streptavidin-horse radish peroxidase protocol. Color development was converted to moles HSP bound using a standard curve that was provided with the assay kit (R&D Systems).

Results and Discussion

Our experimental data indicated that caspase expression in the myocardium was greatest at the extreme temperatures over the temperature range of 22˚C to 42˚C, suggesting an increased myocardial injury at lower (22˚C) and higher temperatures (42˚C) (**Figure A-1**). Caspase expression appeared to be lowest over the temperature range 27-32˚C, consistent with our hypothesis.

HSP expression was similarly highest at the lowest temperature tested (22˚C), but declined with increasing temperature to 42˚C. Therefore, there was no direct correlation between caspase expression levels and HSP70 expression levels (**Figure A-2**). However, the temperature range of 27-32˚C provided an increased HSP level combined with a minimal caspase level, which would be better for the myocardial cells than other temperatures. Dr. Wyeth's project also examines sex differences in myocardial viability during transplation. When tabulated according to the sex of the rat heart, we found that HSP70 expression at extreme hypothermia (27˚C) was significantly higher in females, suggesting females may be better protected against cardiac damage than males (**Figure A-3**).

This study provides a first attempt at using HSP70 and caspase expression as a biochemical tool to assess the cellular state in explanted hearts. The scatter in the data makes drawing conclusions difficult, apart from general trends. However, Dr. Wyeth and Dr. Taylor found that the surgical removal and perfusion procedure on the Langendorf apparatus improved with each heart tested, such that the last five hearts studied provided the most reproducible data. This suggests that re-testing a new series of hearts may well provide much better data and clearer answers to the question of temperature dependence of cardiac caspase and HSP expression. At this time, Dr. Wyeth would carry out physiological studies of cardiac function to correlate with the biochemical data for hearts perfused at the various temperatures studies. We hope that continuation of this study will provide insight into optimal conditions for storage and transport of explanted hearts for transplantation.

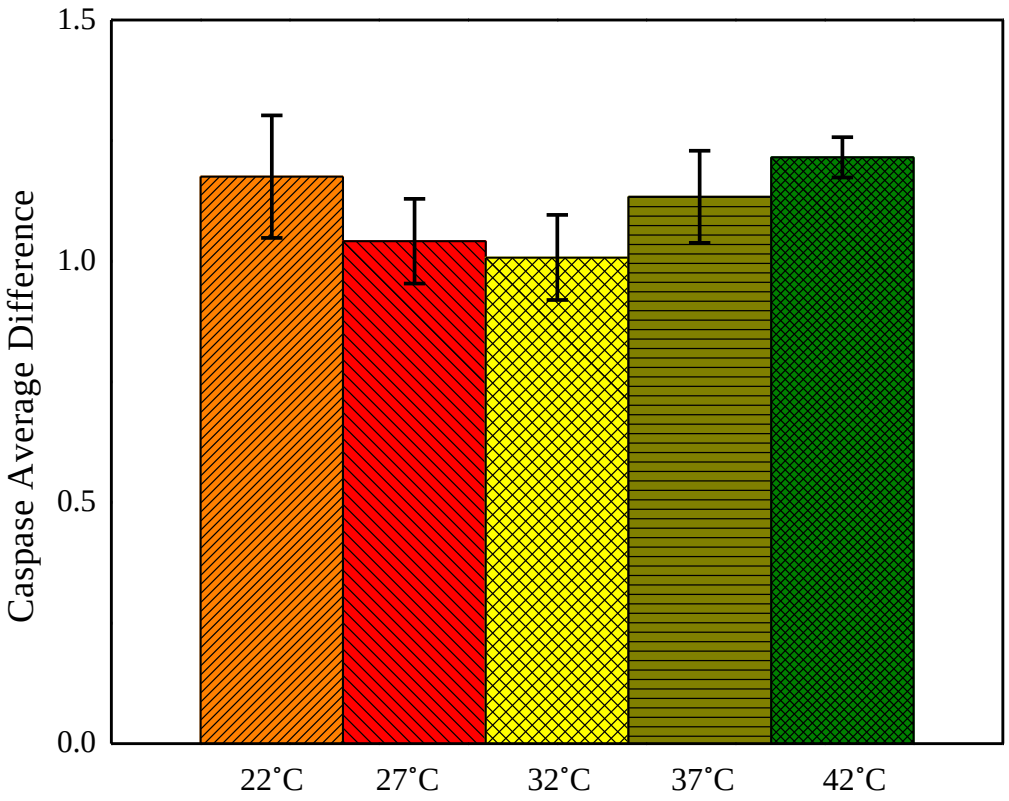

Figure A-1. Change in caspase activity with temperature in perfused explanted heart homogenates. Sprague-Dawley rat hearts were explanted and cannulated on a Langendorf apparatus, then perfused with oxygenated Krebs-Henseleit buffer for 30 min at the indicated temperatures. The hearts were homogenized and the homogenate was assayed colorimetrically for caspase activity, as described in the text. Bars represent the average of duplicate measurement, and the errors represent the high-low values for the repeats.

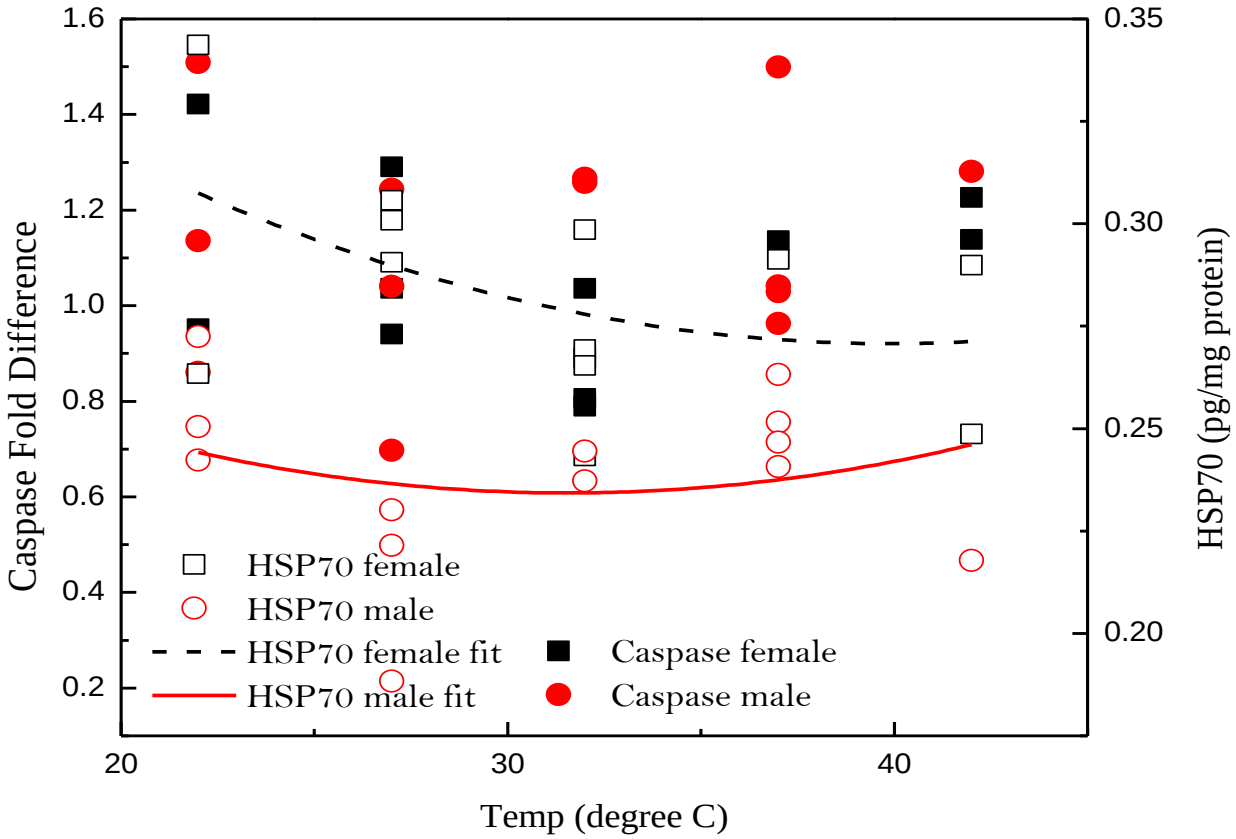

Figure A-2. Relationship of caspase and HSP70 in perfused hearts. The cardiac homogenates described in Figure A-1 were analyzed for HSP70 expression levels by ELISA immuno-assay as described in Methods. Symbols represent single experiments on each homogenate, with multiple determinations for each homogenate, and are separated based on the sex of the rat. The caspase data of figure A-1 was plotted with the HSP70 data to show the correlation of the two parameters.

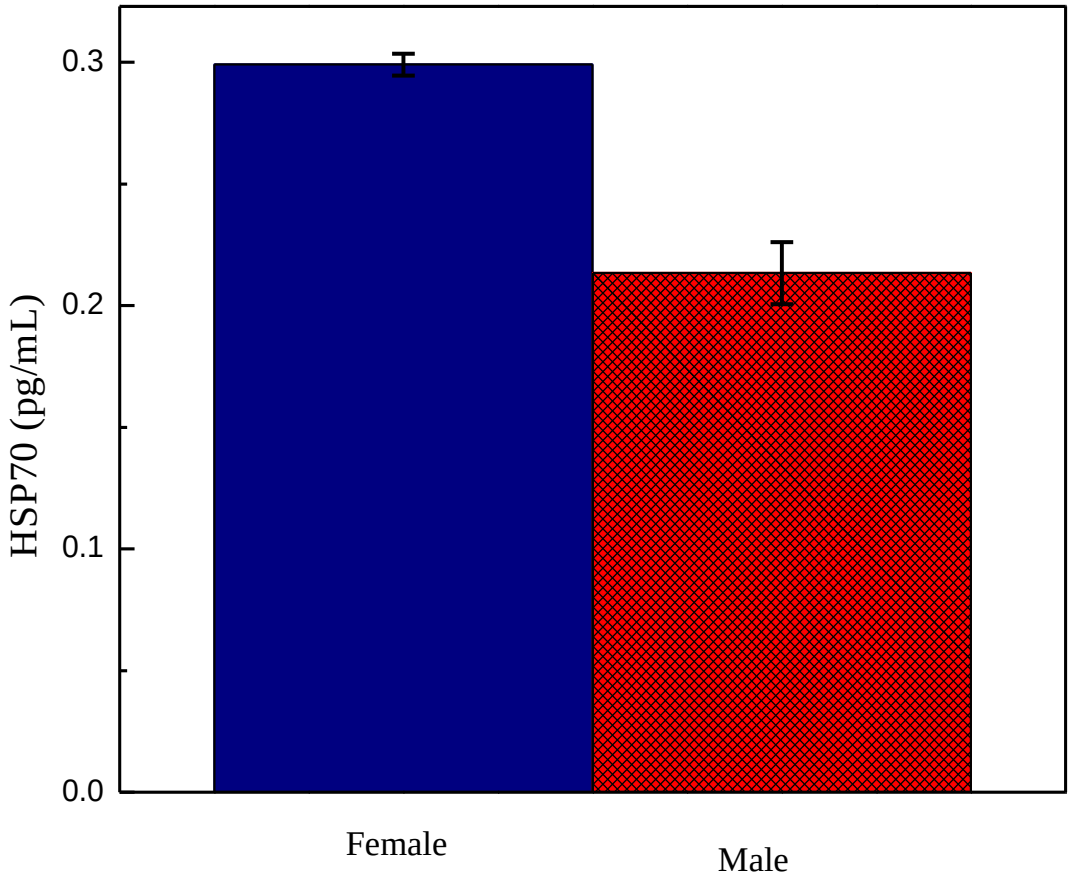

Figure A-3. Differences in HSP70 expression in female versus male rats at 27°C. HSP70 expression at extreme hypothermia (27˚C) was significantly higher in females (left, blue) than males (right, red), suggesting females are better protected against cardiac damage.

REFERENCES

ARNAUD, C., JOYEUX, M., GARREL, C., GODIN-RIBUOT, D., DEMENGE, P. & RIBUOT, C. 2002. Free-Radical Production Triggered by Hyperthermia Contributes to Heat Stress-Induced Cardioprotection in Isolated Rat Hearts. *British Journal of Pharmacology,* 135**,** 1776-1782.

DEGTEREV, A., BOYCE, M. & YUAN, J. 2003. A Decade of Caspases. *Oncogene,* 22**,** 8543-8567.

GORNALL, A. G., BARDAWILL, C., J. & DAVID, M., M. 1949. Determination of Serum Proteins by Means of the Biuret Reaction. *Journal of Biological Chemistry,* 177**,** 751-767.

HUTTER, M., SIEVERS, R., BARBOSA, V. & WOLFE, C. 1994. Heat-Shock Protein Induction in Rat Hearts. A Direct Correlation Between the Amount of Heat-Shock Protein Induced and the Degree of Myocardial Protection. *Circulation,* 89**,** 355-360.

KUKREJA, R. & HESS, M. 2000. Heat Shock Proteins in Myocardial Protection. *Virginia Commonwealth University*.

LINDQUIST, S. & CRAIG, E. A. 1988. The Heat-Shock Proteins. *Annual Review of Genetics,* 22**,** 631-677.

SCHMITT, J. P., SCHUNKERT, H., BIRNBAUM, D. E. & AEBERT, H. 2002. Kinetics of Heat Shock Protein 70 Synthesis in the Human Heart After Cold Cardioplegic Arrest. *European Journal of Cardio-Thoracic Surgery,* 22**,** 415-420.